Cell-ECM Interactions Promote Invadopodia Maturation

By

Kevin M. Branch

Dissertation

Submitted to the Faculty of the

Graduate School of Vanderbilt University

in partial fulfillment of requirements

for the degree of

DOCTOR OF PHILOSOPHY

in

Cancer Biology

December, 2012

Nashville, Tennessee

Approved:

Dr. Donna Webb

Dr. Steven Hanks

Dr. Irina Kaverina

Dr. Roy Zent

Dr. Alissa Weaver

To my mother – 11 years cancer free!

ACKNOWLEDGEMENTS

I would like to thank the Breast Cancer Program training grant at Vanderbilt for funding my first two years and the Vanderbilt University Graduate Fellowship. I would also like to thank the Department of Cancer Biology for their support and assistance throughout graduate school.

I am very grateful for my committee members, Dr. Donna Webb, Dr. Steven Hanks, Dr. Irina Kaverina, and Dr. Roy Zent, for their advice, guidance, and, of course, reagents. Their suggestions and advice greatly helped to drive and strengthen the project. I am also indebted to a number of brilliant microscopists at Vanderbilt and elsewhere. Specifically, Dr. Sam Wells, Dr. Bob Matthews, and CarolAnn Bonner of the Vanderbilt Cell Imaging Shared Resource; Dr. Joe Roland of the Epithelial Biology Core Imaging Resource; Dr. Donna Webb and Dr. Irina Kaverina for usage of their confocal and total internal reflection microscopes; Nichole Lobdell of Dr. Al Reynolds lab; and, finally, Dr. Kevin Elicieiri and Dr. Patricia Keely of the Laboratory for Optical and Computational Instrumentation at the University of Wisconsin-Madison. Their access, training, and guidance have been critical to the success of the microscopy and subsequent analyses in this project and have also been a driving force for my own interest in advanced imaging.

I am very thankful for my advisor, Dr. Alissa Weaver, for her mentorship throughout graduate school. I am grateful for her guidance and appreciate the encouragement and training she provided me. I am also thankful for past and

present members of the Weaver lab. Dr. Nicole Bryce, Dr. Emily Clark, and Dr. Nelson Alexander were immensely helpful and patient when I entered the lab. I am grateful for the scientific discussions and friendship of labmates Dr. Aron Parekh, Dr. Bong Hwan Sung, Dr. Kellye Kirkbride, Dr. Daisuke Hoshino, Christi Lynn French, Seema Sinha, and Nan Hyung Hong. Lab managers make the world go around, so I would also like to thank Julie Clark (Maier), Tyne Miller, and Kaitlin Costello.

I would like to thank my friends and family for their unwavering support. I could not have gotten by without my graduate school friends, who put up with my constant intramural sports enthusiasm for our numerous “IGP Class of ’13...ish” intramural teams, and the graduate students, post-docs, and professors in the Tuesday/Thursday morning basketball games. I am eternally grateful for the support from afar of my parents, brother, and sister, and my Xavier family. Finally, I would like to thank my wife, Megan, and our pup, Cooper, and kitty, Zoey. They brighten every day and strengthen me with their unconditional love and support.

TABLE OF CONTENTS

LIST OF FIGURES

Page

LIST OF PUBLICATIONS

Branch KM, Hoshino D, Weaver AM. (2012). “Adhesion rings surround invadopodia and promote maturation.” *Biol Open.,* **1:** 711-722.

Cleghorn WM, Branch KM, Kook S, Bulus N, Gurevich EV, Zent R, Weaver AM, Gurevich VV. “Arrestins regulate cell spreading and motility via focal adhesion dynamics.” (in preparation).

Parekh A, Ruppender NS, Branch KM, Sewell-Loftin MK, Lin J, Boyer PD, Candiello JE, Merryman WD, Guelcher SA, Weaver AM. (2011). “Sensing and modulation of invadopodia across a wide range of rigidities.” *Biophys. J.,* **100:** 573-82.

Anderson AR, Hassanein M, Branch KM, Lu J, Lobdell NA, Maier J, Basanta D, Weidow B, Narasanna A, Arteaga CL, Reynolds AB, Quaranta V, Estrada L, Weaver AM. (2009). “Microenvironmental independence associated with tumor progression.” *Cancer Res.,* **69:** 8797-8806.

Blaine SA, Ray KC, Branch KM, Robinson PS, Whitehead RH, Means AL. (2009). “Epidermal growth factor receptor regulates pancreatic fibrosis.” *Am J Physiol Gastrointest Liver Physiol.*, **297(3):** G434-41.

Alexander NR*, Branch KM*, Parekh A, Clark ES, Iwueke IC, Guelcher SA, Weaver AM. (2008). “Extracellular matrix rigidity promotes invadopodia activity.” *Curr Biol.,* **18:** 1295-9. (*contributed equally)

Enderling H, Alexander NR, Clark ES, Branch KM, Estrada L, Crooke C, Jourquin J, Lobdell N, Zaman MH, Guelcher SA, Anderson AR, Weaver AM. (2008). “Dependence of invadopodia function on collagen fiber spacing and cross-linking: computational modeling and experimental evidence.” *Biophys J.,* **95:** 2203-18.

LIST OF ABBREVIATIONS

A disintegrin and metalloprotease ..... ADAM

ADP-ribosylation factor 6 ..... Arf6

American Cancer Society ..... ACS

Basement membrane ..... BM

Bovine serum albumin ..... BSA

Caveolin-1 ..... Cav-1

Cell division control protein 42 homolog Cdc42

Colony stimulating factor-1 ..... CSF-1

Cortactin ..... Cort

Dimethyl sulfoxide ..... DMSO

Electron microscopy ..... EM

Epidermal growth factor ..... EGF

Extracellular matrix ..... ECM

Extracellular signal-regulated kinases ..... ERK

Fetal bovine serum ..... FBS

Fibronectin ..... FN

Fluorescein isothiocyanate ..... FITC

Fluorescence recovery after photobleaching ..... FRAP

Focal adhesion ..... FA

Focal adhesion kinase ..... FAK

Glyceraldehyde 3-phosphate dehydrogenase ..... GAPDH

Green fluorescent protein ..... GFP

Growth factor receptor-bound protein 2 ..... Grb2

Guanosine triphosphate ..... GTP

Head and neck squamous cell carcinoma ..... HNSCC

Hepatocyte growth factor ..... HGF

Human Epidermal Growth Factor Receptor 2 ..... HER2

Immunofluorescence ..... IF

Inositol polyphosphate 5-phosphatases 5-ptases

Inositol-trisphosphate 3-kinase A ..... ITPKA

Integrin linked kinase ..... ILK

Knockdown ..... KD

Matrix metalloproteinase ..... MMP

Membrane-type matrix metalloproteinase ..... MT-MMP

MT1-MMP-phLuorin MT1-pHLuor

MyosinIIA/B ..... MyoIIA/B

Myosin light chain kinase ..... MLCK

N-ethylmaleimide-sensitive factor ..... NSF

National Heart, Lung, and Blood Institute ..... NHLBI

National Institutes of Health ..... NIH

Neural Wiskott-Aldrich Syndrome protein ..... N-WASp

Non-catalytic region of tyrosine kinase adaptor protein 1 ..... Nck

Non-targeting shRNA control ..... NTC

NSF-attachment protein receptors ..... SNARE

Optical density ..... OD

Overexpressed ..... OE

p130 Crk-associated substrate ..... p130Cas or Cas

Particularly interesting new cysteine-histidine-rich protein ..... PINCH

Pascals ..... Pa

Paxillin ..... Pax

Phosphatidylinositol (3,4,5)-triphosphate ..... PI(3,4,5)P3 or PIP3

Phosphatidylinositol (3,4)-bisphosphate ..... PI(3,4)P2

Phosphatidylinositol (4,5)-bisphosphate ..... PI(4,5)P2

Phosphatidylinositol 4-phosphate 5-kinase type I-alpha PIP5KIα

Phosphatidylinositol phosphate ..... PIP

Phospho-myosin light chain ..... pMLC

Phosphoinositide-3-kinase PI3K

Phosphoinositide-dependent protein kinase 1 ..... PDK1

Platelet-derived growth factor ..... PDGF

Polyacrylamide ..... PA

Poly-D-lysine ..... PDL

Protein kinase C ..... PKC

Ras-related C3 botulinum toxin substrate 1 ..... Rac1

Ras homolog gene family, member A ..... RhoA

Reactive oxygen species ..... ROS

Rho-associated protein kinase ..... ROCK

Rous sarcoma virus ..... RSV

SH2-containing 5′-inositol phosphatase..... SHIP2

Short hairpin ribonucleic Acid ..... shRNA

Short interfering ribonucleic acid ..... siRNA

Standard error of the mean ..... SEM

Stromal cell derived factor 1 alpha SDF-1α

Synaptojanin-2 ..... SJ-2

Td-Tomato F-Tractin ..... Tom-Tract

Tetramethyl rhodamine isothiocyanate ..... TRITC

Tissue inhibitor of metalloproteinases 2 ..... TIMP-2

Transforming growth factor beta ..... TGF-β

Tyrosine kinase substrate with 5 Src-homology 3 domains Tks5

Tyrosine-protein phosphatase non-receptor type 12 ..... PTP-PEST

V-abl Abelson murine leukemia viral oncogene homolog ..... Abl

Vascular endothelial growth factor ..... VEGF

Vascular smooth muscle cell ..... VSMC

Vesicular stomatitis virus G glycoprotein ..... VSVG

Vesicle-associated membrane protein 7 ..... VAMP7

Vinculin ..... Vinc

CHAPTER I

INTRODUCTION

Cancer Progression

Cancer is the second leading cause of death in the United States behind heart disease. The American Cancer Society (ACS) estimates that more than 1.6 million people will be diagnosed with cancer in 2012, with over 577,000 deaths (Siegel *et al.*, 2012). Specific phenotypes are acquired by normal cells as they develop into a tumor: sustained proliferative signaling, evasion of growth suppressive signals, resistance to cell death signals, induction of angiogenesis, replicative immortality, and invasion into the surrounding extracellular matrix (ECM) leading to metastasis (Hanahan & Weinberg, 2000, 2011). Invasion of cancer cells from the primary site is the key step in the progression of a tumor from a benign to a malignant state. Furthermore, the main cause of mortality from cancer is metastatsis: the colonization of tumor cells at sites distant from the primary tumor (Sporn, 1996; Pantel & Brakenhoff, 2004).

Metastasis is a multi-step process during which cells must bypass several obstacles (Fidler, 2003). This begins with local proteolysis of the surrounding basement membrane (BM), a densely packed meshwork of laminin, type IV collagen, proteoglycans and glycoproteins (Rowe & Weiss, 2008). The cell may then invade into and through the surrounding stroma, a more loosely packed

connective tissue area surrounding the tumor that is comprised primarily of type I collagen fibers, along with fibroblasts and immune cells (Kufe *et al.*, 2006). If an invading cell comes in contact with a blood vessel, it may intravasate into the vessel, which can be facilitated by leaky vessels recruited via angiogenesis by the primary tumor (Folkman, 1971). From there, the cancer cell must survive in the bloodstream and attach to the blood vessel wall at a distant site in order to extravasate out of the vessel, invade through the new local tissue, and begin to proliferate, forming a metastasis. Micrometastatic lesions consisting of single or small groups of cells can lead to macroscopic tumors in a process termed colonization, which can be preceded by a period of dormancy that can last decades in some cancer types (Aguirre-Ghiso, 2007). Each of these steps can be rate-limiting to the process of metastasis (Poste & Fidler, 1980). Therefore, understanding mechanisms of cancer cell invasion is critical to develop therapies to decrease cancer mortality.

Cancer Cell Invasion

Tumor cells can adopt varying modes of migration and invasion to traverse the complex structure of BM and stroma surrounding the primary tumor (Friedl & Alexander, 2011). The first step of invasion is breaching the surrounding BM (Barsky *et al.*, 1983; Spaderna *et al.*, 2006), which requires membrane type matrix metalloproteinase (MT-MMP) activity (Hotary *et al.*, 2006; Rowe & Weiss, 2008). This invasion type can also be used while invading the BM surrounding blood vessels (Laug *et al.*, 1983; Blood & Zetter, 1990).

Cancer cells can adopt varying modes of migration to navigate the more fibrillar tissue stromal areas surrounding the tumor (Friedl & Alexander, 2011). Single cells can migrate in amoeboid or mesenchymal fashion, dependent on the organization and structure of the stromal ECM. Amoeboid migration requires Rho-associated protein kinase (ROCK) and activity of the molecular motor myosin to contract the cell body and provide the force to move the cell through pores in the fibrillar matrix in a protease-independent fashion (Wolf *et al.*, 2003; Wyckoff *et al.*, 2006). This mode of migration is likely to be used in areas of sparse, lightly cross-linked, or otherwise disrupted or defective ECM (Sabeh *et al.*, 2009; Madsen & Sahai, 2010). Mesenchymal migration is protease-dependent and requires adhesion to the ECM through focal adhesions (FAs) (Cukierman *et al.*, 2001; Li *et al.*, 2003; Wolf *et al.*, 2007). The protease activity serves to both clear space for the cell to move through the connective tissue and create tracks of reorganized ECM fibers (Wolf *et al.*, 2007) along which advancing cells can migrate more efficiently (Provenzano *et al.*, 2008b; Doyle *et al.*, 2009). Cancer cells can also invade collectively from the primary tumor (Giampieri *et al.*, 2009). This process requires “leader” cells migrating in a mesenchymal fashion to create the path as well as intact cell to cell adhesion (Wolf *et al.*, 2007; Scott *et al.*, 2010). These invasive modes of migration can occur in combination to allow cancer cells to invade from the primary tumor. There are many sub-cellular structures that can facilitate these modes of invasion.

Invadopodia

Overview and History

A cellular structure thought to be important in degradation of the BM ECM is an invadopodium (Weaver, 2006; Parekh & Weaver, 2009). Invadopodia are small, sub-cellular structures that require actin polymerization machinery to protrude from the ventral surface of the cell and degrade matrix.

Evidence for invasive ventral sub-cellular protrusions was first observed in Rous sarcoma virus (RSV)-transformed fibroblasts, as proteins previously localized at FAs (vinculin and α-actinin) were relocated into "rosette" structures upon RSV infection (David-Pfeuty & Singer, 1980). These structures were called cellular feet or "podosomes" due to electron microscopy (EM) images showing ventral protrusions on fibronectin (FN)-coated plastic (Tarone *et al.*, 1985). These protrusions presented as punctate and clustered rosette podosome structures localizing actin and phospho-tyrosine by immunofluorescence. Meanwhile, Wen-Tien Chen, with others, demonstrated a punctate loss of underlying fluorescently-labeled FN in RSV-transformed fibroblasts suggesting that these podosomes could degrade ECM (Chen *et al.*, 1984; Chen *et al.*, 1985). The loss of FN localized with vinculin, α-actinin, and viral-Src, a form of the Src tyrosine kinase lacking its C-terminal auto-inhibitory domain responsible for the transforming ability of RSV (Martin, 1970). FN clearing was dependent on MMPs (Chen *et al.*, 1984), which localized to the structures, which were then called "invadopodia" (Chen, 1989).

The terms podosome and invadopodium have often been used interchangeably, especially in cells transformed with viral-Src or Src Y527F, which abrogates regulatory phosphorylation resulting in an active Src kinase (Cooper *et al.*, 1986; Hunter, 1987). Currently, the term podosome is generally used to describe these actin-based invasive structures in normal cells, while invadopodia is used in cancer cells. In various Src-transformed cells, podosomes, invadopodia, and a new term, “invadosome” have all been used to describe these structures, with invadopodia and podosomes as classes of invadosomes (Linder *et al.*, 2011). For the sake of this dissertation, invadopodia will refer to those structures in cancer cells, while invadosomes and podosomes will refer to the structures in Src-transformed and normal cells, respectively (Figure 1).

Both invadopodia and podosomes are important for invasive cellular functions in various cell types. Podosomes contribute to formation of the sealing zone in osteoclasts and are important for bone resorption (Kanehisa *et al.*, 1990; Miyauchi *et al.*, 1990). Podosomes also form in other normal cells including macrophages, dendritic cells, endothelial cells, and vascular smooth muscle cells (VSMCs) (Gaidano *et al.*, 1990; Burns *et al.*, 2001; Hai *et al.*, 2002; Moreau *et al.*, 2003). Invadopodia form and degrade matrix in multiple types of human cancer cells (Chen *et al.*, 1994; Monsky *et al.*, 1994; Seals *et al.*, 2005; Clark *et al.*, 2007a) and are important for cellular invasion (Coopman *et al.*, 1998; Schoumacher *et al.*, 2010). Therefore, these structures play important roles in traversing ECM barriers in normal and pathologic cellular contexts.

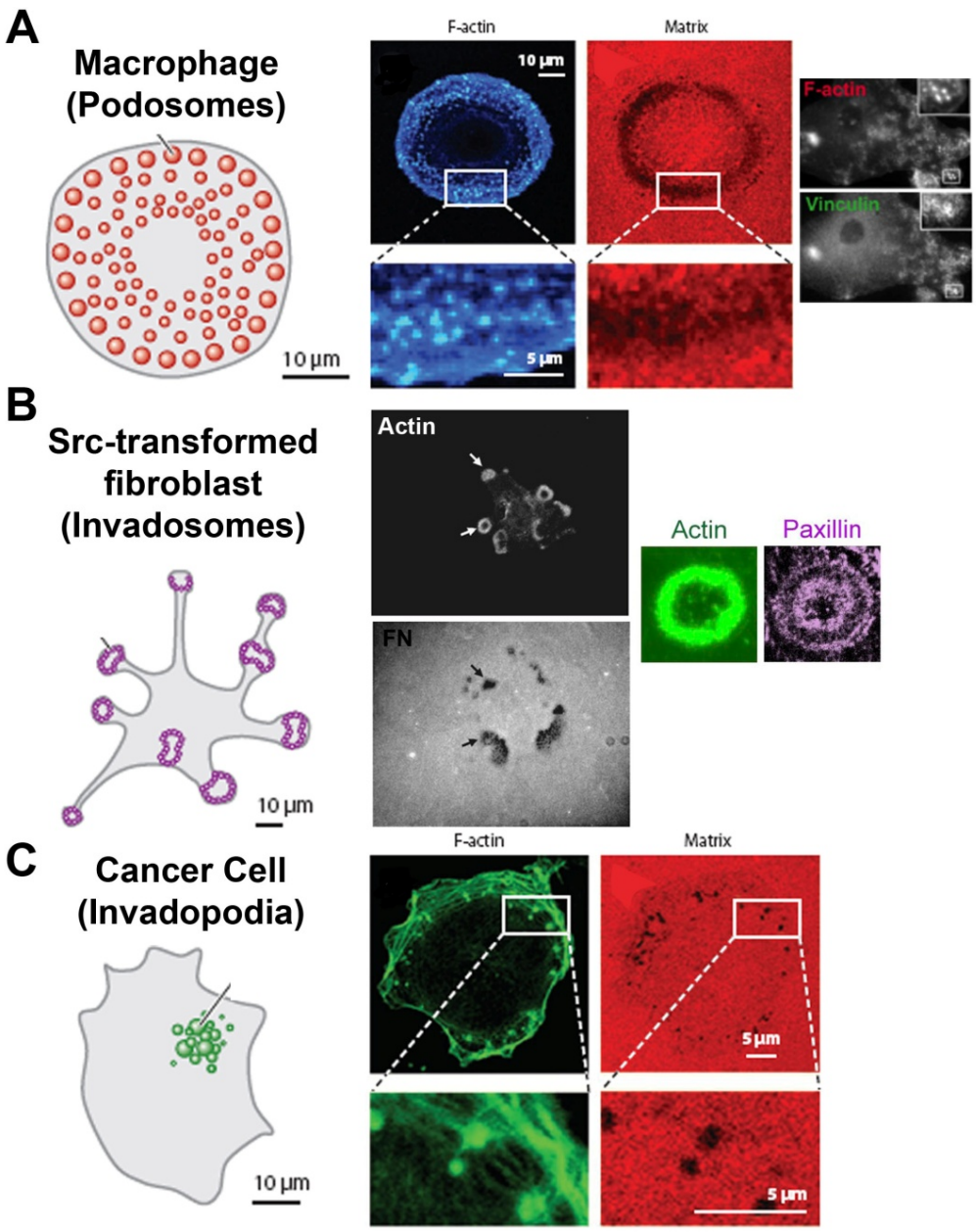

Figure 1. Cellular Invasive Structures. A. Cartoon and IF of podosomes in primary human macrophages localizing F-actin with holes in fluorescent gelatin (matrix, black holes). **B.** Cartoon and IF of podosome/invadosome rosettes in Src-transformed fibroblasts localized with degraded fluorescent FN. Images on right show typical adhesion structures surrounding F-actin-containing podosomes in murine macrophages (vinculin, A) or Src-transformed fibroblasts (paxillin, B). **C.** Cartoon and IF of F-actin containing invadopodia in MDA-MB-231 breast cancer cell line localized with degraded fluorescent gelatin. Adhesion localization data is sparse, but paxillin, integrins, and possibly vinculin may localize at or around invadopodia (see text). Images adapted from Linder *et al.,* 2011: All cartoons, center of A and C, Cougoule *et al.,* 2009: Right of A, (Webb *et al.*, 2007): Center of B, Pan *et al.,* 2011: Right of B.

Src-transformed cells have been a popular model for studying invasive cellular structures due to the robust formation of invadopodia-like puncta and more extensive rosette structures (Tarone *et al.*, 1985; Badowski *et al.*, 2008; Winograd-Katz *et al.*, 2011). Expression of constitutively active Src generally leads to a loss of classic FAs replaced by invadosomes (David-Pfeuty & Singer, 1980; Chen, 1989; Fincham *et al.*, 1995; Winograd-Katz *et al.*, 2011). Therefore, invadosomes represent the primary adhesive structure in Src-transformed cells, similar to podosomes in many normal cells such as macrophages. Meanwhile, cancer cells that produce invadopodia continue to form FAs, which could lead to a more complex and even competitive relationship between the two actin-based structures (Chan *et al.*, 2009; Liu *et al.*, 2009b).

While invadosomes in Src-transformed cells share many similar features to invadopodia in cancer cells, there are some critical differences. First, the presence of constitutively active Src inherently bypasses and/or alters some upstream signals that would otherwise come from growth factors and/or adhesions. Thus, Src-transformed cells may not be the best model for studying how upstream signals lead to an invasive phenotype. Second, invadosome rosettes have a somewhat different structure from podosomes, invadopodia, and higher order organizations of podosomes, such as osteoclast sealing rings. Finally, for unknown reasons, it is extremely rare for cancer cells to express constitutively active Src kinase mutant molecules (Yeatman, 2004). Therefore, there may be some key differences in how cancer cell invadopodia are activated and function, as compared to otherwise normal cells that are transformed with

constitutively active Src.

Structure of Invadopodia and Podosomes

Both invadopodia and podosomes have been well characterized by indirect immunofluorescence (IF) and electron microscopy (EM). Both appear as punctate structures by IF at which actin, actin regulatory proteins such as Arp2/3, cortactin, Tks5, and N-WASp, proteases such as MT1-MMP, active Src, and tyrosine phosphorylated proteins have been localized (Weaver, 2006; Murphy & Courtneidge, 2011). The punctate structures are generally composed of the same components in invadopodia and podosomes, although differences have been noted in scaffolding proteins upstream of N-WASp and membrane dynamics (Artym *et al.*, 2011; Oser *et al.*, 2011). Invadosomes can further assemble into a secondary rosette structure as observed in Src-transformed cells. Podosomes also assemble into higher order structures, such as the sealing zone in osteoclasts.

By EM, the invadosomes of Src-transformed fibroblasts form protrusions or large swaths of membrane in contact with the underlying glass coverslip or matrix protein (Tarone *et al.*, 1985; Chen, 1989). Podosomes in normal cells are characterized as dome-shaped structures above the plasma membrane (Gawden-Bone *et al.*, 2010), and exhibit a dense actin core with radial actin fibers extending outward that may anchor the podosome to the membrane (Luxenburg *et al.*, 2007). On surfaces with ample space and a satisfactory ECM substrate in the ventral direction, podosomes in VSMCs, dendritic cells and

macrophages are protrusive and degrade into the underlying matrix (Gawden-Bone *et al.*, 2010; Quintavalle *et al.*, 2011; Van Goethem *et al.*, 2011). Invadopodia begin as multiple small, finger-like protrusions on the ventral surface of the cell (Bowden *et al.*, 1999) that can mature into protrusions with branched actin filaments through most of the protrusion with bundled filaments at the tip (Schoumacher *et al.*, 2010). These data suggest that, in a proper environment, invadopodia and podosomes similarly form protrusions, degrade and invade into the ECM.

Podosomes are further characterized by a ring of adhesion proteins that surrounds the individual actin puncta or the rosette structure. In normal cells such as macrophages, podosomes are often the primary adhesive structure and are used for motility and invasion (Marchisio *et al.*, 1984; Marchisio *et al.*, 1987). Podosome formation induced in Src-transformed cells or VSMCs results in a local disassembly of FA (Chen *et al.*, 1984; Kaverina *et al.*, 2003; Burgstaller & Gimona, 2004). Invadopodia studies also demonstrated localization of adhesion-related proteins including $\alpha V\beta 3$ integrin and paxillin at the invadopodia puncta of normal fibroblasts and cancer cells (Bowden *et al.*, 1999; Deryugina *et al.*, 2001). Paxillin and its family member Hic-5 also localize in a ring surrounding the invadopodia core, as in podosomes (Desai *et al.*, 2008; Pignatelli *et al.*, 2012). The localization of adhesion proteins around and adhesion ability of invadopodia in cancer cells has been controversial, however, and has been suggested as a defining difference between invadopodia and podosomes (Linder *et al.*, 2011; Murphy & Courtneidge, 2011).

A key feature of these structures is the localization with degraded holes in an underlying ECM. MT1-MMP is regarded as the primary invadopodial protease (Nakahara *et al.*, 1997; Sabeh *et al.*, 2004), and knockdown of MT1-MMP protein levels greatly reduces invadopodia function (Artym *et al.*, 2006). Interestingly, invadopodia number is also decreased, to a lesser extent, by MMP inhibition, suggesting a positive feedback to invadopodia formation from degradation of the ECM (Artym *et al.*, 2006; Clark *et al.*, 2007a). Soluble proteases such as MMP-2 and MMP-9 can be secreted from or activated by MT1-MMP at invadopodia (Deryugina *et al.*, 2001; Artym *et al.*, 2006). The serine protease seprase also localizes to invadopodia and is important for matrix degradation (Monsky *et al.*, 1994). Finally, a disintegrin and metalloprotease 12 (ADAM12) localizes to Src-induced podosomes by binding to Tks5 (Abram *et al.*, 2003). Therefore, a number of proteases facilitate ECM degradation by these structures, but MT1-MMP is considered indispensable.

Invadopodia and Podosomes in vivo

Due to their small size, invadopodia and podosomes have primarily been studied *in vitro,* as ventral protrusions into a thin ECM layer on glass coverslips. While cells can encounter these geometries *in vivo*, it has been unclear if podosome and invadopodia structures would assemble or behave similarly *in vivo*. Recently, direct evidence of podosome and invadopodia formation *in vivo* has come to light. In invading cells, traditional invadopodia and lamellipodia may merge to create invasive protrusions at the cell front. Breast cancer cells form

such invasive protrusions in 3D Matrigel culture that degrade ECM at the cell front which localize invadopodia markers such as cortactin and Tks5 (Magalhaes *et al.*, 2011). Fibroblast or breast cancer cell invasion through 3D collagen gels can occur through similar protrusive structures that demonstrate collagenolytic activity at the base of the protrusion rather than the front, although no invadopodia markers were used in this study (Wolf *et al.*, 2007). Invadopodia and podosomes have also recently been described *in vivo*. Immunoelectron microscopy of murine aortas shows localization of cortactin and Tks5 in podosome rosette structures in VSMCs (Quintavalle *et al.*, 2011). In a breast cancer mouse model, tumor cells at the invasive front of the primary tumor exhibit leading edge protrusion with degradative ability in cryosections immunostained for cortactin, actin, N-WASp, and degraded collagen, with N-WASp knockdown greatly reducing collagenolytic activity (Gligorijevic *et al.*, 2012). This is the first demonstration of invadopodia-like structures with degradative ability and canonical invadopodia markers *in vivo*.

Stages of Invadopodia and Podosomes

Invadopodia have been shown to assemble in a step-wise fashion. Cortactin and actin aggregates form first, followed quickly by MT1-MMP recruitment to the invadopodia within minutes (Artym *et al.*, 2006). Noticeable degradation of a thin layer of fluorescent ECM (~50 nm) can occur in the few minutes following MT1-MMP recruitment (Artym *et al.*, 2006; Artym *et al.*, 2009), while thicker layers (~1 μm) do not show holes in the matrix for 30 minutes to an

hour following cortactin appearance (Oser *et al.*, 2009). This study also demonstrated immediate recruitment of MT1-MMP to cortactin punctate structures formed upon epidermal growth factor (EGF) stimulation (Oser *et al.*, 2009). However, cells treated with a pan-MMP inhibitor or with small interfering RNA (siRNA) targeting MT1-MMP exhibit a nearly complete loss of ECM degradation but only a 2- to 4-fold decrease in invadopodia number (Artym *et al.*, 2006; Clark *et al.*, 2007a; Steffen *et al.*, 2008). These data suggest that actin polymerization precedes MT1-MMP recruitment and local matrix degradation, while also implying a positive feedback loop between matrix degradation and invadopodia formation.

Soluble Extracellular Signals Induce Invadopodia and Podosomes

There are many extracellular cues that regulate invadopodium and podosome formation and function, including growth factor receptors and cell-ECM interactions. Macrophages form podosomes in response to colony stimulating factor 1 (CSF-1), with phosphoinositide-3-kinase (PI3K) activity required downstream (Wheeler *et al.*, 2006). Transforming growth factor beta (TGF-β) induces podosome formation in and invasion by endothelial cells through Src, PI3K, RhoA, and Cdc42 signaling (Varon *et al.*, 2006; Rottiers *et al.*, 2009). Podosomes also form in endothelial cells in response to vascular endothelial growth factor (VEGF) with Src, RhoA, Rac1, and Cdc42 as crucial downstream components (Osiak *et al.*, 2005; Wang *et al.*, 2009). Finally, platelet derived growth factor (PDGF) induces podosome formation in VSMCs

(Quintavalle *et al.*, 2011).

Invadopodia are also induced by many of these growth factors and utilize the same downstream signaling pathways. EGF is a key signaling input for invadopodia formation in cancer cells. EGF stimulation induces actin polymerization at invadopodia sites through a well-defined pathway involving Nck1 and N-WASp (Yamaguchi *et al.*, 2005; Mader *et al.*, 2011). VEGF induces invadopodia in head and neck squamous cell carcinoma (HNSCC) cells (Lucas *et al.*, 2010). Hepatocyte growth factor (HGF) and stromal cell derived factor 1 alpha (SDF1α) increase breast cancer cell invadopodia formation through Src and cortactin or Abl kinases, respectively (Smith-Pearson *et al.*, 2010; Rajadurai *et al.*, 2012). TGF-β induces non-invasive mammary epithelial cells to produce invadopodia and degrade matrix through RhoC-ROCK, Rac1-p38MAPK signaling, the paxillin family member Hic-5, focal adhesion kinase (FAK), and Src signaling (Pignatelli *et al.*, 2012), while TGF-β treatment of invasive cells enhances invadopodia formation through Src and PI3K and matrix degradation through extracellular signal-regulated kinases (ERK) signaling (Mandal *et al.*, 2008). These data indicate that many types of growth factor stimulation converge upon similar or identical signaling hubs for both invadopodia and podosome activity, including Src, PI3K and Rho family small GTPases.

Lipid Regulation of Invadopodium and Podosome Formation

At numerous cellular sites, phosphatidylinositol lipids serve as critical activators of actin polymerization (Wennstrom *et al.*, 1994; Ueno *et al.*, 2011).

With respect to invadopodium and podosome formation, PI3K signaling was recently shown to be critical (Oikawa *et al.*, 2008; Yamaguchi *et al.*, 2011; Hoshino *et al.*, in revision). Regulators of phosphatidylinositol phosphates (PIPs) have been implicated in the regulation of invadopodia and podosome formation. PI3Ks phosphorylate phosphatidylinositides at the D-3 position primarily creating PI(3,4,5)P3 (PIP3) from PI(4,5)P2 (Fruman *et al.*, 1998). PI3Ks are activated downstream of a number of extracellular signals, especially downstream of growth factor receptor signaling (Cantley, 2002). Knockdown of class I PI3Ks reduces invadopodia number and degradation of ECM by a similar amount, suggesting a specific effect on invadopodia formation (Yamaguchi *et al.*, 2011; Hoshino *et al.*, in revision). Classic signaling downstream of PI3K involves phosphoinositide-dependent protein kinase 1 (PDK1)-mediated phosphorylation and activation of Akt serine-threonine kinases (Cantley, 2002). Indeed, both PDK1 and Akt were shown to be required for invadopodia formation in breast cancer cells and inhibition of each abrogates increased ECM degradation in response to constitutively active PI3K (Yamaguchi *et al.*, 2011). PI3K inhibition also reduces podosome formation induced by phorbol ester treatment to activate protein kinase C (PKC) in epithelial cells (Xiao *et al.*, 2012). These data suggest that PI3Ks may signal through a classical pathway to promote invadopodia and podosome formation, although the downstream mechanism is unclear.

In addition to classic signaling via PIP3, it is possible that a critical function of PIP3 is to serve as a precursor lipid for PI3,4P2. Inositol polyphosphate 5-phosphatases (5-ptases) such as SHIP2 or synaptojanin-2 (SJ-2) can form

PI(3,4)P2 from PIP3 (Ooms *et al.*, 2009). SJ-2 is required for ECM degradation and localizes to invadopodia in glioma cells (Chuang *et al.*, 2004) and is required for invadosome formation in Src-transformed fibroblasts (Oikawa *et al.*, 2008). We also recently found that SHIP2 overexpression increases invadopodia formation and function dependent on PI3K activity (Hoshino *et al.*, in revision). Interestingly, using specific PIP probes, Oikawa *et al.* demonstrated that PI(3,4)P2 is specifically localized at invadosomes while PIP3 localized to invadosomes but also to other areas in the cell (Oikawa *et al.*, 2008). Overexpression of these probes sequesters the lipid, and the PI(3,4)P2 probe reduced invadosome number. Live cell imaging demonstrated that PI(3,4)P2 clustering is an early event in invadosome formation following washout of the Src inhibitor PP2. These data suggest that PI(3,4)P2 is critical in the initial formation stage of invadosomes and invadopodia.

Although few binding partners have been determined for PI(3,4)P2, the Src substrate Tks5 is a likely effector at invadosomes (Lock *et al.*, 1998). Tks5 preferentially binds to PI(3,4)P2 and PI(3)P, and its PX domain that mediates this binding is required for localization to invadosomes (Abram *et al.*, 2003). Tks5 localizes to invadopodia and podosomes and is required for ECM degradation in cancer cells and formation of podosomes (Seals *et al.*, 2005; Crimaldi *et al.*, 2009). In non-tumorigenic cells, Tks5 is required for Src-induced invadosome formation, and Tks5 expression amplifies the invadopodia formation in cancer cells transfected with active Src (Seals *et al.*, 2005; Stylli *et al.*, 2009). Tks5 is believed to affect invadopodia/podosome formation in two ways. First, Tks5 can

form a complex with N-WASp and upstream scaffolding proteins Grb2 and Nck in response to Src activity in Src-transformed and cancer cells, respectively, to presumably promote actin polymerization at nascent invadopodia (Oikawa *et al.*, 2008; Stylli *et al.*, 2009). Tks5 is also important for the generation of reactive oxygen species (ROS) downstream of active Src (Gianni *et al.*, 2009). ROS localize to and promote invadopodia and podosome formation, possibly by inactivation of the phosphatase PTP-PEST, which could otherwise inhibit Src activity (Diaz *et al.*, 2009; Weaver, 2009). Thus, Tks5 may serve as both a scaffold protein and a feedback amplifier of Src signaling to facilitate the assembly of nascent invadopodia at PI3,4P2-rich membrane sites. Another possible effector which localizes to the plasma membrane via binding to PI(3,4)P2 and PIP3 is Akt. Akt was recently implicated in invadopodia and podosome formation (Yamaguchi *et al.*, 2011; Xiao *et al.*, 2012). Downstream effectors of Akt at invadopodia are unclear. However, PI3K-mediated Akt activation at the leading edge induces cell motility and actin re-organization, perhaps through phosphorylation of the actin-binding protein Girdin (Enomoto *et al.*, 2005).

Other PIPs have been localized to invadopodia and can regulate localized protein activation to promote actin assembly. PI(4,5)P2 surrounds the invadopodium protrusion and may be locally generated by phosphatidylinositol 4-phosphate 5-kinase type I-alpha (PIP5KIα), which localizes to invadopodia in breast cancer cells (Yamaguchi *et al.*, 2010). Both PI(4,5)P2 and PIP5KIα are required for ECM degradation by invadopodia, although invadopodia formation

itself was not assessed in that study (Yamaguchi *et al.*, 2010). Interestingly, the Ras family GTPase Arf6, which activates PIP5KIα downstream of EGF (Honda *et al.*, 1999), localizes to and is required for invadopodia activity (Hashimoto *et al.*, 2004; Tague *et al.*, 2004). PI(4,5)P2 affects a wide range of actin regulators (Saarikangas *et al.*, 2010). N-WASp, which promotes actin nucleation via activation of the Arp2/3 complex (Machesky *et al.*, 1999), is activated by binding to PI(4,5)P2 and active Cdc42 (Rohatgi *et al.*, 1999; Kim *et al.*, 2000; Rohatgi *et al.*, 2000). N-WASp localizes to invadosomes or podosomes in both Src-transformed fibroblasts and macrophages as well as to invadopodia in its active form (Mizutani *et al.*, 2002; Lorenz *et al.*, 2004; Isaac *et al.*, 2010). N-WASp knockdown or inhibition of its binding to the Arp2/3 complex reduces invadopodia or podosome formation, or ECM degradation by podosomes in macrophages (Mizutani *et al.*, 2002; Yamaguchi *et al.*, 2006; Nusblat *et al.*, 2011). PI(4,5)P2 also regulates the activity of Nck and Grb2, which are binding partners and weak activators of N-WASp (Rohatgi *et al.*, 2001), and critical for invadopodia and/or podosome formation (Yamaguchi *et al.*, 2005; Oikawa *et al.*, 2008).

Protease Trafficking is Crucial for Functionality of Invadopodia and Podosomes

Cellular protein trafficking machinery is thought to be critical for polarized localization of proteins to invadopodia (Poincloux *et al.*, 2009). Although the Golgi complex has been localized in close proximity to invadopodia (Baldassarre *et al.*, 2003) and was initially assumed to be the major source of secretory vesicles, recent data suggest that a late endosomal/lysosomal compartment is critical for

delivery of MT1-MMP (Steffen *et al.*, 2008). Although MT1-MMP is probably initially exocytosed via the biosynthetic pathway from the Golgi, a large fraction of internalized MT1-MMP is recycled back to the membrane from endosomes and localizes with late endosome/lysosome markers. Endolysosomal recycling may provide a mechanism to relieve TIMP-2 mediated inhibition of MT1-MMP activity (Remacle *et al.*, 2003; Itoh & Seiki, 2006; Li *et al.*, 2008).

Some components of the pathway regulating delivery of MT1-MMP to invadopodia have been identified. The exocyst complex consists of eight proteins and functions to tether post-Golgi and endocytic recycling vesicles to the plasma membrane (Prigent *et al.*, 2003; Hsu *et al.*, 2004). The exocyst plays a role in both invadopodia formation via the Arp2/3 complex (Liu *et al.*, 2009a) and invadopodia function via MT1-MMP localization to invadopodia dependent on the polarity protein IQGAP (Sakurai-Yageta *et al.*, 2008). Phosphorylation of the exocyst subunit Exo70 by ERK1/2 enhances exocytosis from the biosynthetic pathway as measured by vesicular stomatitis virus G glycoprotein (VSVG) exocytosis and partially regulates ECM degradation by invadopodia, suggesting a role for exocyst mediated post-Golgi vesicle docking in invadopodia function (Ren & Guo, 2012). However, the localization of VSVG as a measure of biosynthetic secretion at invadopodia has been controversial (Caldieri *et al.*, 2012). Therefore, MT1-MMP recycled through a late endosome/lysosome compartment may be the key population trafficked to invadopodia. In fact, bafilomycin treatment to inhibit the acidification of lysosomes reduces MT1-MMP accumulation at invadopodia as measured by fluorescence recovery after

photobleaching (FRAP) (Hoshino *et al.*, 2012). Also, knockdown of the late endosomal/lysosomal vesicular N-ethylmaleimide-sensitive factor (NSF)-attachment protein receptors (SNARE) VAMP7, which localizes to MT1-MMP-containing vesicles, reduces MT1-MMP surface localization and invadopodia-related degradation of the ECM by 60-70%, suggesting a prominent role for recycled MT1-MMP at invadopodia (Steffen *et al.*, 2008). It is currently unclear, however, if exocyst- and VAMP7-mediated MT1-MMP localization on the cell surface are linked or receive MT1-MMP from different cellular trafficking pathways. The extracellular signals that induce MT1-MMP recruitment to invadopodia are also unclear.

Cell-ECM adhesion has recently emerged as an important regulator of membrane trafficking. Loss of cell-ECM attachment results in internalization of raft domains dependent on caveolin-1 (Cav-1) (del Pozo *et al.*, 2004; del Pozo *et al.*, 2005), while reattachment induces recycling of lipid rafts from endosomes to the plasma membrane dependent on interaction of the small GTPases Arf6 and RalA with the exocyst complex (Balasubramanian *et al.*, 2007; Balasubramanian *et al.*, 2010). Intriguingly, Arf6 regulates ECM degradation by cancer cells (Hashimoto *et al.*, 2004; Tague *et al.*, 2004), while the exocyst affects MT1-MMP localization to invadopodia (Sakurai-Yageta *et al.*, 2008). Invadopodia contain lipid raft components and Cav-1-containing vesicles dynamically traffic with MT1-MMP (Yamaguchi *et al.*, 2009). MT1-MMP also fractionates with lipid raft components (Yamaguchi *et al.*, 2009; Grass *et al.*, 2012). Cav-1 is also required for functional invadopodia formation and MT1-MMP overexpression-induced

increases in ECM degradation (Yamaguchi *et al.*, 2009). Therefore, cell-ECM adhesion may play a key role in promoting exocytosis of lipid raft-rich vesicles containing MT1-MMP and other cargo.

Adhesion Regulation of ECM Degradation by Cellular Organelles

The main focus of the work in this dissertation is the regulation of invadopodia by cell-ECM interactions. Podosomes in normal cells are often the primary adhesion structures (Marchisio *et al.*, 1984; Marchisio *et al.*, 1987), while invadosome formation in Src-transformed cells or podosome formation induced by PKC activation adhesions leads to complete disassembly of FAs with recruitment of adhesion proteins to the new invadosome/podosome structures (Chen *et al.*, 1984; Kaverina *et al.*, 2003; Burgstaller & Gimona, 2004). Podosomes and invadosomes form specifically on adherent surfaces, and knockout of β1 integrins or activation of CD44 can reduce or increase the number of invadosome secondary rosette structures, respectively (Chabadel *et al.*, 2007; Destaing *et al.*, 2010). Interestingly, osteoclast podosome organization into belts and bone resorption, but not actin core formation, was reduced with combinations of β1, β2, and αV integrin knockout (Schmidt *et al.*, 2011). Furthermore, podosome or invadosome rosette expansion, actin core turnover, and matrix degradation, but, again, not actin core formation, are affected by knockdown or perturbation of paxillin phosphorylation, FAK, p130Cas, RhoA-ROCK signaling, and calpain (Berdeaux *et al.*, 2004; Brabek *et al.*, 2004; Calle *et al.*, 2006; Tatin *et al.*, 2006; Badowski *et al.*, 2008; Pan *et al.*, 2011).

Interestingly, these proteins have previously been shown to control focal adhesion turnover (Franco *et al.*, 2004; Webb *et al.*, 2004; Ezratty *et al.*, 2005; Schober *et al.*, 2007). These data implicate cell-ECM adhesion and downstream signaling in the turnover, expansion, and functionality, but not formation, of these structures.

Focal adhesions have long been considered non-degradative structures that mediate attachment to the ECM and serve as signaling scaffolds (Geiger & Yamada, 2011). A recent study localizes degradation of a very thin ECM layer underneath FAs in a subset of fibrosarcoma and pancreatic cells dependent on MT1-MMP, Src, FAK and p130Cas (Wang & McNiven, 2012). Due to the increased sensitivity of this ECM degradation system compared to classic invadopodia assays, this study likely revealed a low level of degradative ability by FAs. Interestingly, these structures were determined to be separate from invadopodia, as the streak-like degradation underneath FAs was distinct from the dot-like invadopodia-related ECM degradation underneath the same cell. Src, FAK, and p130Cas inhibition or knockdown appeared to primarily affect FA-related rather than invadopodia-related degradation in cells that exhibited ECM degradation underneath FAs. However, Src inhibition completely abolished ECM degradation in cells which form classic invadopodia, while FAK and p130Cas knockdown had no effect. These data suggest that FAK and p130Cas may specifically affect MT1-MMP recruitment to FAs. In certain physiological invasive situations, cells likely combine protrusive, invasive, and adhesive machinery (Friedl & Wolf, 2009; Gligorijevic *et al.*, 2012). In fact, adhesions have been

observed in 3D and *in vivo* (Cukierman *et al.*, 2001; Kubow & Horwitz, 2011), and β1 integrin has been localized with MT1-MMP and degraded collagen at the base of cellular protrusions in 3D (Wolf *et al.*, 2007). Therefore, adhesion-mediated protease recruitment is an attractive model to facilitate cellular invasion in physiologic environments.

The role of FA proteins at or around invadopodia has been controversial (Linder *et al.*, 2011; Murphy & Courtneidge, 2011). Initial studies demonstrated localization of α3, β1 integrin, and paxillin at invadopodia and α5β1 around the protrusion in melanoma or breast cancer cells (Bowden *et al.*, 1999; Mueller *et al.*, 1999) with ligation of β1 integrin increasing ECM degradation underneath these cells (Nakahara *et al.*, 1996; Nakahara *et al.*, 1998). However, in rat bladder carcinoma cells, antibody blocking of α3 or β1 integrin increased invadopodia formation, potentially by blocking binding to laminin-332, which these cells secrete liberally (Liu *et al.*, 2009b). Downstream of integrins, knockdown or inhibition of FAK activity was shown to increase invadopodia numbers (Chan *et al.*, 2009; Liu *et al.*, 2009b), perhaps by releasing retention of Src kinase at competing FAs. However, other studies have shown a requirement for FAK in invadopodia-associated matrix degradation downstream of p190RhoGEF or an increase in matrix degradation with FAK overexpression (Alexander *et al.*, 2008; Yu *et al.*, 2011; Pignatelli *et al.*, 2012). Altogether, the localization and effect of adhesion proteins at invadopodia remains an open question, especially given the coincident expression of focal adhesions in the same cancer cells that form invadopodia. The relative lack of live imaging

studies has also made it difficult to distinguish at which stage adhesion proteins act to regulate invadopodia and podosome formation and/or function.

Purpose of this study

The BM and surrounding stromal ECM are often viewed as a barrier to tumor cell invasion. However, chemical and physical signals from the ECM can be sensed by the cell and transmitted into biochemical responses. Tumors are often associated with an increase in tissue rigidity due to proliferation and packing of tumor cells against the surrounding BM as well as the desmoplastic response, which involves increased collagen deposition in the immediate tumor environment (Li *et al.*, 2005). Interestingly, increased breast density associated with collagen deposition is a prognostic indicator of breast tumor development and invasive capacity (Boyd *et al.*, 2005; Gill *et al.*, 2006). *In vitro* studies have demonstrated a progressively invasive phenotype in tumor cells grown in 3D environments of increasing rigidity (Paszek *et al.*, 2005; Provenzano *et al.*, 2008a). However, when this study began, it was unclear by what cellular mechanisms tissue rigidity might promote invasive behavior.

These studies tested the hypothesis that cell-ECM interactions promote the maturation of invadopodia to fully functional, ECM degrading structures. This work demonstrates that invadopodia-associated ECM degradation is modulated by substrate stiffness and the stiffness with maximum activity can vary depending on tumor cell type. Overexpression of the mechanosensing proteins FAK and p130Cas can augment the invadopodial response to stiffness.

In addition, integrins, which are key receptors for ECM, are investigated as promoters of invadopodia formation and function. Adhesion proteins were found to distinctly localize in ring-like structures around invadopodia. Inhibition of integrins with either a blocking antibody or by use of a peptide inhibitor of ECM-integrin interaction specifically affected cellular ECM degradation by reducing MT1-MMP recruitment to invadopodia. This process requires the integrin effector integrin-linked kinase (ILK) and apparently involves downstream recruitment of the scaffold protein IQGAP. These data support a model in which cell-ECM interactions specifically promote the maturation stage of invadopodia to promote matrix degradation and tissue invasion.

CHAPTER II

MATERIALS AND METHODS

Antibodies and reagents

Antibodies

Cortactin, 4F11, FAK, clone 4.47 (Upstate Biotechnology, Lake Placid, NY); non-muscle myosin IIA, IIB, β-actin, AC-74, and vinculin, hVin-1 (Sigma, St. Louis, MO); p130Cas (clone 21, BD Biosciences, San Jose, CA); phosphorylated serine 19-myosin light chain 2 (pMLC), Src pY416, #2101, GAPDH, 14C10, and pY165-p130Cas (Cell Signaling, Danvers, MA); pY397 FAK (BioSource, Carlsbad, CA); Paxillin (Y113, Abcam, Cambridge, MA); IQGAP, H-109, normal mouse IgG, and integrin β1, active, 12G10, (Santa Cruz, Santa Cruz, CA); integrin β1, blocking, AIIB2 (a gift from Dr. Roy Zent, Vanderbilt University); integrin αVβ3, blocking, LM609 (Millipore, Billerica, MA); and fluorescent Alexa Fluor secondary antibodies and phalloidin (Invitrogen, Grand Island, NY).

Reagents

Blebbistatin, ML-7, and Y-27632 were from Calbiochem (Merck KGaA, Darmstadt, Germany). Gly-Arg-Gly-Asp-Ser-Pro (GRGDSP, Sigma), and Gly-Arg-Gly-Glu-Ser-Pro (GRGESP, American Peptide Co., Sunnyvale, CA).

tdTomato-F-tractin (Tom-Tract) was a gift of Dr. Robert Fischer (NHLBI, Bethesda, MD) and was created by cloning the 9-52 stretch of the F-actin binding protein ITPKA (Johnson & Schell, 2009) into pCMV-tdTomato (Clontech, Mountain View, CA). GFP-paxillin was PCR cloned from pEGFP-N3-Paxillin, a gift of Dr. Donna Webb (Vanderbilt), into the pENTR-TOPO vector and recombined into the LZRS-GW-Neo retroviral vector, a gift from Dr. Al Reynolds (Vanderbilt), using the Gateway recombination system (Invitrogen). LZRS-MS-Cas and LZRS-MS-FAK were gifts from Dr. Steven Hanks (Vanderbilt). MT1-MMP-pHLuorin (MT1-pHLuor) was a gift from Dr. Philippe Chavrier (Institut Curie, Paris). MT1-pHLuor was PCR-cloned into the pLenti6 lentiviral vector by Dr. Daisuke Hoshino (Invitrogen). Control (non-targeting shRNA (NTC), Addgene, Cambridge, MA) and two shRNA constructs targeting ILK (sh1- 5'-CUGAACAAACACUCUGGCAUU -3' (Thermo Scientific, Lafayette, CO), sh2- 5'-GCAAUGACAUUGUCGUGAAGG -3' (Sigma)) were obtained in the lentiviral vector pLKO.1-puro (Sigma). MT1-MMP targeting shRNA (MT1 sh1- 5'-CAGCGATGAAGTCTTCACTTA -3', sh2- 5'-CAGCCTCTCACTACTCTTTC -3') or shLacZ as a control were subcloned into the lentiviral vector pLenti-BlockIt by Dr. Daisuke Hoshino (Invitrogen).

Cell Culture and Manipulation

Cell Culture

MCF10A-CA1d breast cancer cells were obtained from Dr. Fred Miller

(Karmanos Institute, MI) (Santner *et al.*, 2001). Cells were cultured in DMEM/F12 supplemented with 5% horse serum (HyClone, Thermo Scientific), 0.1 ug/ml cholera toxin (Calbiochem), 10 ug/ml insulin (Gibco, Invitrogen), 0.5 ug/ml hydrocortisone (Sigma), and 20 ng/ml EGF (Invitrogen) at 37° C with constant humidity. SCC61 HNSCC cells were previously described (Weichselbaum *et al.*, 1986) and were cultured in DMEM supplemented with 20% fetal bovine serum (FBS, HyClone) and 0.4 mg/ml hydrocortisone (Sigma) at 37° C.

Transfection and Transduction

Tom-Tract was transiently transfected into SCC61 cells at a 1:1 µg DNA:µl Lipofectamine 2000 (Invitrogen) ratio for 6 hours per the manufacturer's instructions. Cells were imaged 1-2 days later. Retrovirus or lentivirus were produced using Phoenix (Dr. Garry Nolan, Stanford) or 293FT cells, respectively, and SCC61 cells were incubated with viral supernatant overnight and later selected with the appropriate antibiotics.

Invadopodia Assay

MatTek culture dishes pre-coated with poly-D-lysine (PDL) (MatTek Corp., Ashland, MA) were coated with 1% gelatin + 1% sucrose (different percentages are noted for Figure 2) in PBS for 1 minute. The gelatin was then wicked away until only a very thin layer remained, which was allowed to dry at a >70° angle for 45 minutes. The gelatin was then crosslinked with 0.5% glutaraldehyde for 15 minutes on ice followed by 30 minutes at room temperature. Glutaraldehyde was

then deactivated with 1 mg/ml sodium borohydride for 3 minutes. Then, the gels were coated with 50 μg/ml FITC-conjugated fibronectin (FITC-FN). Finally, dishes were sterilized with 70% ethanol. Cells were cultured at a density to allow single cells (i.e. 25,000 in a 35mm dish) in a 1:1 ratio of DMEM:RPMI-1640 (or L-15 for live cell imaging) with 5% NuSerum (Gibco), 10% FBS, and 100 ng/ml EGF for 20 hours before fixation with 4% paraformaldehyde and immunostaining. For integrin-blocking studies, RGD, RGE (250 μg/ml), or specific integrin blocking antibodies (10 μg/ml each) were added immediately upon plating of the cells.

Fluorescent-FN Conjugation

6 mg fluorescein isothiocyanate isomer I (FITC, Sigma) was dissolved in 200 ml borate buffer. FN was diluted to 0.5 mg/ml in 10 ml borate buffer in a dialysis bag. FN was then placed in the FITC-borate buffer solution in the dark at room temperature with spinning for 1.5 hours. To remove un-conjugated FITC, the now FITC-labeled FN was dialyzed against PBS for 2-3 days with 3 changes per day at 4° C. The concentration of labeled FITC-FN was determined by measuring the optical density (OD) of the FITC-FN at 280nm and 493nm. The protein concentration was determined with the following equation: FITC-FN (mg/ml) = [OD280 – (0.36 x OD493)] / 1.34. If a fluorescent protein with an ester attacking group was used to label FN (i.e. Alexa Fluor 633 succinimidyl ester), then 0.2M sodium bicarbonate buffer was used rather than borate buffer.

Polyacrylamide gels

3-aminopropyltrimethoxysilane functionalized MatTek dishes were coated with polyacrylamide (PA) gels (Pelham & Wang, 1997). The gels used contained 8% acrylamide and 0.05% bis-acrylamide (soft) or 0.35% bis-acrylamide (hard). The thin (~75 μm) PA gels were coated with gelatin (~1 μm thickness) and FITC-FN and cells were cultured as outlined for the invadopodia assay.

Rheology

Gelatin and PA gels (both hard and soft) were analyzed on a TA Instruments ARG2 rheometer at 37°C using a 25 mm circular head. Strain sweeps were first performed at 1 Hz to identify the range where the storage modulus was constant as a function of strain, which ranged from 0.025 to 0.1% depending on the material. Frequency sweeps (0.1 – 10 Hz) were then performed for each material at constant applied strain. Storage modulus data reported were measured at 1 Hz.

Microscopy and Analysis

Immunofluorescence

CA1d and SCC61 cells plated for invadopodia or adhesion analyses were fixed with 4% paraformaldehyde (Avantor, Center Valley, PA), permeabilized with 0.5% Triton X-100 (Research Products International Corp., Mt. Prospect, IL), blocked for 1 hour with 3% bovine serum albumin fraction V (BSA, Merck KGaA),

incubated with indicated primary antibodies in 3% BSA for 1 hour or overnight followed by appropriate fluorescently-conjugated secondary antibodies, or fluorescently-labeled phalloidin to mark actin filaments, for 1 hour in 3% BSA. 1x PBS was used for all washes. Imaging was performed as detailed below.

Polyacrylamide Gel Invadopodia Analysis, Widefield

Widefield fluorescent images were captured on a Nikon Eclipse TE2000-E microscope with a 40X Plan Fluor oil immersion objective lens. Degradation area per cell was determined using MetaMorph software (Molecular Devices, Sunnyvale, CA) by tracing a region around the cellular actin footprint and measuring the thresholded area of dark spots in the FITC-FN in that region. Functional invadopodia were manually counted as morphologically characteristic round actin or cortactin puncta ≥1 μm in diameter found at the basal surface of the cell which also localized with dark holes in the FITC-FN (Clark *et al.*, 2007a).

Adhesions and Invadopodia Analyses, Confocal

Fixed cell confocal images were taken using a Zeiss LSM 510 microscope with the pinhole set at 1 Airy unit, with a Plan Apo 63X oil immersion objective lens with Argon-488nm, HeNe-543nm, and HeNe-633nm lasers. Images were taken at a scan speed of 8 and 4 scans were averaged per acquisition. Degradation areas per cell and invadopodia numbers were determined as above. If ECM degradation was associated with an invadopodia, it was classified as “active”; otherwise it was classified as “inactive”. The presence of an adhesion ring was

defined as paxillin or vinculin fluorescence above background surrounding the invadopodia. Invadopodia metrics (adhesion ringed, non-ringed, total, active and inactive invadopodia) were manually counted. For focal adhesion analyses on paxillin-immunostained cells, the central region of the cell with high background cytoplasmic fluorescence was excluded and the remaining periphery was thresholded. The number and area of peripheral focal adhesions per cell was then determined with the "Analyze Particles" function in ImageJ (NIH). For IQGAP localization analyses, SCC61 cells were plated on invadopodia substrates and fixed and stained for actin and IQGAP. Images were obtained with the Zeiss LSM 510 confocal as described above. The pinhole was opened slightly (1.4 μm optical slice) to account for the slightly higher Z-axis localization of IQGAP at invadopodia. Equal laser power, digital gain and offset settings were used in each experiment and actin and IQGAP signals were within the dynamic range. Invadopodia were traced using the actin immunostaining and average intensity of the actin and IQGAP signals within the traced regions was obtained using ImageJ. Linescans were created with Metamorph. Confocal Z-slices were taken at 0.05 μm per slice for FAK and Cas and 0.1 μm per slice for IQGAP.

Live Cell Imaging

For adhesion ring imaging, live cell confocal images of SCC61 cells stably expressing GFP-Paxillin and transiently transfected with Tom-Tractin were taken using a Zeiss LSM 710 confocal microscope with the pinhole set at 1 Airy unit, with a Plan Apo 63X oil immersion objective lens with Argon-488nm and HeNe-

561nm lasers. Time-lapse images were obtained every 15 seconds at a scan speed of 8 with 4 images averaged per acquisition. Time of invadopodia and paxillin ring appearance was manually determined. For invadopodia and MT1-MMP imaging with Tom-Tractin alone or with MT1-pHLuorin, an Applied Precision DeltaVision Core microscope with a Plan Apo 60X oil immersion objective lens was used. SCC61 cells expressing Tom-Tractin and/or MT1-pHLuorin, with ILK-KD or NTC shRNA where noted, were seeded in the ECM degradation assay on 1% gelatin/unlabeled-FN and placed in a heated microscope chamber at 37°C 2 hours prior to imaging. When used, RGE or RGD peptides were added at the time of cell seeding. Images were then obtained every 15 seconds and processed with 10 iterations of constrained iterative deconvolution using Softworx 5.0 (Applied Precision, Issaquah, WA). For live-cell invadopodia analyses, the actin-containing invadopodia were traced at their largest area and fluorescence intensity of Tom-Tract and MT1-pHLuorin was determined at each time point using Metamorph. The Tom-Tract and MT1-pHLuorin signal at each time point was background corrected at each invadopodia with an identical traced region placed in a similar area of the cell but lacking an invadopodium. With these data, invadopodia formation rate, lifetime, and MT1-pHLuorin accumulation at invadopodia were determined as described in the manuscript. For MT1-pHLuorin accumulation, the data were binned into 1 minute intervals.

Statistics

Data sets were tested for normality using the Kolmogorov-Smirnov normality test in GraphPad InStat3 (GraphPad Software, La Jolla, CA). Groups of non-normal data were compared using the Mann-Whitney rank sum test, while parametric data were compared with an unpaired t-test. Non-normal data were plotted as box and whiskers, which show respectively the 25-75th and 5-95th percentiles with the dotted red line indicating the mean and the black line indicating the median. For the Spearman rank analysis, comparisons between degradation area/cell and each other data set were performed in GraphPad InStat3. A perfect positive correlation = 1, no correlation = 0 and a perfect negative correlation = -1, and p values represent a correlation significantly different than no correlation.

CHAPTER III

SUBSTRATE RIGIDITY PROMOTES INVADOPODIA ACTIVITY

Introduction

Tumor metastasis is a leading cause of mortality from cancer due to an increased tumor load at multiple sites in the body. An initial step in metastasis is invasion of cancer cells from the primary tumor site, which is often surrounded by a dense BM. Proteolytic degradation is required to breach the BM and allow cell invasion beyond the primary site (Hotary *et al.*, 2006). In fact, loss of BM surrounding the tumor is observed in aggressive versus benign tumors (Barsky *et al.*, 1983).

Although the BM and surrounding ECM are often viewed as barriers to cancer progression, cancerous phenotypes can be promoted by physical and chemical signals from the ECM. The physical stiffness of the ECM in particular can affect tumor progression. High mammographic density is a strong prognostic indicator for breast tumor formation and progression (Boyd *et al.*, 2005; Gill *et al.*, 2006). An increase in collagen deposition in the surrounding environment is also associated with tumor development (Li *et al.*, 2005). Therefore, physical signals from the ECM may promote cancer cell invasiveness.

Cells are known to sense mechanical signals from the surrounding environment via integrin-actomyosin interactions at FA through a process termed mechanotransduction. Forces are transmitted into the cell via contraction of non-

muscle myosin II (MyoII) to generate intracellular tensile forces (Giannone & Sheetz, 2006; Clark *et al.*, 2007b). Cells respond to extracellular forces at the protein level to elicit a number of cellular responses. At the protein level, stretching of purified FA proteins talin or Cas induce binding to vinculin or extensive tyrosine-phosphorylation, respectively (Sawada *et al.*, 2006; del Rio *et al.*, 2009). FAK may also unfold to induce paxillin binding (Mofrad *et al.*, 2004). At the cellular level, fibroblasts preferably migrate toward stiffer matrices dependent on FAK auto-phosphorylation at Y397 (Wang *et al.*, 2001), while phosphorylation at Y397 increases in cells on stiffer matrices (Paszek *et al.*, 2005). Increasing rigidity also results in a more dispersed and migratory phenotype in fibroblasts with fewer aggregations similar to a model of epithelial-to-mesenchymal transition (Guo *et al.*, 2006). *In vitro* studies have demonstrated an increasingly invasive phenotype in breast cancer cells growing in increasingly stiff 3D collagen I gels (Paszek *et al.*, 2005). The cellular mechanism for increased cancer cell invasion in response to stiffness is unknown, however.

Invadopodia are sub-cellular, actin-rich, protrusive structures important for cancer cell invasion. Invadopodia localize actin polymerization machinery and protease activity to locally degrade and invade ECM (Weaver, 2006). Formation of invadopodia by cancer cells often correlates with tumor aggressiveness in *in vivo* models (Coopman *et al.*, 1998; Bowden *et al.*, 1999). Despite close ECM contact, it is unclear how chemical or physical signals from the ECM affect invadopodia.

In this chapter, we demonstrate that invadopodia activity is enhanced by

increasing substrate rigidity. The degradation of ECM by invadopodia is dependent on MyoII activity. MyoIIA localized in rings surrounding a subset of invadopodia, highlighting an area where mechanosensing may occur. Over-expression of proteins known to be involved in mechanosensing, FAK and Cas, primed the invadopodial response to rigidity and increased degradation of the ECM on “hard,” but not “soft” PA gels.

Results

ECM Rigidity Promotes Invadopodia Activity

We first tested the role of ECM density on invadopodia function. MCF10A CA1d invasive breast cancer cells were cultured on increasing concentrations of gelatin from 0.5% - 5% which was overlaid with fluorescently-labeled FN (FITC-FN) to visualize degradation by invadopodia. Rather than acting as an increasing barrier to invasion, high concentrations of gelatin promoted degradation of FITC-FN (Fig. 2A). The degradation area per cell was quantified and increased with higher concentrations of gelatin, with the largest increase between 2.5% and 5% (Fig. 2B, black line). The number of functional invadopodia per cell, measured as actin puncta co-localized with degradation of FITC-FN, increased similarly to the degradation area (Fig. 2B, red line). Increasing the density of gelatin gels is likely to increase their rigidity. Therefore, we performed rheology with an oscillatory shear deformation of the gelatin gels to obtain their storage modulus. The storage modulus increased with increasing gelatin concentration

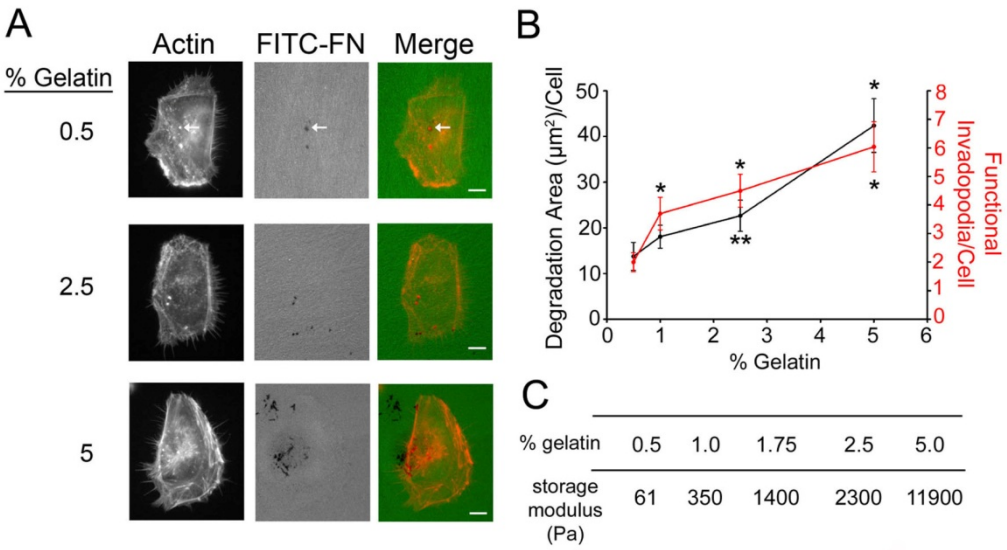

Figure 2. Increased density of gelatin cushions regulates invadopodia functions. A. Widefield fluorescence images of invadopodia in CA1d cells cultured on FITC-FN/gelatin cushions with increasing gelatin percentage. Scale bars = 10 μm. **B.** Quantification of ECM degradation area/cell and number of functional invadopodia/cell (actin puncta associated with degradation sites). Data are represented as mean +/- standard error (SE) * $p < 0.05$, ** $p < 0.06$, compared with 0.5% gelatin. n=3. **C.** The storage moduli of gelatin cushions were measured by rheology. The mean values are reported from 2 independent experiments performed in triplicate. (Performed by Nelson Alexander)

and, again, the largest increase occurred between 2.5% and 5% gelatin (Fig. 2B-C). These data suggest a causal relationship between gelatin concentration and degradation of ECM by invadopodia.

While increasing the gelatin concentration increases the rigidity of the gels, it also serves to increase the ECM ligand availability, which can affect phenotypes such as cell spreading (Engler *et al.*, 2004). Therefore, we cast two different stiffnesses of PA gels by altering the amount of bis-acrylamide cross-linker (Pelham & Wang, 1997) and coated them with an equal concentration of gelatin (1%), which was then overlaid with FITC-FN to visualize degradation. When measured by rheology, the storage modulus of the “soft” and “hard” PA gels were 360 and 3300 Pascals (Pa), respectively (Fig. 3A). These values are on the order of magnitude of measured values in a mouse normal mammary gland compared to a mammary tumor (Paszek *et al.*, 2005). Interestingly, the degradation of FITC-FN underneath the cells increased on the hard gels compared to the soft (Fig. 3B, C). Coating the PA gels with gelatin alone or gelatin/FN had little effect on the storage modulus (Fig. 3A). Cells cultured on the PA gels were immunostained for cortactin and actin, as co-localization of these two proteins with degradation of the underlying ECM represents a functional invadopodium. An increase in functional invadopodia per cell was observed on the hard PA gels (Fig. 3D). Matrix stiffness can enhance invadopodia activity across a variety of cancer cell lines, as these effects were also observed in SCC61 HNSCC and 804G rat bladder carcinoma cells (Fig. 3E-H). These data suggest that substrate rigidity alone promotes invadopodia activity.

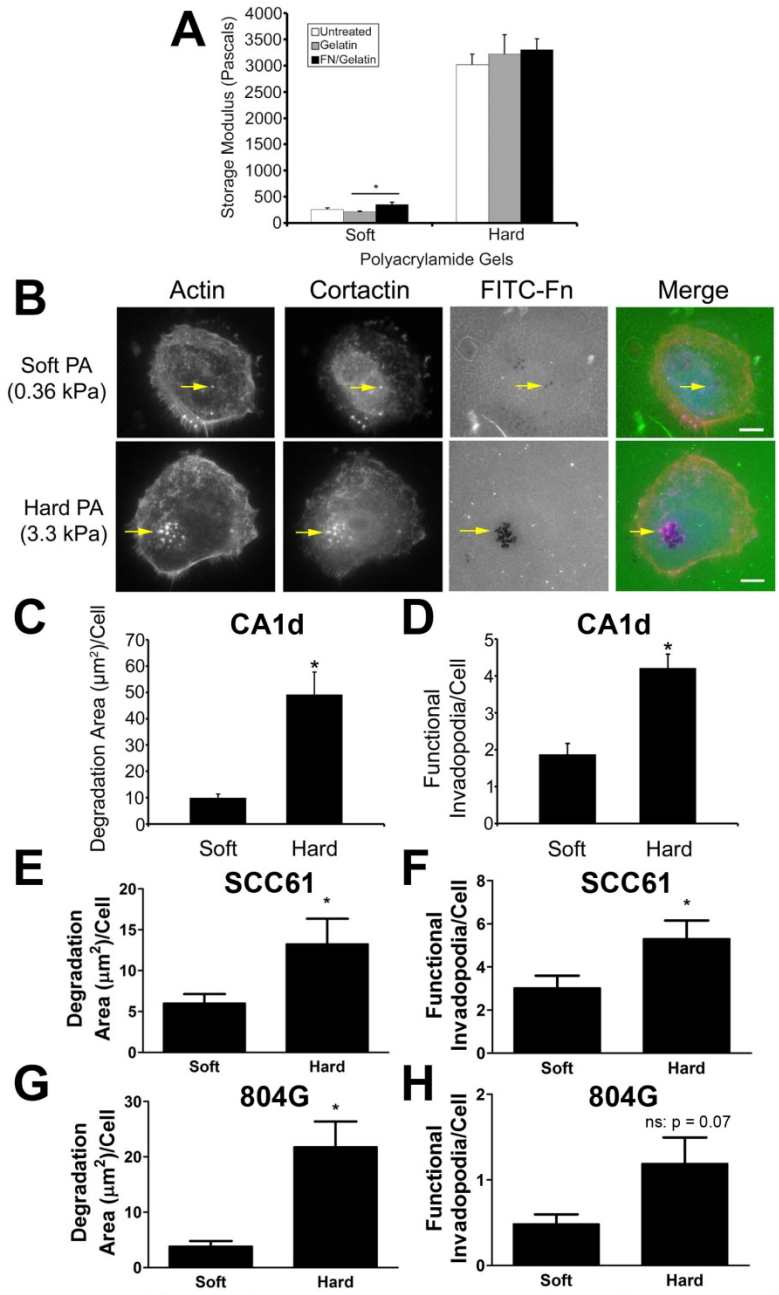

Figure 3. ECM rigidity promotes invadopodia formation and function. **A.** The storage moduli for the PA gels were measured by rheometry. PA gels were prepared as described for the invadopodia assays. **B.** Images of cells cultured on FITC-Fn/1% gelatin-coated PA gels with different rigidities ("Soft" or "Hard"). Storage moduli reported for PA gels are in kiloPascals (kPa). Yellow arrows point to example invadopodia. **C, E, G.** Quantification of invadopodia degradation area/cell. **D, F, H.** Number of F-actin/cortactin dual staining invadopodia associated with ECM degradation ("Functional Invadopodia") per cell. Data are represented as mean +/- SEM. * indicates p value < 0.05, ns = not significant. Scale bars = 10 μm. (A-D performed by Nelson Alexander)

Myosin II Contractility is Required for Invadopodia Functionality

Because cells sense the rigidity of the surrounding environment via integrin-actomyosin interactions at the cell surface, we then wanted to test the role of MyoII contractility in invadopodia activity. Therefore, we treated CA1d cells in a dose-dependent manner up to 25 μM with the specific MyoII inhibitor blebbistatin (Straight *et al.*, 2003), an inhibitor of the upstream activator of MyoII, myosin light chain kinase (MLCK) (ML-7) (Saitoh *et al.*, 1987; Vicente-Manzanares *et al.*, 2009), or an inhibitor of Rho-associated kinase (ROCK, Y-27632) (Uehata *et al.*, 1997), which can act upstream of MyoII through a variety of pathways (Vicente-Manzanares *et al.*, 2009). In all three cases, there was a significant dose-dependent decrease in degradation area per cell (Fig. 4A-B). Interestingly, the proportion of functional to total invadopodia was decreased with blebbistatin or ML-7 treatment (Fig. 4C). In fact, in blebbistatin treated cells, the total number of invadopodia increased while the functional invadopodia decreased (Fig. 4C). Confocal Z-analysis revealed that, in comparison to control DMSO, blebbistatin treated cells formed a large number of actin puncta that were not protrusive or degradative into the ECM (Fig. 4D-E). These actin puncta could represent early invadopodia precursors. This suggests that MyoII contractility in response to substrate rigidity specifically induces the maturation of invadopodia rather than their formation.

Immunofluorescence studies were then performed to determine the localization of MyoII in relation to invadopodia. Although MyoII was important in invadopodia function, no localization of MyoIIA, IIB, or phospho-MLC was

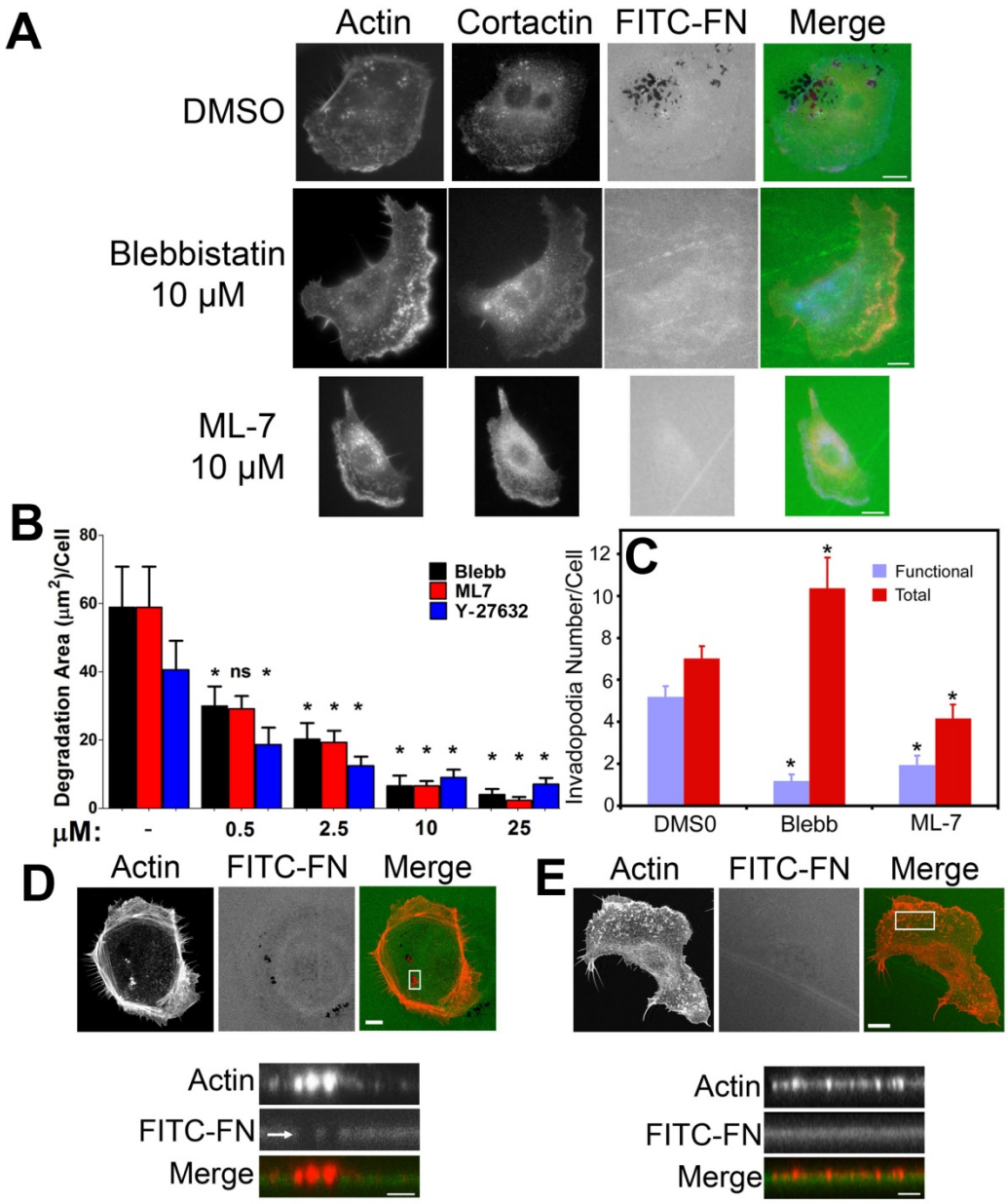

Figure 4. Inhibition of Myosin II activity eliminates invadopodia-associated ECM degradation. A. Images of CA1d cells treated with the myosin inhibitor blebbistatin, the MLCK inhibitor ML-7, and the Rho-associated kinase inhibitor Y-27632 after plating on FITC-FN/2.5% gelatin on glass coverslips. **B.** Quantification of the dose dependent inhibition of ECM degradation area/cell following treatment with the indicated doses of blebbistatin or ML-7. **C.** Quantification of the number of total invadopodia (all cortactin/actin-positive puncta) and functional invadopodia (cortactin/actin-positive puncta colocalized with FITC-Fn degradation) in cells treated with 10 µM blebbistatin or ML-7. * $p < 0.05$, compared with DMSO-treated cells. Data from B and C are represented as mean+/-SE. **D.** Confocal image of control cell with invadopodia degrading FITC-FN/gelatin. **E.** Confocal image of a cell treated with 10 µM blebbistatin. For D & E, the cell areas within the white boxes were further imaged using Z-section analysis. Scale bars are 10 µm for A. and 2 µm for D. & E. (Performed by Nelson Alexander)

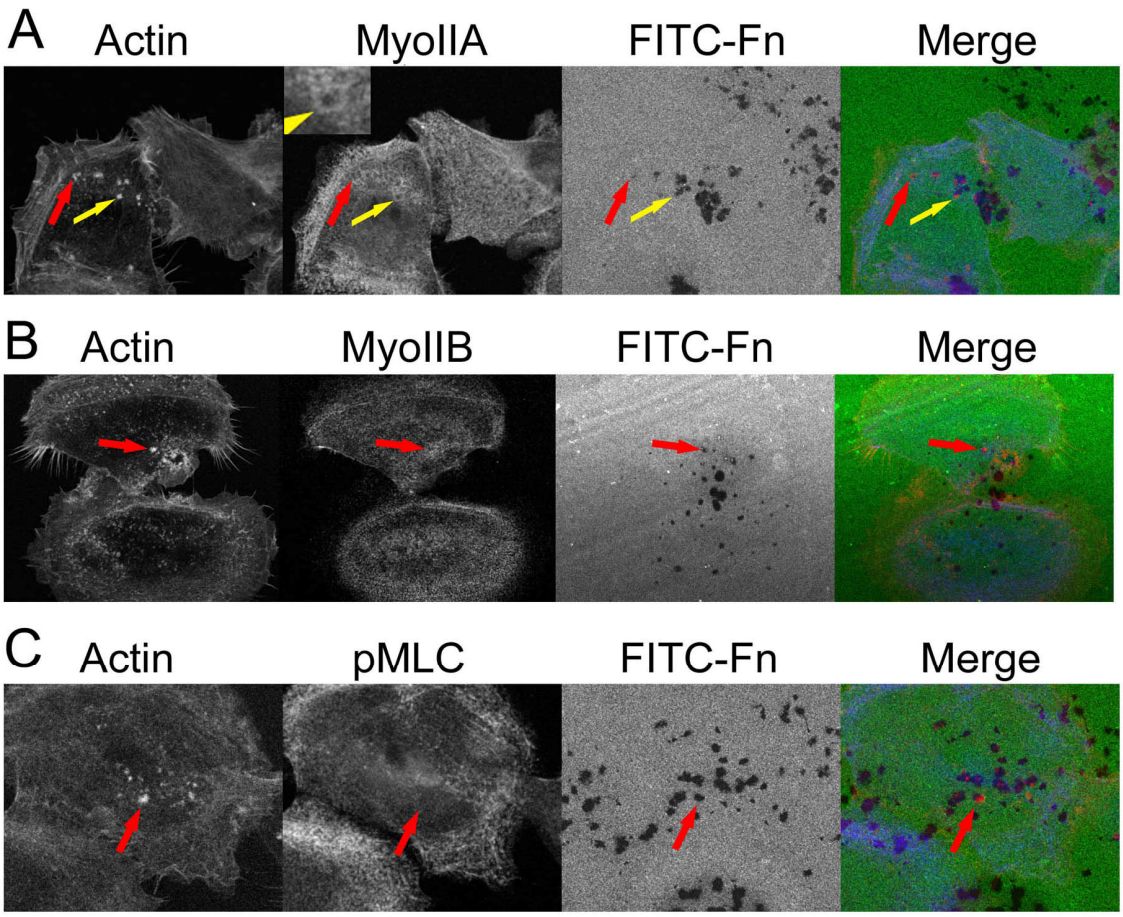

Figure 5. The contractile proteins myosin IIA, IIB, and pMLC do not localize to invadopodia. A. Confocal immunofluorescent localization of actin filaments (Actin, red in merges) and myosin IIA (MyoIIA, blue in merge) in CA1d cells. Degradative invadopodia are identified by co-localization with dark areas of degradation in FITC-FN (green in merges) images. **B.** Immunolocalization of myosin IIB (MyoIIB, blue in merge) in CA1d cells. **C.** Immunolocalization of phosphomyosin light chain (pMLC, blue in merge) in CA1d cells. Red arrows demonstrate lack of co-localization of MyoIIA, IIB, and pMLC with actin-containing invadopodia. Yellow arrow points out ring structure of MyoIIA surrounding actin-containing invadopodia. Zoom in MyoIIA highlights this ring structure. All cells plated on FITC-FN overlying 2.5% gelatin.

observed at the invadopodia puncta (Fig. 5). In fact, there was a noticeable lack of immunofluorescence for all three proteins at the puncta. Interestingly, ~40% of the cells with invadopodia presented with rings of MyoIIA immunostaining surrounding at least one invadopodium (Fig. 5A, yellow arrow, zoom), while MyoIIB or pMLC did not demonstrate this localization (Fig. 5B-C, red arrows). This localization is reminiscent of rings of adhesion proteins that form surrounding the actin cores of podosomes (Marchisio *et al.*, 1984; Marchisio *et al.*, 1987) and suggests a possible localization of MyoII contraction to affect invadopodia function. Regardless, MyoII contraction does not occur at the invadopodia puncta itself, but can still affect invadopodia function.

FAK and Cas Prime the Rigidity-related Invadopodia Response

FAK and Cas are proteins known to be involved in transmitting mechanical force signals into cellular responses (Wang *et al.*, 2001; Mofrad *et al.*, 2004; Sawada *et al.*, 2006). Therefore, we first immunostained for phosphorylated forms of FAK and Cas, specifically phospho-Y397FAK and phospho-Y165Cas, since each of these sites exhibits increased phosphorylation in response to mechanical force (Paszek *et al.*, 2005; Sawada *et al.*, 2006). Both pY397 FAK and pY165Cas localized at the actin puncta of the invadopodia as well as at FA (Fig. 6A-B). Each phospho-protein localized throughout the invadopodial protrusion by confocal Z-stack analysis (Fig. 6A-B). Furthermore, immunofluorescence with antibodies against total FAK or Cas also showed localization of these proteins at invadopodia, although this localization was

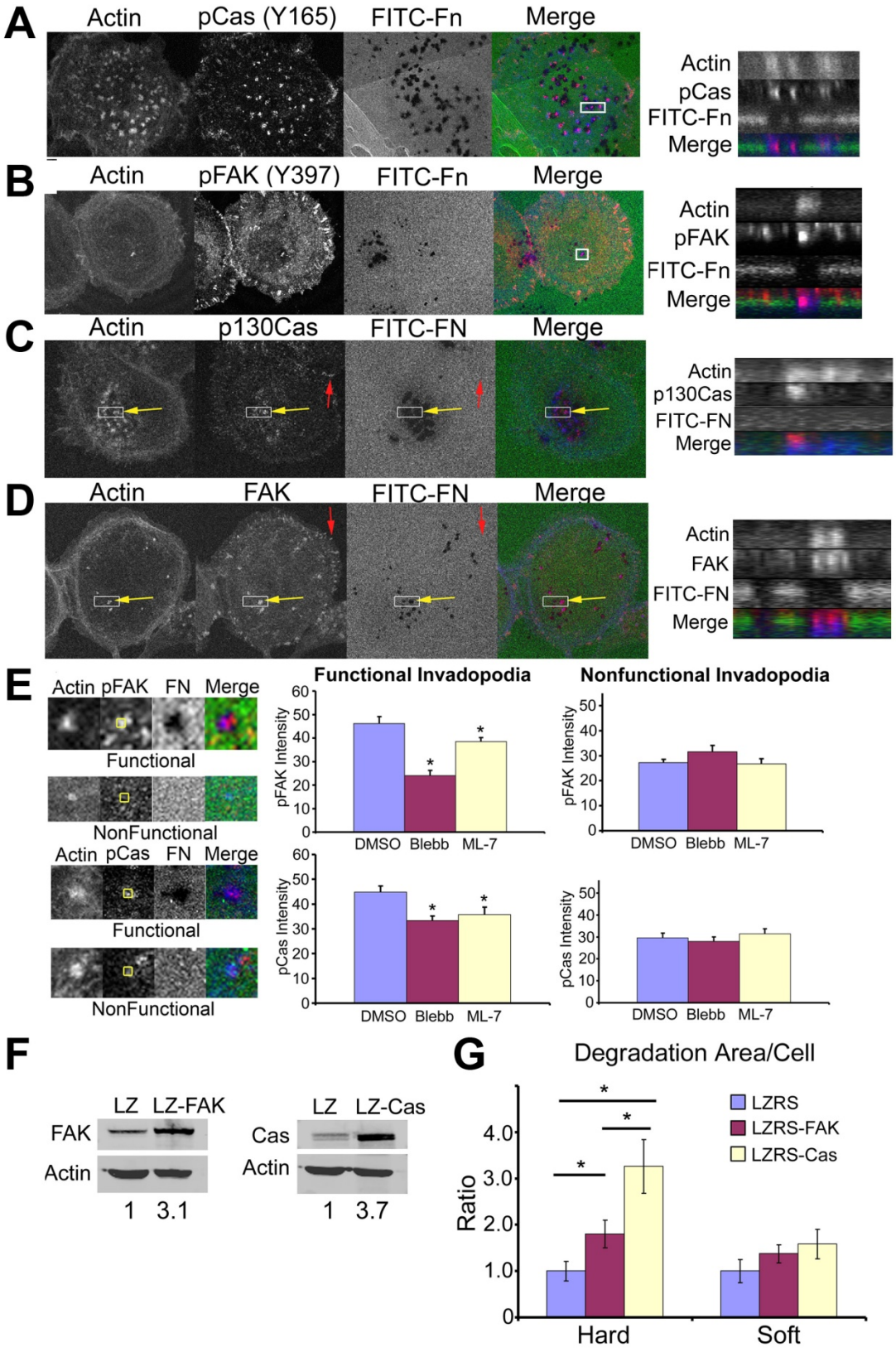

Figure 6. Figure legend on next page.

Figure 6. The mechanosensing signaling proteins FAK and p130Cas localize to and regulate invadopodia. A-D. Confocal immunofluorescent localization of actin filaments (Actin, blue in merges) and **(A)** phospho-p130cas (Y165), **(B)** phosphorylated FAK (Y397), **(C)** total p130cas, or **(D)** total FAK to invadopodia (all red in merges). ECM degradation is evident as dark areas on the FITC-fibronectin image (FITC-FN, green in merges). White boxes in the merged images indicate areas analyzed in the Z-sections. **E.** Quantitation of phosphoFAK (Y397, "pFAK") and phosphoCas (Y165, "pCas") was performed by measuring absolute intensity of antibody stainings in a 4x4 pixel box (yellow boxes in zoomed images show examples) placed in the center of invadopodia, as defined by punctate actin staining. Functional invadopodia were defined to have associated ECM degradation, whereas nonfunctional did not. For A-E, cells were plated on FITC-Fn overlying 2.5% gelatin. * indicates $p<0.05$ vs. DMSO control. **F.** Western blot of total cell lysates from CA1d cells transduced with LZRS-MS-FAK or -p130Cas. Protein level of each is increased 3.1- or 3.7-fold, respectively, compared to LZRS only control. **G.** Degradation area per cell was measured on Hard or Soft PA gels coated with 1% gelatin/TRITC- or FITC-Fn. Results are presented as the ratio of degradation area/cell for FAK- or Cas-overexpressing cells compared with LZRS controls. Asterisks indicate $p<0.05$ vs. LZRS only control. Statistical significance was calculated from raw data. Error bars were converted: [raw data SEM/raw data mean] x ratio difference. Scale bar = 10 μm. (G performed by Aron Parekh)

sometimes weaker at the invadopodia and also occasionally surrounded the puncta instead (Fig. 6C-D, yellow arrows). These proteins clearly localize at invadopodial structures distinct from classic FA which do not localize with degradation of the FITC-FN matrix (Fig. 6C-D, red arrows).

We hypothesized that these phosphorylation events on FAK and Cas occurred downstream of substrate rigidity sensing dependent on MyoII contractility. Therefore, we measured the intensity of pY397 FAK or pY165 Cas immunostaining specifically at functional and non-functional invadopodia with blebbistatin or ML-7 treatment to inhibit MyoII contractility (Fig. 6E). Interestingly, in the control DMSO condition, functional invadopodia exhibited a higher intensity of both pY397 FAK and pY165 Cas staining compared to non-functional invadopodia, suggesting a role for these phosphorylation events in the maturation of an invadopodium (Fig. 6E). Inhibition of MyoII contractility also decreased the fluorescent intensity of pY165 Cas and pY397 FAK at invadopodia, specifically at those few invadopodia that degraded the underlying matrix with MyoII inhibition (Fig. 6E). Meanwhile, no significant change was observed at non-functional invadopodia, although this may be due to the low levels of localization already observed at non-functional invadopodia without drug treatment (Fig. 6E).

To further test the roles of FAK and Cas in the invadopodia response to mechanical signals, we over-expressed (OE) each protein 3-4 fold in the CA1d cells (Fig. 6F). These cells were then cultured overnight on the soft and hard PA gels with fluorescent matrix to assess invadopodia activity. Interestingly, OE of

either protein only slightly increased the amount of degradation underneath the cells cultured on the soft PA gels (Fig. 6G). However, increased FAK or Cas expression each increased the amount of degradation area per cell on the hard PA gels, with Cas OE having a greater effect, perhaps due to increased protein levels compared to FAK OE (Fig. 6G). These data suggest that the mechanosensing proteins FAK and Cas play a role in the invadopodia response to rigidity.

Discussion

These results indicate that cellular degradation of the ECM is regulated by the physics of the surrounding environment. Because MyoII does not localize to the invadopodial protrusion, rigidity sensing does not appear to occur there. However, a subset of invadopodia exhibit MyoIIA ring localization surrounding the invadopodia puncta. This MyoII could represent a structure that can transmit ECM rigidity responses resulting in a local increase in invadopodia function. Contractile forces can also be transmitted long distances across the cell via cellular actin fibers attached to FA. In fact, activation of Src kinase occurs locally and at distal areas of the cell in response to forces applied to a FN-coated bead attached to the cell, dependent on intact microtubules and actin filaments (Wang *et al.*, 2005). Therefore, FAK or Cas may be activated at invadopodia via whole-cell, distant, or local rigidity sensing. Alternatively, FAK or Cas may be activated elsewhere and transported to the invadopodia site to promote maturation.

In many cell types, FA are regarded as the primary mechanosensing sites

where actin fibers connect to integrin-ECM adhesions via a myriad of signaling and scaffolding proteins such as talin, vinculin, paxillin, Src kinase, FAK, and Cas (Katsumi *et al.*, 2004). Meanwhile, normal cells that traverse ECM or cell monolayers as part of their normal function use podosomes as a primary adhesive structure that also degrades underlying matrix (Gaidano *et al.*, 1990; Burns *et al.*, 2001; Hai *et al.*, 2002; Moreau *et al.*, 2003). Podosomes exhibit a well-characterized adhesion ring surrounding the actin core and podosome dynamics are altered by substrate rigidity as well (Collin *et al.*, 2006). In fact, podosomes were recently demonstrated to be mechanosensors themselves (Collin *et al.*, 2008). While invadopodia and podosomes share many components, the role of adhesion proteins in invadopodia activity is not well characterized (Mueller & Chen, 1991; Bowden *et al.*, 1999; Deryugina *et al.*, 2001). Interestingly, Cas is required for invadosome formation, Matrigel invasion, and lung metastasis in Src-transformed fibroblasts (Brabek *et al.*, 2004; Brabek *et al.*, 2005). The Cas substrate domain tyrosines, which are increasingly phosphorylated in response to stretch (Sawada *et al.*, 2006), are required for these Src-induced phenotypes (Brabek *et al.*, 2005). FAK has long been linked to invasive phenotypes in cancer (Weiner *et al.*, 1993; Owens *et al.*, 1995) and may play a role in cellular invasion downstream of active Src (Hauck *et al.*, 2002). We demonstrate a role for FAK in transmitting rigidity signals for increased invadopodia function. However, the role of FAK at invadopodia has since been controversial. FAK knockdown or inhibition of phosphorylation at Y397 increases invadopodia formation and activity on glass coverslips coated with gelatin and

FN, presumably by releasing Src from FA to create more invadopodia (Chan *et al.*, 2009; Liu *et al.*, 2009b). FAK has also been shown to weakly or possibly only transiently localize to invadopodia (Bowden *et al.*, 2006). Therefore, FAK may play differing roles in invadopodia activity dependent on substrate rigidity. Because FAK and Cas OE can enhance the rigidity-induced invadopodia response and phosphorylation of FAK and Cas at invadopodia is affected by MyoII inhibition, rigidity signals from the ECM may be an important input to these mechanosensing proteins to promote invasion. Other FA proteins, such as talin, vinculin, and integrins themselves, are affected by tension or ECM rigidity at FAs (del Rio *et al.*, 2009; Friedland *et al.*, 2009; Kong *et al.*, 2009; Pasapera *et al.*, 2010). Therefore, it is likely that other proteins also regulate cellular invasion in response to physical signals.

Many cancer phenotypes are regulated by the physical cues in the surrounding environment. Increased mammographic density is a risk factor for tumor incidence and aggressiveness (Boyd *et al.*, 2005; Gill *et al.*, 2006). Increased collagen deposition in the tumor microenvironment leads to increases in local stiffness and enhanced tumor invasion (Li *et al.*, 2005; Provenzano *et al.*, 2008a). These data provide a novel mechanism for increased degradation of the ECM and a potential cellular mechanism for these observed cancer phenotypes.

CHAPTER IV

ADHESION RINGS SURROUND INVADOPODIA AND PROMOTE MATURATION

Introduction

An increasing number of studies demonstrate that deregulated cell-ECM signaling promotes multiple phases of tumor progression from initiation to metastasis (Stewart *et al.*, 2004; Lahlou & Muller, 2011). A key step in the progress of a tumor to metastasis that is driven by ECM attachment is cancer cell invasion, which involves regulation of cell motility and degradation of the ECM (Guo & Giancotti, 2004). ECM degradation is especially important, as cells cannot cross the highly cross-linked BM that surrounds the primary tumor without degradation and remodeling (Hotary *et al.*, 2006; Parekh & Weaver, 2009).

Invadopodia are key cellular processes that can carry out this degradation of ECM and further protrude and invade the degraded areas (Chen, 1989; Schoumacher *et al.*, 2010). Membrane-tethered (MT) proteases are critical for invasion through BM (Hotary *et al.*, 2006; Rowe & Weiss, 2008). MT1-MMP is a MT protease critical for invadopodia activity (Nakahara *et al.*, 1997; Sabeh *et al.*, 2004). Live cell imaging demonstrates a rapid localization of MT1-MMP to invadopodia shortly after invadopodia formation (Artym *et al.*, 2006; Artym *et al.*, 2009). Recent studies have shed light on polarized delivery mechanisms leading to MT1-MMP localization to invadopodia (Poincloux *et al.*, 2009). MT1-MMP is

trafficked from a late endocytic/lysosomal compartment dependent on the vesicular SNARE VAMP7, the scaffold protein IQGAP, and the exocyst complex (Sakurai-Yageta *et al.*, 2008; Steffen *et al.*, 2008; Hoshino *et al.*, 2012).

In the previous chapter, I demonstrated that the chemical composition and physical rigidity of the ECM regulate the activity of invadopodia. I also implicated MyoII contractility in the maturation of invadopodia. Meanwhile, integrins and downstream signaling proteins have been shown to either promote or disrupt invadopodia formation (Nakahara *et al.*, 1998; Chan *et al.*, 2009; Liu *et al.*, 2009b). The formation or stability of invadosomes in Src-transformed cells is affected by integrin blocking as well (Badowski *et al.*, 2008; Destaing *et al.*, 2010). Alternatively, integrin attachment to ECM proteins also promotes MT1-MMP trafficking directly to the attachment site (Galvez *et al.*, 2002; Bravo-Cordero *et al.*, 2007), and integrins have been suggested to play a role in protease docking at invadopodia (Mueller *et al.*, 1999). We and others have observed adhesion protein localization, including MyoII (Figure 5), FAK (Figure 6), RhoC (Bravo-Cordero *et al.*, 2011), and α5 integrin (Mueller *et al.*, 1999) at or surrounding invadopodia, similar to structures seen in podosomes (Linder & Aepfelbacher, 2003; Gimona *et al.*, 2008). However, the presence of adhesion proteins at or around invadopodia remains controversial and this localization is suggested to be a defining difference between invadopodia and podosomes (Linder *et al.*, 2011; Murphy & Courtneidge, 2011). Unlike podosomes in normal cells, cancer cells also interact with the ECM via FA that may compete with invadopodia for signaling proteins (Chan *et al.*, 2009) or transmit signals from a

distance to affect invadopodia formation and function (Wang *et al.*, 2005). Therefore, whether invadopodia act as adhesive structures is unclear and the role of integrin-ECM adhesion in invadopodia progression remains to be seen. This chapter will describe the characterization of invadopodia as adhesion structures and the role of a subset of integrins and downstream signaling proteins in invadopodia maturation.

Results

Podosome-like Adhesion Rings Surround Invadopodia and Correlate with Their Activity

FAs are important mechanosensing structures in the cell and Chapter III demonstrates that invadopodia activity is promoted by extracellular rigidity. However, invadopodia have been shown to compete with FAs for components (Chan *et al.*, 2009). Therefore, I characterized the invadopodia and adhesion phenotypes in CA1d breast cancer and SCC61 HNSCC cells cultured on soft and hard PA gels as well as 1% gelatin/FITC-FN on a glass coverslip, which represents an extreme rigidity not seen physiologically (69 GPa vs 10-30 GPa for bone) (Callister, 2000; Nemir & West, 2009; Moore *et al.*, 2010) in order to compare FA phenotypes with invadopodia characteristics. Immunostaining revealed paxillin or vinculin localization surrounding cortactin- or actin-containing invadopodia in adhesion rings similar to those around podosome actin core subunits, along with localization of these proteins at classical FAs (Fig. 7). Other

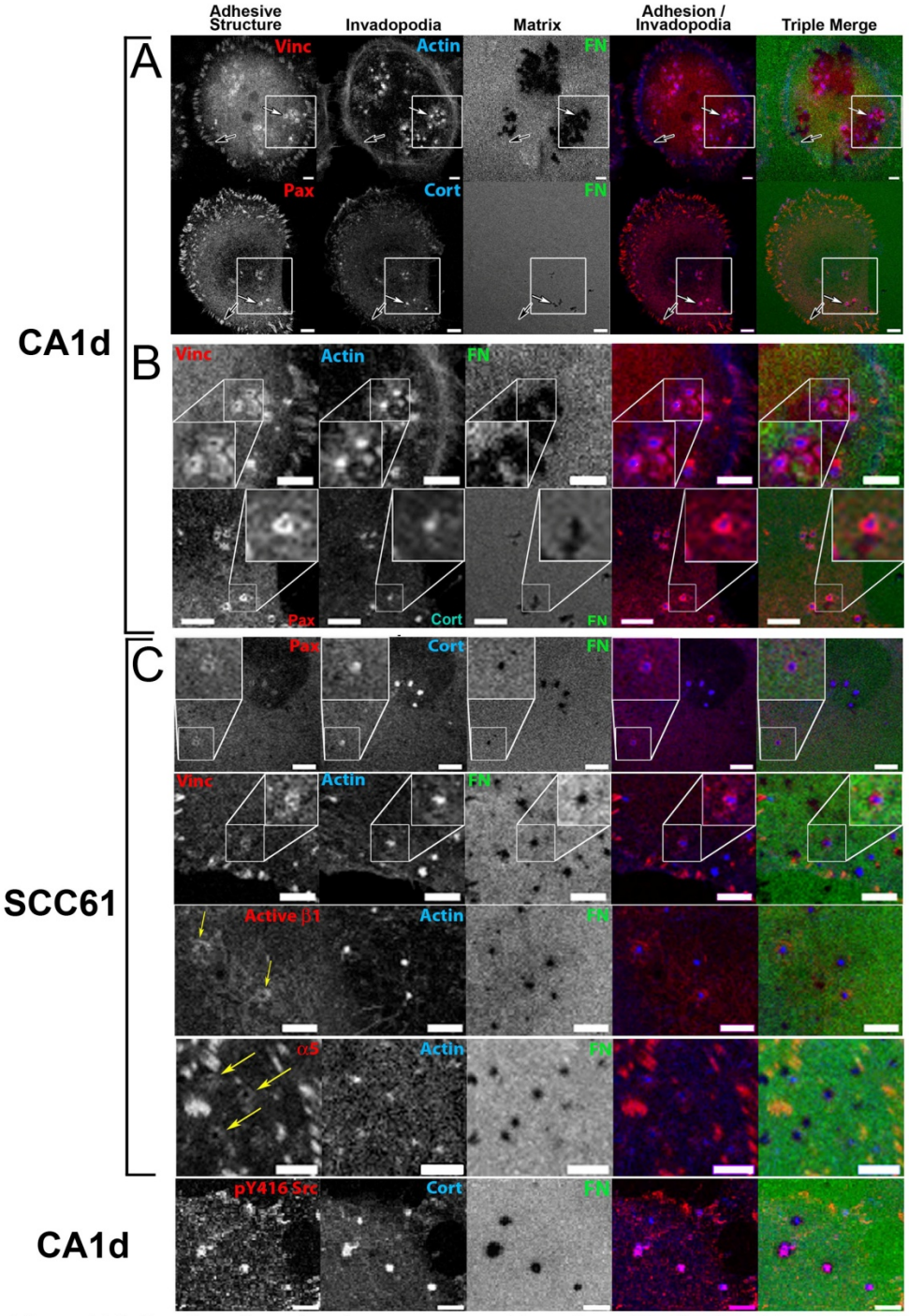

Figure 7. Adhesion ring structures surround invadopodia. Confocal images of CA1d or SCC61 cells cultured on 1% gelatin/FITC-FN coated glass coverslips (Matrix, green in triple merge) and immunostained with antibodies against paxillin (Pax), vinculin (Vinc), active β1 integrin (Active β1), or active Src (pY416 Src) or transfected with GFP-α5 integrin (α5) to visualize adhesion structures (Adhesive Structure, red in merges). Cells were also immunostained for cortactin (Cort) or with fluorescent phalloidin (Actin), or stably expressing mCherry-Lifeact (Actin in α5 row) to visualize invadopodia (blue in merges). White boxes in A represent zoomed area in B. White/yellow arrows designate adhesion rings around invadopodia, black arrows represent focal adhesions.. Scale bars = 5μm

adhesion proteins including α5 and active β1 integrin also localized around the invadopodium protrusion, while active pY416 Src localized at the cortactin puncta (Fig. 7C).

In order to better understand the relationship between adhesion rings, FA, and invadopodia activity, we performed a correlative analysis of invadopodia-associated ECM degradation with the number of adhesion-ringed invadopodia or FA. To provide a richer dataset for analysis and because we previously found that cells modulate invadopodia activity according to substrate rigidity, we chose 3 rigidity conditions for the analysis and cultured CA1d or SCC61 cells on FITC-FN/1% gelatin overlaying polyacrylamide (PA) or glass invadopodia substrates of defined rigidity (Soft PA=1 kPa, Hard PA=10 kPa, glass=1 GPa) as previously described (Alexander *et al.*, 2008; Parekh *et al.*, 2011). After 18 h, the cultures were fixed and immunostained for cortactin and paxillin. Cortactin-positive invadopodia puncta have a characteristic morphology and size ≥1 μm (Clark *et al.*, 2007a), and were analyzed for association with ECM degradation and number per cell. FA number and size were analyzed from paxillin-positive structures at the periphery of the cell, and invadopodia-associated adhesion rings were identified manually. Overall, analysis across all conditions revealed that a higher percentage of adhesion-ringed invadopodia puncta were associated with degraded ECM than were non-ringed invadopodia (Fig. 8A), suggesting that adhesion rings may promote invadopodia-associated degradation. We also correlated the number of FA and invadopodia ring structures per cell with the amount of degradation per cell. Interestingly, the number of paxillin-ringed

invadopodia peaked on the same rigidity that elicited the highest invadopodia activity per cell, on the hard PA gel for the CA1d cells and on the glass surface for the SCC61 cells (Fig. 8B-C). Using a Spearman's rank correlation to test the statistical dependence between two variables, we found that the number of adhesion-ringed invadopodia per cell significantly and positively correlated with ECM degradation area/cell on a cell-by-cell basis (Fig. 8D). The number of non-adhesion-ringed invadopodia also significantly correlated with ECM degradation/cell but to a lesser extent than adhesion-ringed invadopodia. By contrast, except for SCC61 cells plated on glass substrates, neither the number nor size of FA correlated with the degradation area/cell on a cell-by-cell basis (Fig. 8D, 9). Altogether, these correlative data indicate that adhesion ringed-invadopodia are highly associated with ECM degradation.

Adhesion Rings form Shortly After Invadopodia Formation

Because SCC61 cells on the glass surface formed the most adhesion ringed-invadopodia and degraded the most ECM, this condition was used to test the roles of adhesion rings in invadopodia function. Invadopodia have been shown to develop in a step-wise process, with cortactin and actin accumulation rapidly followed by MT1-MMP arrival and degradation of the underlying ECM (Artym *et al.*, 2006). In VSMCs, rings surrounding podosomes form shortly after punctate localization of an actin marker (Kaverina *et al.*, 2003). However, the dynamics of adhesion formation at invadopodia is not clear. The adhesion proteins could assemble prior to the actin accumulation to promote invadopodia formation at that site, or after actin accumulation to stabilize the protrusion into

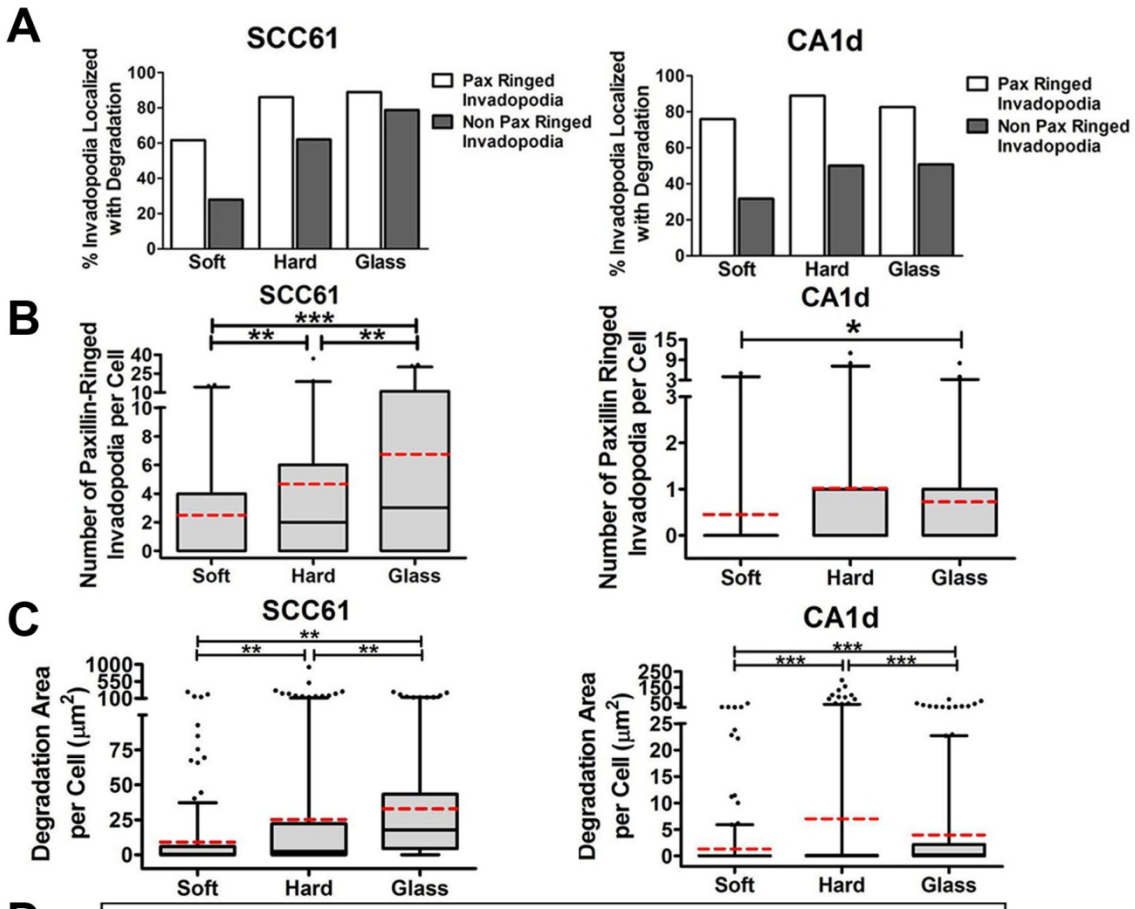

D

Spearman Correlation with Degradation Area per Cell				
Conditions	**Number of ringed-invadopodia per cell**	**Number of non-ringed-invadopodia per cell**	**Number of focal adhesions per cell**	**Average focal adhesion area per cell**
CA1d Soft PA	0.3593***	0.3653***	-0.0591	0.03277
CA1d Hard PA	0.6214***	0.2885**	-0.1533	0.1639
CA1d Glass	0.527***	0.2743**	-0.1196	0.1456
SCC61 Soft PA	0.3735***	0.2475*	-0.03218	0.1434
SCC61 Hard PA	0.4751***	0.3167**	0.1329	-0.08346
SCC61 Glass	0.5285***	0.4372***	0.3632**	0.2049

Figure 8. Invadopodia adhesion rings strongly correlate with degradation of ECM. A-B. Percent **(A)** or number **(B)** of paxillin-ringed or non-ringed invadopodia associated with or without degradation on soft or hard PA gels, or glass coverslips coated with 1% gelatin/FITC-FN, as indicated in SCC61 and CA1d cells. **C.** Degradation area per cell measured as area of dark holes in FITC-FN matrix underneath cells. **D.** Spearman correlations comparing degradation area per cell with invadopodia or FA characteristics from A-B & Fig. 9. Data presented as box and whisker plots indicating 25-75th and 5-95th percentiles with the red dotted line indicating the mean and the black line indicating the median. *p<0.05, **p<0.01, ***p<0.001 vs indicated comparison.

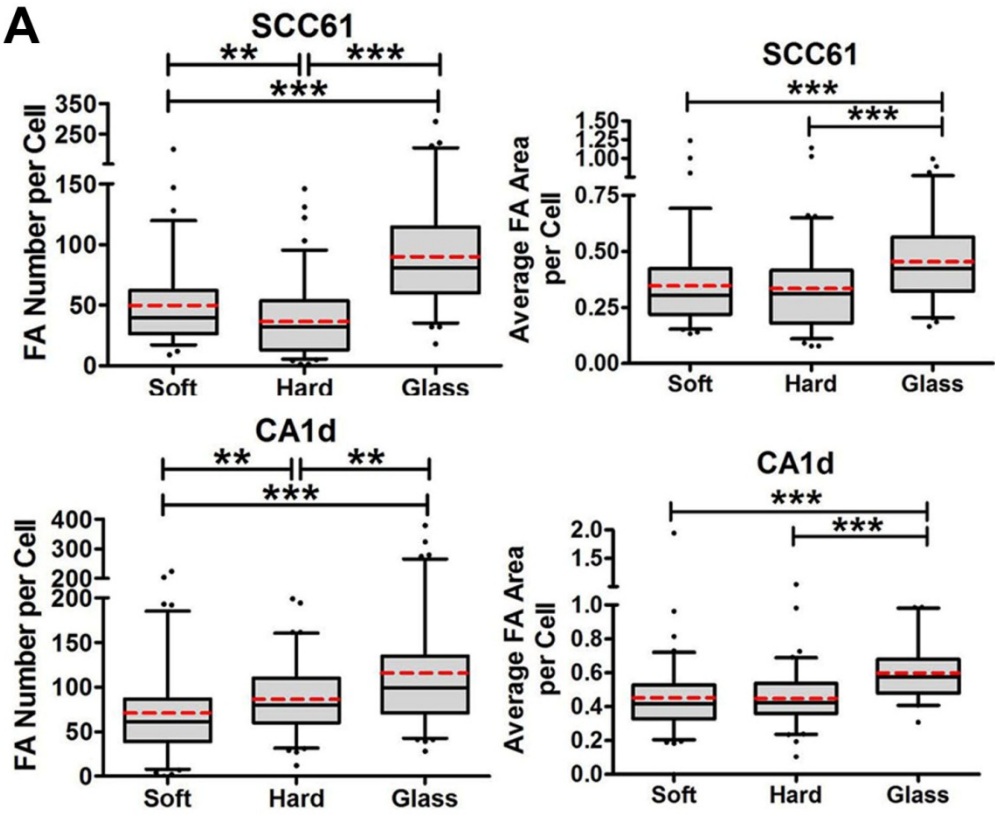

Figure 9. Focal adhesion characteristics do not correlate with degradation area per cell. Quantification of focal adhesion characteristics on a per cell basis in SCC61 and CA1d cells. Box and whiskers indicate respectively the 25-75th and 5-95th percentiles with the dotted red line indicating the mean and the black line indicating the median. *p<0.05, **p<0.01, ***p<0.001 vs. indicated comparison

the matrix and/or facilitate the delivery of MMPs. To this end, SCC61 cells expressing Tom-Tract to mark actin as well as GFP-Paxillin were cultured on 1% gelatin/unlabeled FN on glass coverslips and serum starved overnight. Directly before imaging, complete invadopodia media was added to stimulate invadopodia formation. The basal surface of the cells was then imaged with confocal microscopy with images acquired every 15 seconds for 1 hour (Fig. 10A). In general, adhesion rings formed quickly after appearance of the actin puncta with a mean of 2.6 minutes and median of 2 minutes after formation of the invadopodium (Fig. 10B). In addition, ~90% of invadopodia formed in the 1 hour movies developed an adhesion ring (Fig. 10C). As previously observed (Bravo-Cordero *et al.*, 2011), I also recorded oscillations of the actin signal at invadopodia. The GFP-Paxillin ring also oscillated in intensity similarly to the actin, although its recovery was slightly delayed compared to the reappearance of the actin puncta (Fig. 10D). Occasionally, adhesion rings did not recover with the actin or did not appear at all during the hour of time-lapse imaging, which may explain the lower percentage of adhesion ringed invadopodia observed in fixed cell analyses (Fig. 10E). These data indicate that adhesion rings form after invadopodia formation.

Integrin-ECM Interactions are Critical for Adhesion Ring Formation and Invadopodial ECM Degradation

To test the role of integrins in invadopodia formation, adhesion ring formation, and invadopodia activity, SCC61 cells were incubated with an RGD peptide

(gRGDsp) which blocks the RGD-binding integrins from binding their ligands (Hayman *et al.*, 1985), or with a combination of β1- and αvβ3 integrin blocking antibodies (AIIB2 + LM609) (Cheresh, 1987; Hall *et al.*, 1990). These integrin targets were chosen based on the ECM substrate in the invadopodia assay (FN) and their described roles in invadosome or podosome activity (Nakamura *et al.*, 2007; Destaing *et al.*, 2010). The cells were incubated on FITC-FN to quantify matrix degradation and immunostained with cortactin to mark invadopodia and paxillin to mark adhesion structures (Fig. 11A). Compared with gRGEsp or IgG antibody controls, inhibition of RGD-binding or β1 and αVβ3 integrins attachment to FN reduced the median area of ECM degradation/cell from 4 to 1.4 μm^2 and 6.4 to 3.1 μm^2, respectively (Fig. 11B, D). The latter effect was specific to β1 integrin blocking, as αVβ3 inhibitory antibody treatment did not significantly affect ECM degradation by the cells (Fig. 11F-G). The immunostaining for cortactin and paxillin was utilized to quantify the number of cortactin-positive invadopodia puncta ("Total"), the number of invadopodia surrounded by paxillin-containing adhesion rings ("Ringed"), and whether or not cortactin puncta had associated ECM degradation ("Active" or "Inactive"). Although it is possible that some of the "Inactive" invadopodia may represent other cortactin-positive structures, the size criteria of ≥1 μm diameter minimizes this possibility and use of this metric allows analysis of invadopodia maturation. Furthermore, we complement such analyses with live cell imaging (next paragraph). Integrin inhibition with gRGDsp or combined AIIB2 and LM609 treatment resulted in a significant reduction in the number of invadopodia with surrounding paxillin rings, while having a lesser

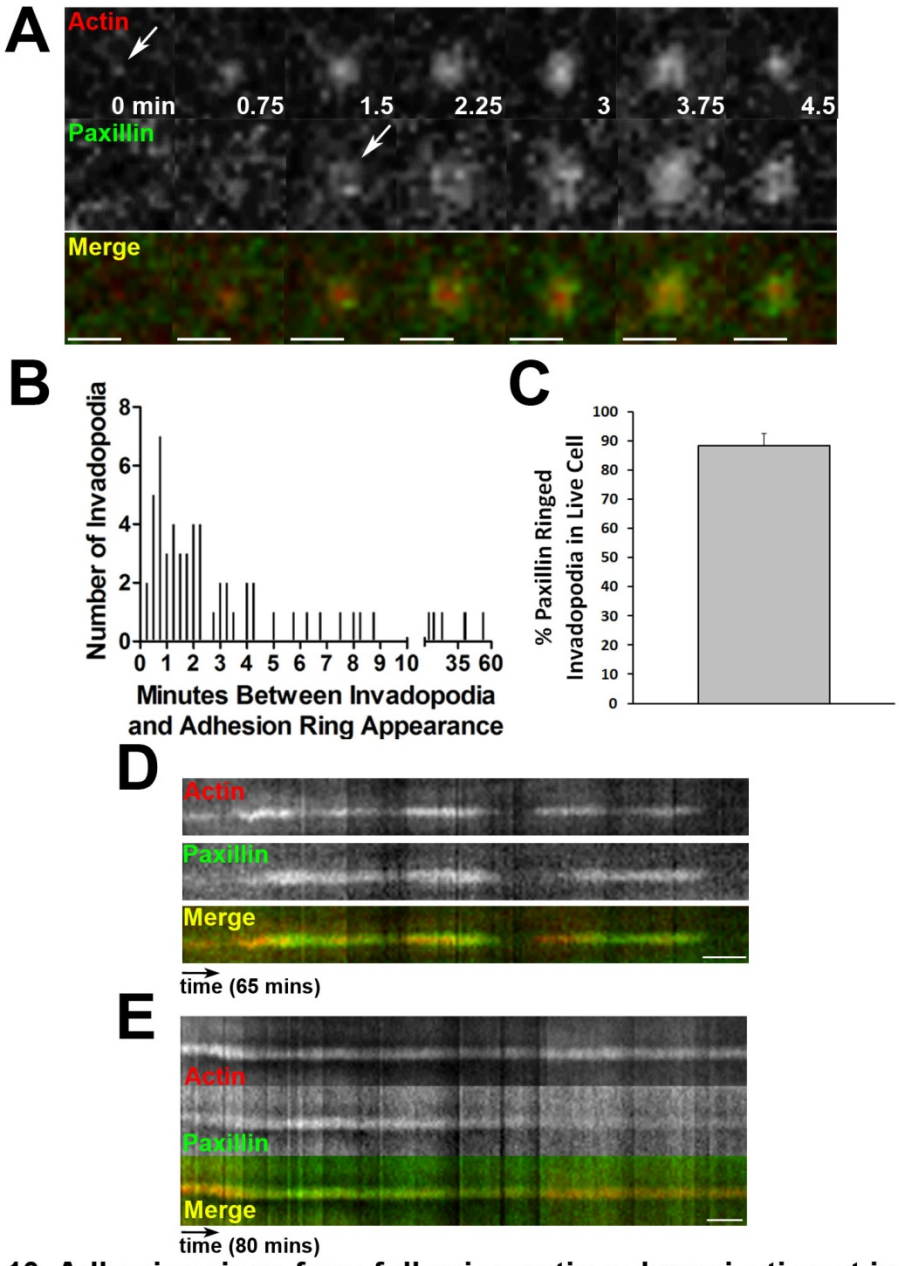

Figure 10. Adhesion rings form following actin polymerization at invadopodia. A. Zoomed images of a single invadopodia over time from time-lapse confocal imaging of SCC61 cells expressing GFP-Paxillin (green in merge) and Tom-Tractin (Actin, red in merge). Scale bar = 3 μm. **B.** Histogram showing the time between actin puncta formation and paxillin adhesion ring formation in live cell images from A. **C.** Quantification of the percentage of invadopodia with GFP-paxillin ring localization at any time during the movie. Data are mean and SEM. **D.** Kymograph showing the lifetime of a typical invadopodia from time-lapse imaging in A. Oscillations occur in both the actin and paxillin signal. **E.** Kymograph representing a subset of invadopodia from time-lapse imaging in A. For these invadopodia, the paxillin ring disappears prior to invadopodia disassembly. Time scale bars for D and E = 5 min.

effect on total invadopodia numbers (Fig. 11C, E). Furthermore, RGD-binding integrin inhibition with these reagents resulted in a significant decrease in the number of active invadopodia from a median of 3 to 1 per cell, while increasing or not affecting the inactive invadopodia per cell (Fig. 11C, E). Overall, these data indicate that integrins significantly contribute to adhesion ring formation and invadopodia-associated ECM degradation.

To directly determine if inhibition of integrins leads to a loss of proteinase recruitment or conversely to alterations in invadopodia dynamics, I performed live cell imaging. To specifically detect extracellular MT1-MMP, SCC61 cells were engineered to stably express low levels of the critical invadopodia protease MT1-MMP tagged with superecliptic-pHLuorin-GFP (MT1-pHLuor). The pHLuorin tag exhibits greatly enhanced fluorescence at the extracellular pH of 7.4 compared to the more acidic intracellular vesicles (Miesenbock *et al.*, 1998; Lizarraga *et al.*, 2009). After transient transfection with Tom-Tractin to visualize invadopodia, dual color widefield images were captured on a Deltavision microscope every 15 seconds and computationally deconvolved to remove out of focus light. From these movies, times of invadopodia formation and disassembly were determined as the IC50 points of the background-subtracted Tom-Tractin fluorescence intensity fit to a sigmoid curve at the initiation or disappearance of the invadopodia. Invadopodia lifetime was calculated as the time between formation and disassembly (Fig. 12C). Invadopodia formation rate was manually calculated as the number of invadopodia/cell/hour (Fig 12A). MT1-MMP recruitment to invadopodia over time was measured as the background-subtracted

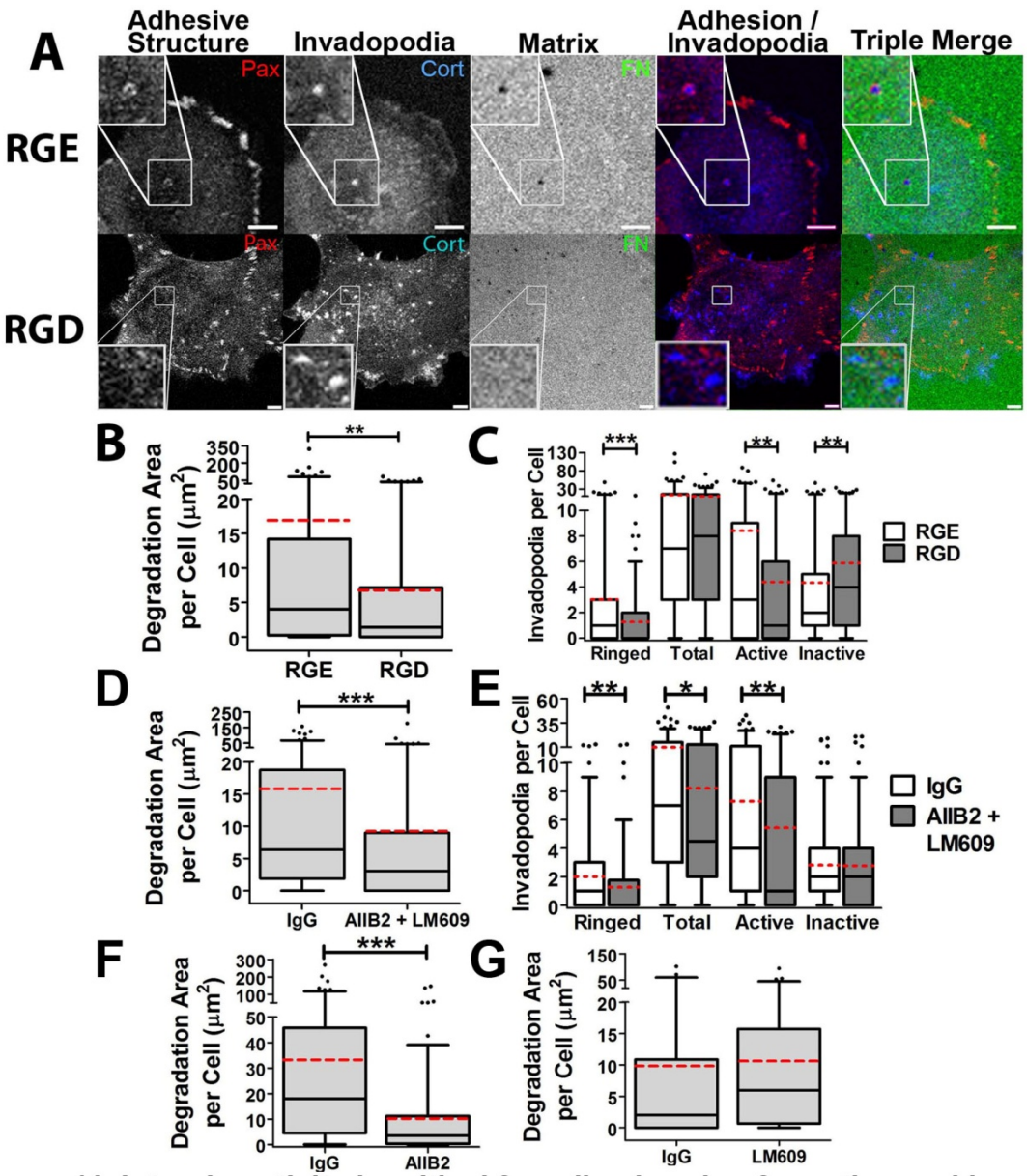

Figure 11. Integrin activity is critical for adhesion ring formation and invadopodia activity. A-C: SCC61 cells were cultured on FITC-FN/1% gelatin (FN, green) and treated with RGD or RGE peptide control (250 μg/ml) overnight then immunostained for paxillin (Pax, red) and cortactin (Cort, blue). **A.** Confocal images. Zooms indicate typical invadopodia for condition. Scale bars = 5 μm. **B.** Quantification of degradation area/cell. **C.** Quantification of the number of paxillin-ringed cortactin-containing invadopodia (Ringed), total cortactin-positive invadopodia (Total), invadopodia localized with degradation of the FITC-FN matrix (Active), and invadopodia localized with intact FITC-FN (Inactive) **D-G.** SCC61 cells cultured as above treated with 10μg/ml AIIB2 + 10 μg/ml LM609 **(D-E)** or either alone **(F-G)**. **D, F-G.** Quantification of degradation area/cell. **E.** Quantification of invadopodia numbers as in B. n ≥ 60 cells per condition from ≥3 independent experiments. *p<0.05, **p<0.01, ***p<0.001 vs. indicated comparison

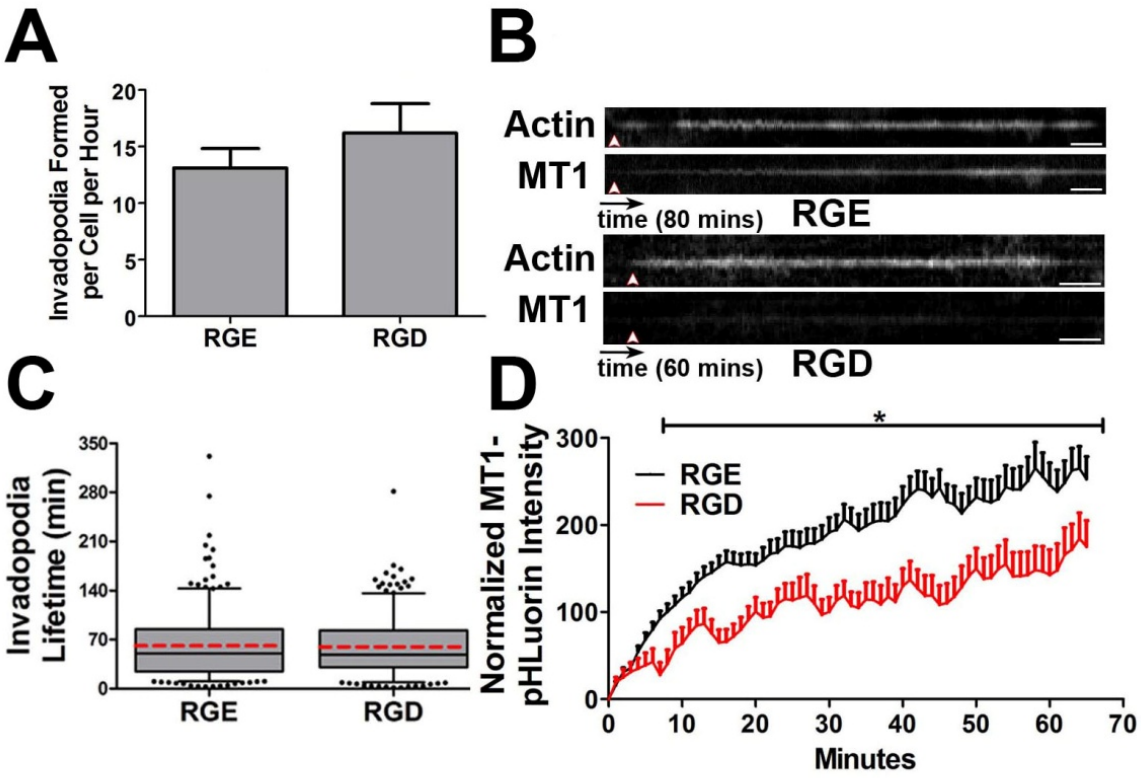

Figure 12. Integrin activity regulates MT1-MMP recruitment to invadopodia. A. Quantification of invadopodia formation rate. **B.** Representative kymographs of live-cell imaging of SCC61 cells expressing Tom-Tractin (Actin), to mark invadopodia, and MT1-MMP-pHLuorin (MT1), to mark extracellular MT1-MMP accumulation in invadopodia. Arrowheads indicate invadopodia formation time. Time scale bar = 5 min. **C.** Invadopodia lifetime. **D.** Quantification of MT1 accumulation at invadopodia over time, in which time zero is the appearance of the invadopodia and MT1 intensity at each time point is subtracted by the intensity at time zero. n ≥ 11 cells, ≥ 300 invadopodia per condition from ≥ 3 independent experiments. For A, error bars indicate SEM. For C, box and whiskers show respectively the 25-75th and 5-95th percentiles with the dotted red line indicating the mean and the black line indicating the median. *p < 0.05 for RGD vs. RGE at each time point.

fluorescence intensity of MT1-pHLuor at each time point subtracted from the initial fluorescence intensity at the time of invadopodia formation (Fig. 12D). Using this approach, we found that inhibition of RGD-binding integrins with gRGDsp had no significant effect on the rate of invadopodia formation or on invadopodia lifetime compared to treatment with control gRGEsp peptide (Fig. 12A, C). However, there was a significant reduction in the accumulation of MT1-MMP at invadopodia (Fig. 12B, D). Thus, in control gRGEsp-treated cells, the MT1-MMP signal at Tom-Tractin-positive invadopodia increased steadily over the lifetime of individual invadopodia (Fig. 12B, D). By contrast, in gRGDsp-treated cells, the overall MT1-MMP accumulation rate was significantly decreased, suggesting that the major effect of integrin inhibition was on invadopodia maturation (Fig. 12B, D).

Integrin-Linked Kinase Controls Adhesion Ring Formation, Invadopodia Dynamics and Activity

Our live and fixed imaging results with RGD blocking peptide indicated that integrins are involved in both adhesion ring formation and the accumulation of MT1-MMP at invadopodia. Since the majority of invadopodial MT1-MMP is derived from exocytosis of late endocytic/lysosomal vesicles (Steffen *et al.*, 2008; Hoshino *et al.*, 2012), we hypothesized that downstream signals from integrin-ECM attachement might regulate this process. Although little is known about the relationship between integrins and exocytosis (Balasubramanian *et al.*, 2010; Gupton & Gertler, 2010; Wickstrom & Fassler, 2011), a possible downstream

candidate is integrin-linked kinase (ILK), based on its reported function connecting caveolar vesicles to IQGAP at adhesions (Wickstrom *et al.*, 2010). Since cholesterol-rich caveolin-positive membranes and IQGAP have been separately shown to mediate proteinase trafficking to invadopodia (Sakurai-Yageta *et al.*, 2008; Caldieri *et al.*, 2009; Yamaguchi *et al.*, 2009), ILK is likely an important link between integrins and MT1-MMP-containing vesicles to promote the degradative activity of invadopodia. To test this hypothesis, I knocked down ILK in SCC61 cells. Using two separate shRNA constructs, ILK protein expression was decreased by 58% and 82% in ILK-KD1 and -KD2 cells compared with a non-targeting control (Fig. 13B). When assessed by fixed cell IF, ILK-KD cells exhibited a significant reduction in invadopodia-associated degradation, and the number of total, ringed, and active invadopodia per cell (Figs.13A, C-D). Consistent with the hypothesized role in invadopodia maturation, there was no significant difference between control and ILK-KD cells in the number of inactive invadopodia/cell. Combining gRGDsp treatment with ILK-KD had no further effect on invadopodia-associated ECM degradation compared with RGD treatment alone, suggesting that RGD-binding integrins likely function upstream of ILK (Fig. 13E).

We also performed live cell imaging in MT1-pHLuor, Tom-Tractin-expressing control and ILK-KD cells to analyze the effect of ILK-KD on MT1-MMP accumulation and invadopodia dynamics. Unlike the effect of RGD peptide (Fig. 12), ILK-KD led to a decrease in invadopodia formation, from a median of 28 to 12 invadopodia per cell per hour and invadopodia lifetime from a median of 35 to

21 minutes. (Fig. 14A, C). Similar to the effect of integrin inhibition with gRGDsp peptide, KD of ILK1 led to a large reduction in the rate of MT1-MMP recruitment to invadopodia (Fig. 14B). We note that unlike with RGD-inhibited cells, the decrease in extracellular MT1-MMP accumulation only occurred after the first 20 min (Fig. 14D). However, overall these data indicate that integrin and ILK-mediated adhesion signaling is critical for accumulation of extracellular MT1-MMP at invadopodia. Since the accumulation was quantitated at already-formed invadopodia, the decreases in protease accumulation for both integrin- and ILK-inhibited cells were independent of any effects on invadopodia formation or lifetime.

Integrins and ILK Recruit IQGAP to Invadopodia

Based on our findings that integrins and ILK affect invadopodia activity and MT1-MMP recruitment and the known role of the ILK-binding partner IQGAP in capturing caveolar vesicles (Sakurai-Yageta *et al.*, 2008; Wickstrom *et al.*, 2010), I tested if blocking RGD-binding integrins or knocking down ILK affected IQGAP localization to invadopodia. Confocal sections show IQGAP localization with actin at the invadopodium, similar to previous reports (Sakurai-Yageta *et al.*, 2008), and with paxillin surrounding it (Fig. 15A). Confocal Z-sections demonstrate IQGAP localization skewed towards the top of the invadopodium (Fig. 15B). To determine if IQGAP is recruited to invadopodia based on integrins or ILK, RGD-treated or ILK-KD SCC61 cells were cultured overnight on FITC-FN/1% gelatin, fixed, and immunostained for actin to mark invadopodia and

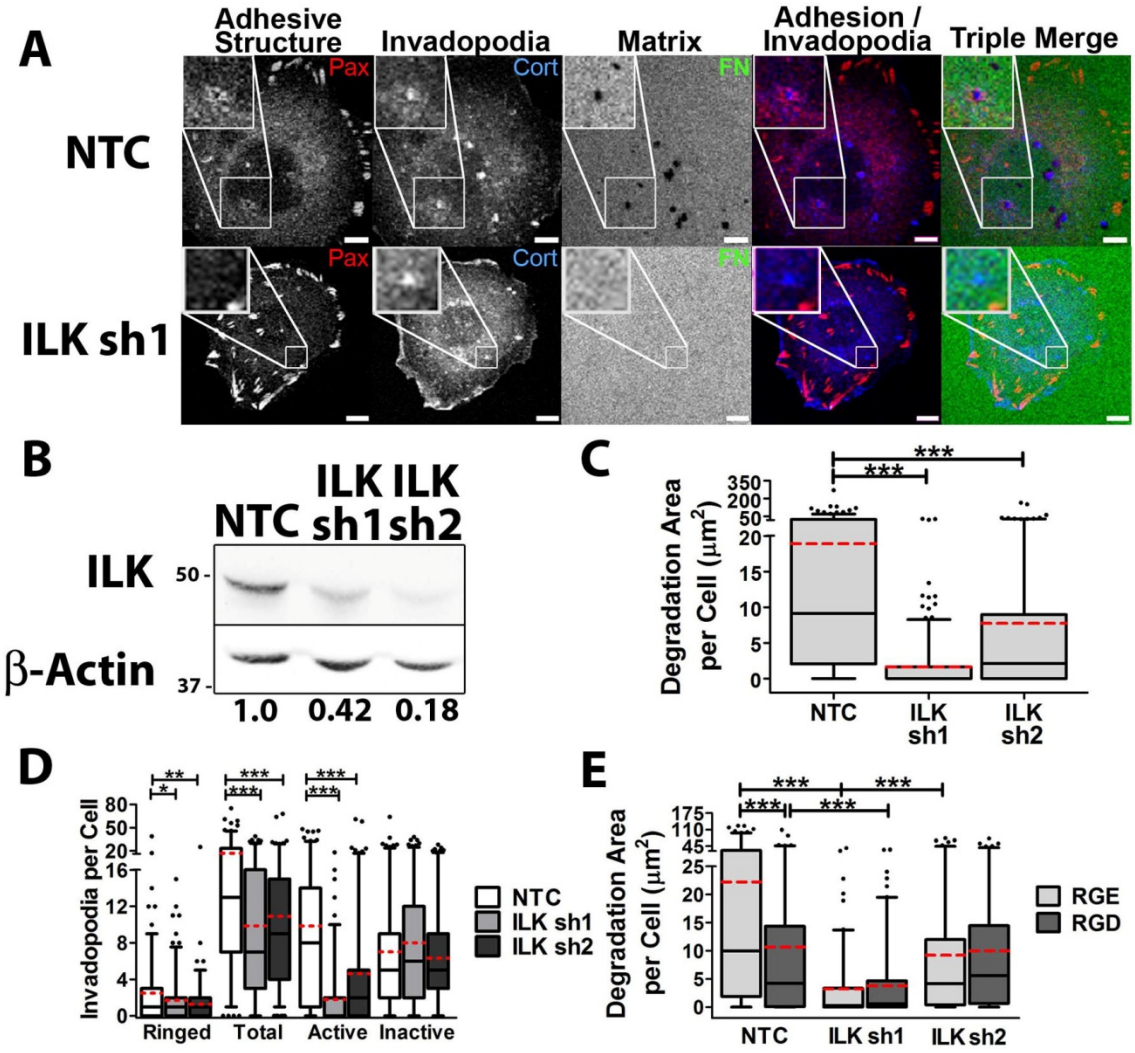

Figure 13. Integrin-linked kinase controls adhesion ring formation, invadopodia formation, and activity. SCC61 cells stably expressing shRNA against ILK1 (sh1, sh2) or non-targeting control (NTC) shRNA were cultured on FITC-FN/1% gelatin (FN) for 16 h, then fixed and immunostained for cortactin (Cort) and paxillin (Pax). **A.** Confocal images. Scale bars = 5 μm. **B.** Western blot for ILK in total cell lysates from SCC61 cells. Numbers indicate ILK band intensity of the indicated cell line as a ratio of the NTC ILK level, after normalization to the β-actin loading control. **C.** Degradation area/cell. **D.** Invadopodia characteristics. **E.** NTC and ILK-KD cells were further treated with RGE or RGD peptides and analyzed for degradation. Note that there is only a significant difference within a cell line for NTC. n ≥ 60 cells per condition from ≥3 independent experiments. For C-E, box and whiskers show respectively the 25-75th and 5-95th percentiles with the dotted red line indicating the mean and the black line indicating the median. *p < 0.05; **p < 0.01, ***p < 0.001 vs. indicated comparison.

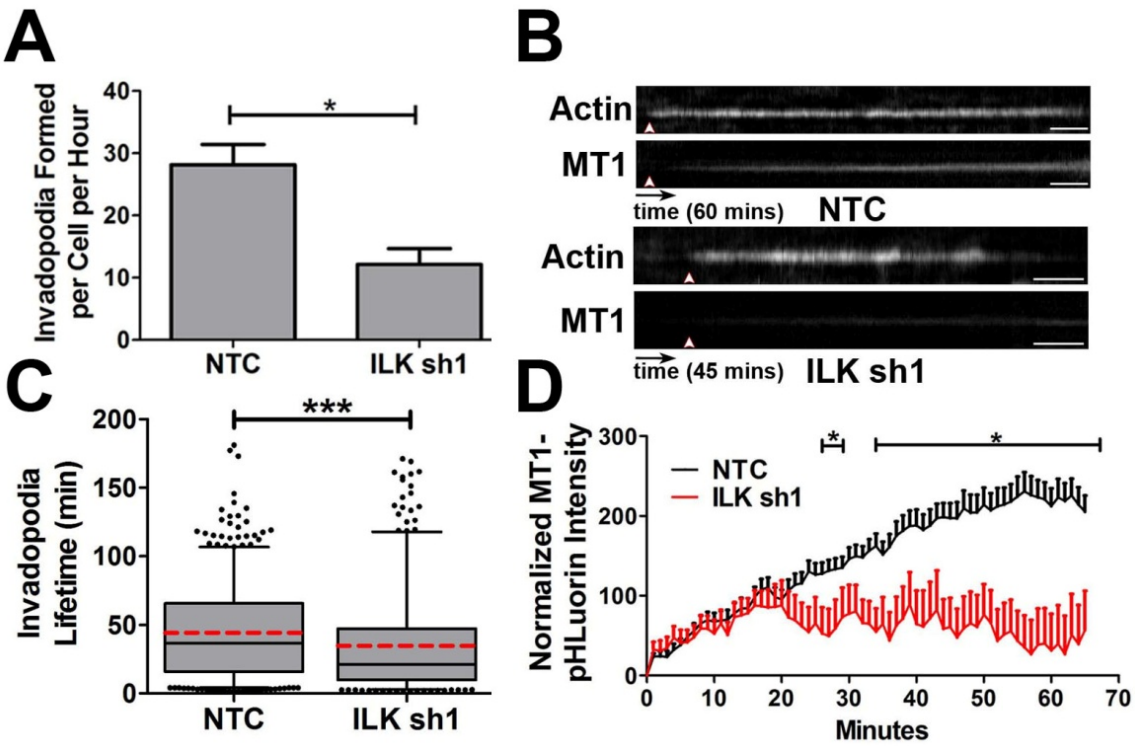

Figure 14. Integrin-linked kinase controls invadopodia formation and activity. Live-cell imaging of NTC or ILK sh1 SCC61 cells expressing Tom-Tractin (Actin), to mark invadopodia, and MT1-pHLuor (MT1), to mark extracellular MT1-MMP was performed and analyzed for **(A)** invadopodia formation rate, **(C)** invadopodia lifetime, **(B, D)** MT1 accumulation over time at invadopodia. Time scale bars = 5 min. n ≥ 11 cells, ≥ 300 invadopodia per condition from ≥ 3 independent experiments. Error bars on invadopodia formation graphs indicate SEM. For C, box and whiskers show respectively the 25-75th and 5-95th percentiles with the dotted red line indicating the mean and the black line indicating the median. *$p < 0.05$; ***$p < 0.001$ vs. indicated comparison.

IQGAP (Fig. 15C). The fluorescent intensities of actin and IQGAP at invadopodia were quantified from images acquired under identical laser and camera conditions. The ratio of IQGAP to actin intensity was then plotted. Consistent with a model whereby integrins and ILK facilitate IQGAP recruitment to invadopodia, inhibition of RGD-binding integrins or ILK-KD led to a decrease in the IQGAP to actin intensity ratio at invadopodia (Fig. 15 C-E). The median ratio of IQGAP to actin intensity decreased from 0.57 to 0.49 with RGD treatment and from 0.49 to 0.34 and 0.37 with ILK shRNA #1 and #2, respectively, compared to controls (Fig. 15D-E).

MT1-MMP Regulates ECM Degradation and Invadopodia Dynamics, but not Adhesion Ring Formation

Recruitment of MT1-MMP and other proteinases is thought to be a late stage in invadopodia formation; however several studies have reported reduced numbers of invadopodia/cell in proteinase-inhibited cells (Artym *et al.*, 2006; Clark *et al.*, 2007a; Steffen *et al.*, 2008), suggesting feedback from proteolytic activity. To test whether MT1-MMP acts upstream or downstream of adhesion ring formation, SCC61 cells were transduced with shRNA targeting MT1-MMP and analyzed for invadopodia and adhesion ring formation and ECM degrading ability in fixed cell assays (Fig. 16A-B). Consistent with previous reports (Artym *et al.*, 2006; Steffen *et al.*, 2008) ECM degradation per cell was almost completely abolished in MT1-MMP knockdown cells (Fig. 16B-C). Furthermore, there was a 4-fold decrease in the number of active invadopodia per cell and a corresponding increase in inactive invadopodia numbers (Fig. 16D). Meanwhile, there was no

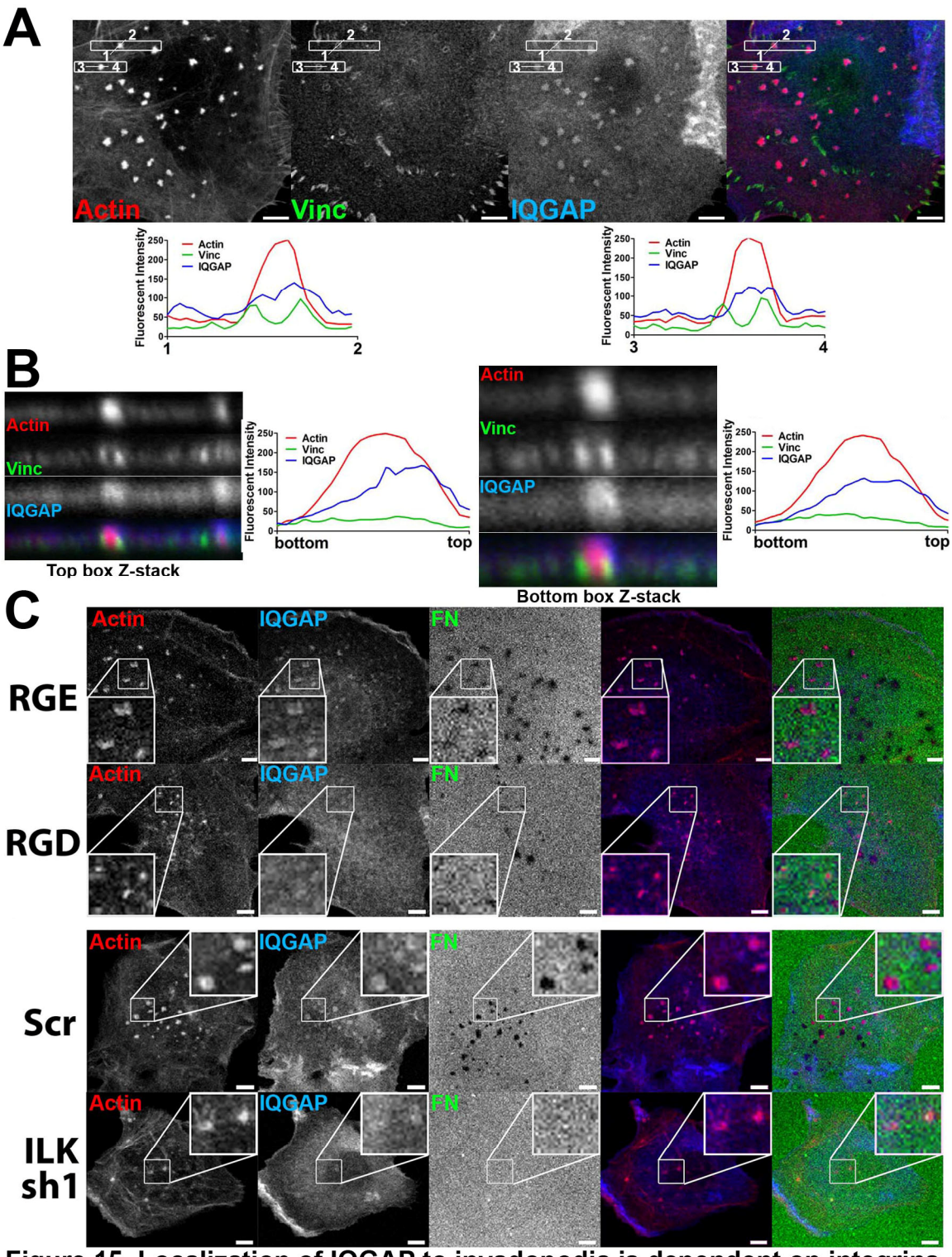

Figure 15. Localization of IQGAP to invadopodia is dependent on integrins and ILK. A. Confocal images of SCC61 cells cultured on unlabeled-FN/1% gelatin for 16 hrs and immunostained for actin (red), IQGAP (blue) and vinculin (Vinc, green). Graphs indicate fluorescent intensity (in arbitrary units) of each marker over the indicated line scan in the X-Y dimension. **B.** Confocal Z-stacks of boxed invadopodia are shown. **Continued on next page**

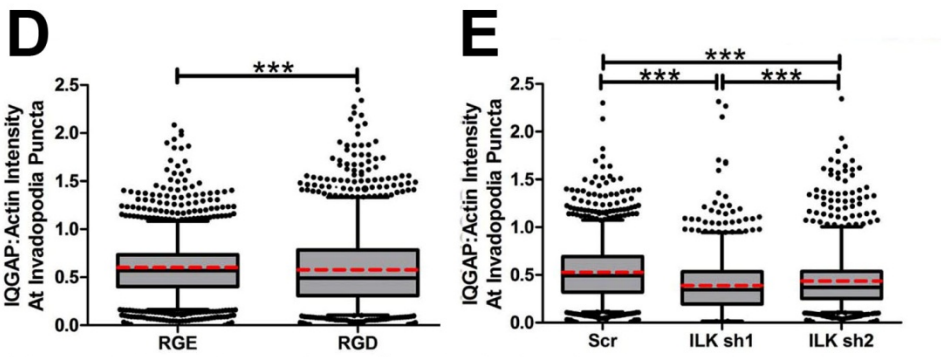

Figure 15 continued: B. Graphs indicate intensity fo each marker in the indicated line scan in the X-Z dimension. **C-E.** SCC61 cells treated with RGD or RGE peptide control (250 µg/ml) **(C,D)** or stably expressing shRNA against ILK1 (sh1, sh2) or non-targeting control (NTC) shRNA **(C,E)** were cultured on FITC-FN/1% gelatin (FN, green) for 16 hours then immunostained for actin (red) and IQGAP (blue). **C.** Confocal images. Zooms indicate typical invadopodia for condition. **D-E.** Ratio of IQGAP to actin intensity at invadopodia. Box and whiskers show respectively the 25-75th and 5-95th percentiles with the dotted red line indicating the mean and the black line indicating the median. ***p < 0.001 vs. indicated comparison. Scale bars = 5 µm.

significant change in either the number of adhesion-ringed invadopodia or the number of total invadopodia. Live cell imaging further revealed that the rate of invadopodia formation was reduced in MT1-MMP-KD cells (Fig. 16E). There was also a small but significant decrease in the median lifetime of invadopodia in MT1-MMP-KD cells from 45.5 to 35.5 minutes (Fig. 16F), suggesting that there is indeed a positive feedback loop that results from MT1-MMP activity at invadopodia (Artym *et al.*, 2006; Clark *et al.*, 2007a; Steffen *et al.*, 2008). These data are consistent with a model in which adhesion rings form upstream of MT1-MMP accumulation to promote ECM degradation. MT1-MMP activity itself also has significant effects on invadopodia dynamics, both in the formation and stability phases.

Discussion

In this chapter, we examined the role of cell-ECM adhesion and downstream signaling in the regulation of invadopodia formation and activity. We find that podosome-like adhesion rings surround invadopodia shortly after their formation and their presence is highly correlated with invadopodia activity. Integrins and ILK are critical for adhesion ring formation, localization of the vesicular adaptor protein IQGAP and the transmembrane proteinase MT1-MMP to invadopodia, and ECM degradation. Overall these data indicate that adhesion is critical for invadopodia maturation.

Adhesion Ring Formation is not a Distinguishing Feature of Podosomes

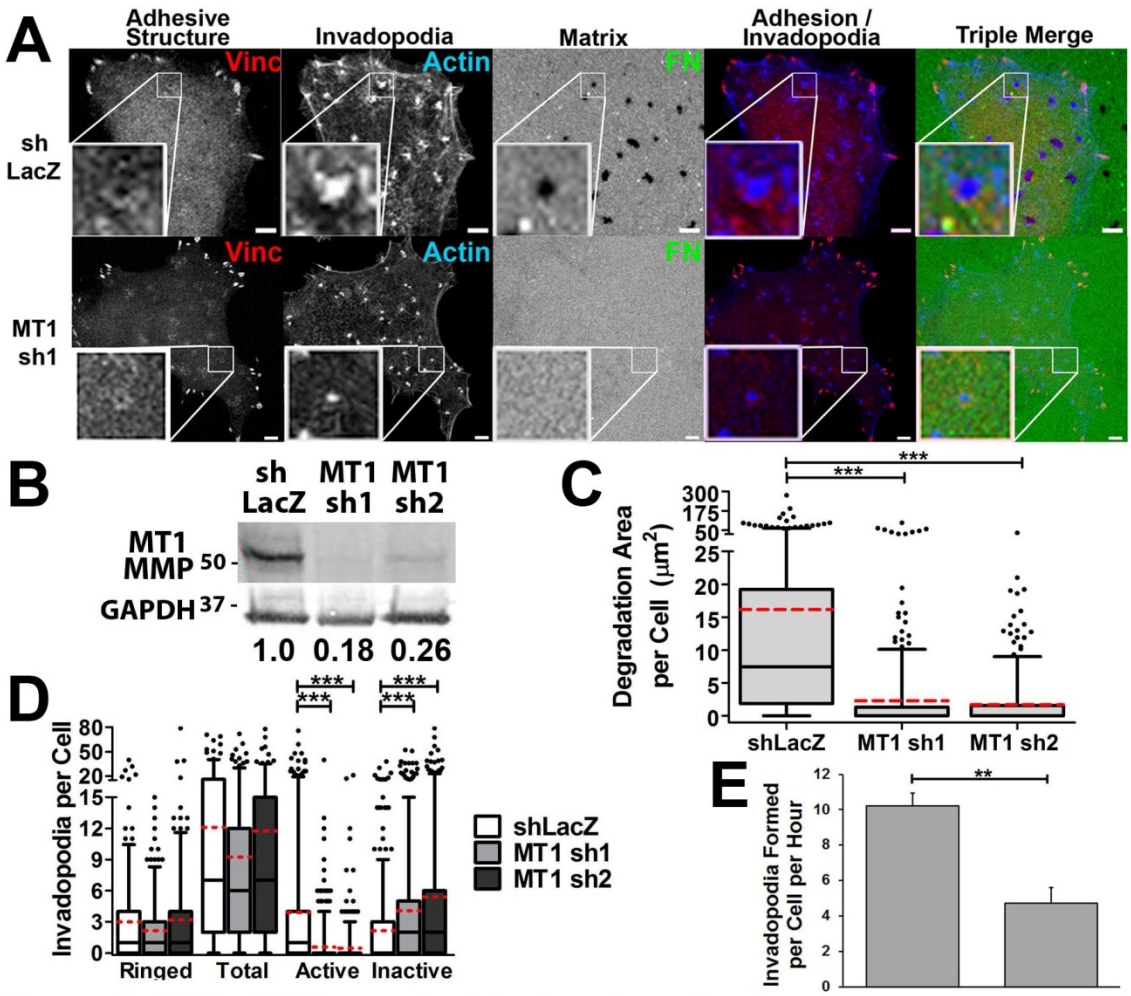

Figure 16. MT1-MMP is required for invadopodia-associated ECM degradation, but not for adhesion ring localization. A-D. SCC61 cells stably expressing shRNA constructs against MT1-MMP (MT1 sh1 or sh2) or shLacZ control oligo were cultured on FITC-FN/gelatin substrates for 16 h and then fixed and immunostained for vinculin (Vinc, red in merges) and actin (blue in merges). **A.** Confocal images. Zoomed images show representative invadopodia for the condition. Scale bars = 5 μm. **B.** Western blot of total cell lysates. Numbers indicate the ratio of MT1-MMP normalized to the GAPDH loading control and then to shLacZ control. **C.** Quantification of degradation area/cell. **D.** Quantification of types of invadopodia per cell. n ≥ 60 cells per condition from ≥ 3 independent experiments. **E-F.** Invadopodia formation **(E)** and lifetime **(F)** of SCC61 cells stably expressing shLacZ or MT1 sh1 transiently transfected with Tom-Tractin to mark invadopodia. n ≥ 12 cells, ≥ 180 invadopodia per condition from ≥ 3 independent experiments. Error bars in E indicate SEM. For C-D, and F, box and whiskers show respectively the 25-75th and 5-95th percentiles with the dotted red line indicating the mean and the black line indicating the median. *p < 0.05; **p < 0.01, ***p < 0.001.

Invadopodia and podosomes are both actin-rich structures that can degrade underlying matrix. Despite many similarities, including common molecular constituents and pathways of activation, invadopodia are often classified as distinct structures that form in cancer cells and have separate properties from podosomes such as longer lifetimes, protrusive behavior, and morphological classifications (Gimona *et al.*, 2008; Murphy & Courtneidge, 2011). A major distinction is the presence of adhesion proteins surrounding the actin-based protrusion (Gimona *et al.*, 2008; Linder *et al.*, 2011; Murphy & Courtneidge, 2011). Here, we demonstrate that two different cancer cell lines exhibit adhesion ring formation around the invadopodial protrusion. These rings consist of multiple components of classic adhesions including paxillin, vinculin, and β1 integrin and localize at the basal surface of the cell by confocal microscopy, suggesting that these are legitimate adhesive structures. However, they were less prominent than adhesion rings normally observed around podosomes, possibly due to competition with FAs for adhesion components (Chan *et al.*, 2009) or a greater cytoplasmic pool of adhesion proteins in cancer cells that obscures observation of the ring structures. Interestingly, in invadosome-producing Src-transformed fibroblasts, β1 integrin was shown to be important not only for the organization but also for the formation of invadosome structures (Destaing *et al.*, 2010). Although an effect on invadopodia formation is observed here with ILK KD in SCC61 cells, the primary role for RGD-binding integrins and ILK appears to be promotion of invadopodia maturation. Similarly,

in osteoclasts, despite a small effect on actin podosome puncta diameter, knockout of combinations of integrins β1, β2, and αv or kindlin-3 led to severe defects in podosome organization and bone resorption (Schmidt *et al.*, 2011). In addition, Badowski *et al.* examined the role of paxillin in invadosome formation by Src-transformed cells and podosome formation by osteoclasts. In those systems, loss or mutation of paxillin primarily affected podosome organization and ECM degradation (Badowski *et al.*, 2008). Our data suggest that adhesion rings are indeed a common component of both invadopodia and podosomes and indicate that a major function of those rings is to promote protease recruitment and invadopodia maturation.

A New Model of Invadopodia Stages

Altogether, our data are consistent with a model in which adhesion rings are assembled shortly after invadopodia actin puncta assembly and promote recruitment of proteinases to allow ECM degradation (Fig. 17). RGD-binding integrins and ILK are crucial components of this process as inhibition or knock-down reduces adhesion ring formation, MT1-MMP recruitment to invadopodia and ECM degradation. Furthermore, inhibiting integrins in ILK-KD cells had no further effect on ECM degradation, suggesting that integrins and ILK reside in the same pathway with respect to invadopodia-associated ECM degradation. We place MT1-MMP at a later stage than adhesion formation since knockdown of MT1-MMP had no effect on the number of adhesion-ringed invadopodia but inhibition of cell-ECM adhesion led to decreased recruitment of MT1-MMP. After

exocytosis, MT1-MMP and other proteases might also interact with integrins via a direct docking mechanism (Mueller *et al.*, 1999; Galvez *et al.*, 2002) that could provide additional positive feedback to enhance invadopodia lifetime and/or ECM degradation.

Whereas integrin inhibition with gRGDsp did not affect invadopodia formation or lifetime, ILK-KD did, indicating that ILK may not function solely downstream of integrins for those activities. Although ILK is thought to primarily function as a downstream effector of integrins in complex with PINCH and parvin (Sakai *et al.*, 2003; Stanchi *et al.*, 2009; Wickstrom *et al.*, 2010), ILK can also be regulated by growth factor signaling (Ho & Dagnino, 2012; Serrano *et al.*, 2012) and PI3K (Wu & Dedhar, 2001). Since invadopodia formation can be activated by both growth factor and PI3K signaling (Yamaguchi *et al.*, 2005; Yamaguchi *et al.*, 2011), one possibility is that the regulation of invadopodia dynamics by ILK may occur downstream of growth factors rather than integrins. Another possibility is that the inhibition of RGD-binding integrins with gRGDsp was less effective at blocking the integrin-ILK-IQGAP-MT1-MMP pathway than ILK-KD. Since knockdown of MT1-MMP itself can affect invadopodia dynamics (Fig. 16), a more complete block of the pathway with ILK-KD might lead to the difference that we noted for invadopodia dynamics.

Regulation of Exocytosis by Integrins and ILK

Integrins and adhesion signaling have recently been shown to affect diverse exocytic processes. Assembly and localization of the exocyst complex

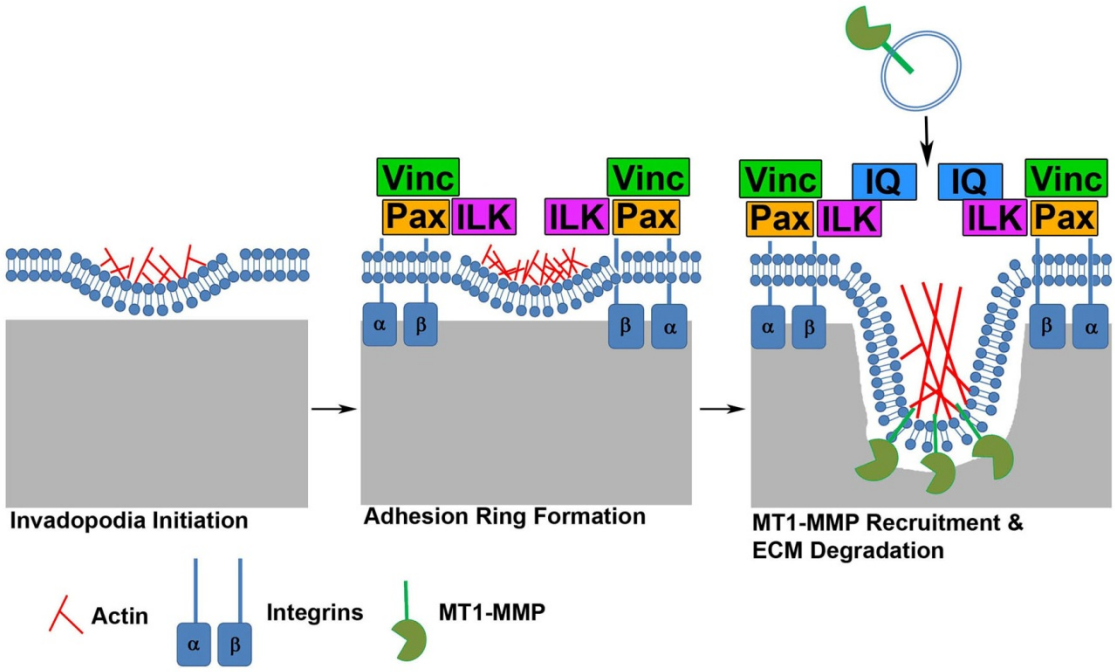

Figure 17. Model of invadopodia maturation. Initial actin puncta appearance is followed by adhesion ring structure formation including integrins (α,β), ILK, paxillin (Pax) and vinculin (Vinc). Ring formation leads to enhanced MT1-MMP recruitment and ECM degradation by invadopodia.

were shown to be regulated by integrin adhesion and paxillin through activation of the RalA GTPase (Spiczka & Yeaman, 2008; Balasubramanian *et al.*, 2010). β1 Integrin-ECM interaction was also recently shown to promote exocytosis of lipid rafts by a mechanism that links ILK, the scaffold protein IQGAP1 and the formin mDia1 to capture of microtubules and subsequent vesicle delivery to the plasma membrane (Wickstrom *et al.*, 2010; Wickstrom & Fassler, 2011). Furthermore, integrin adhesion to collagen in 3D was shown to promote polarized trafficking of MT1-MMP (Bravo-Cordero *et al.*, 2007). Of note, several microtubule motors have been shown to regulate exocytosis of MT1-MMP at podosomes (Wiesner *et al.*, 2010; Cornfine *et al.*, 2011). Furthermore, the exocyst complex localizes to invadopodia through IQGAP1 and is important for MT1-MMP localization to invadopodia (Sakurai-Yageta *et al.*, 2008). In light of these data and our finding that IQGAP localization to invadopodia is reduced in integrin- and ILK-KD cells (Fig. 15), we speculate that adhesion rings surrounding invadopodia may promote targeted MT1-MMP recruitment to invadopodia through capture of vesicles via a similar ILK-IQGAP-mediated mechanism (Fig. 17).

Deregulation of β1 integrin and ILK signaling has been implicated in a wide range of aggressive tumor behaviors, including cancer invasion (Dai *et al.*, 2003; Guo & Giancotti, 2004; Sawai *et al.*, 2006; Lu *et al.*, 2008; Poincloux *et al.*, 2009). With regard to ECM degradation and cancer invasion, our data suggest that at least one key mechanism may be via integrin-ILK-mediated regulation of protease secretion at invadopodia. Interestingly, ILK-regulated secretion has also

been implicated in tumor angiogenesis and caveolar formation (Edwards *et al.*, 2008; Wickstrom *et al.*, 2010). Future studies should address how general the secretory defect is from integrin-ILK signaling and to what extent invadopodia represent “hotspot” secretion sites for lipid raft-carried molecules.

CHAPTER V

DISCUSSION AND FUTURE DIRECTIONS

Mechanosensing at Invadopodia

As a whole, my data support the concept that integrin-mediated mechanotransduction promotes the functionality of invadopodia via recruitment of MT1-MMP. In Alexander *et al.,* we demonstrated that general substrate rigidity specifically promotes invadopodia activity. This response is enhanced by the overexpression of the mechanosensing proteins FAK and p130Cas. We also observed localization of FAK and p130Cas to the invadopodia core and of myosin IIA, active β1 integrin, paxillin, and vinculin to invadopodia rings. As a result, invadopodia appear to be bona fide adhesive structures and mechanosensing organelles. Invadosome/podosome rosettes in fibroblasts and macrophages have in fact been shown to exert force on the substrate similar to FAs (Collin *et al.*, 2006; Collin *et al.*, 2008; Labernadie *et al.*, 2010). This effect has not been demonstrated for invadopodia and might be difficult to assess due to their small size compared to podosome rosettes and FAs. It is interesting to speculate, however, that subcellular force changes mediated by ECM topography or compositional heterogeneity *in vivo* could locally induce ECM degradation. Alternatively, forces induced on a subcellular scale can lead to long distance signaling responses (Wang *et al.*, 2005) which could also mediate rigidity

responses. Overall, these data indicate a strong relationship between ECM rigidity and tissue degradation, which is likely to be enhanced in tumors that are exposed to a more rigid environment than normal epithelial cells experience (Paszek *et al.*, 2005).

Integrin-ECM Regulation of Invadopodia Activity

Integrin heterodimers exert differential effects on cellular phenotypes that are triggered by interactions with specific ECM ligands (Danen et al., 2002; Orr et al., 2006; Roca-Cusachs et al., 2009). Interestingly, treatment of cells with a β1 integrin blocking antibody can lead to differential effects on invadopodia activity depending on the cellular and ECM context (Liu *et al.*, 2009b; Branch *et al.*, 2012). In Liu *et al.,* treatment of bladder carcinoma cells with a β1 integrin blocking antibody mimicked the effect of laminin-332 knockdown, as attachment to laminin-332 reduced invadopodia numbers (Liu *et al.*, 2009b). By contrast, in cells plated on FN, we found that treatment with either an RGD blocking peptide or an antibody that blocks β1 integrin-ligand interactions inhibits invadopodia maturation. Therefore, specific ECM-integrin interactions may lead to divergent effects on invadopodia activity.

Cooperation between Mechanical Signals and Growth Factor Signaling in Invadopodia Progression

Our data show that integrin-ECM attachment and ILK promote maturation of invadopodia, as defined by protease exocytosis. Integrin-mediated

mechanotransduction also results in a specific increase in functional, but not total, invadopodia numbers. Invadopodia formation instead appears to depend on growth factor signaling and can be induced by a number of growth factors including EGF, VEGF, and TGF-β (Yamaguchi *et al.*, 2005; Mandal *et al.*, 2008; Lucas *et al.*, 2010). In many of these situations, growth factor-induced invadopodia formation requires PI3K, possibly leading to formation of PI(3,4)P2 and recruitment of initiators of invadopodia such as Tks5 (Seals *et al.*, 2005; Yamaguchi *et al.*, 2011; Hoshino *et al.*, in revision). These data lead to a model in which growth factor signaling and integrin-mediated mechanotransduction cooperate to promote formation of fully functional invadopodia.

Future Directions

Mechanism of Protease Recruitment to Invadopodia by Integrins

Integrins promote cell surface protease expression through a variety of mechanisms, including alterations in protein expression, direct docking of vesicles, or activation of signaling pathways to promote trafficking (Deryugina *et al.*, 2001; Ellerbroek *et al.*, 2001; Galvez *et al.*, 2002; Matias-Roman *et al.*, 2005; Tomari *et al.*, 2009; Yamaguchi *et al.*, 2009; Balasubramanian *et al.*, 2010). However, the exact mechanism for the observed decrease in MT1-MMP at invadopodia in response to ILK KD or RGD peptide block of integrin adhesion remains undetermined. We did find that blocking integrins or ILK led to a decrease in the intensity of IQGAP staining at invadopodia. We therefore favor a

model in which an integrin-ILK-IQGAP complex recruits lipid raft-rich vesicles (Wickstrom *et al.*, 2010) containing proteases to invadopodia by promoting docking via the exocyst complex (Sakurai-Yageta *et al.*, 2008). However, that model has not yet been formally tested. Therefore, an important future direction is to directly quantitate MT1-MMP-containing vesicle docking by TIRF microscopy or other methods. We could also measure the trafficking of lipid raft-containing vesicles to invadopodia in response to integrin, ILK, or IQGAP inhibition to assess a possible defect in general secretion to invadopodia with blocking or knockdown of these proteins.

Feedback from Adhesions to Invadopodia Formation

Growth factor – PI3K signaling is emerging as a critical initiating factor for invadopodia protrusion (Yamaguchi *et al.*, 2011; Hoshino *et al.*, in revision), while our data point to integrins as mediating protease recruitment for invadopodia maturation (Branch *et al.*, 2012). However, additional data suggests a positive feedback emanating from proteolytic activity at invadopodia. Thus, knockdown or inhibition of invadopodial proteases, or of proteins required for protease recruitment to invadopodia, not only greatly inhibits matrix degradation but also reduces invadopodia number (Artym *et al.*, 2006; Clark *et al.*, 2007a; Steffen *et al.*, 2008). Consistent with those studies and with a positive feedback model, in our live imaging studies, we found that knockdown of MT1-MMP led to both a reduced rate of invadopodia formation, as well as a decreased lifetime of individual invadopodial structures (Branch *et al.*, 2012). The feedback could

occur via the release of growth factors or ECM fragments from the ECM. Alternatively, proteases can cleave and alter the activity of growth factors or growth factor receptors themselves (Lehti *et al.*, 2005; Kessenbrock *et al.*, 2010; Koshikawa *et al.*, 2010). Future studies should determine the roles of proteolytic growth factor release and activation in invadopodia formation.

An increase in integrin activity could also crosstalk with growth factor receptor signaling to provide additional feedback and promote invadopodia formation. We did observe a decrease in the formation of invadopodia with ILK knockdown, although ILK is also implicated in cellular processes downstream of growth factors such as EGF (Esfandiarei *et al.*, 2010; Ho & Dagnino, 2012). Interestingly, EGF-induced Src activation is amplified by cell attachment to FN and this process requires ILK (Azimifar *et al.*, 2012). Also, EGF-induced PI3K-Akt signaling is amplified by auto-clustered β1 integrin or increased ECM stiffness (Levental *et al.*, 2009). Since specific integrin-ECM interactions have apparent varying effects on invadopodia formation and function (Liu *et al.*, 2009b; Branch *et al.*, 2012), one possibility is that divergent downstream signaling interfaces differentially with growth factor signaling pathways. An important future direction is therefore to determine which integrin-ECM interactions promote maximal invadopodia activity as well as to identify synergy of these pathways with growth factor induction of invadopodia formation.

REFERENCES

Abram CL, Seals DF, Pass I, Salinsky D, Maurer L, Roth TM & Courtneidge SA. (2003). The adaptor protein fish associates with members of the ADAMs family and localizes to podosomes of Src-transformed cells. *J Biol Chem* **278:** 16844-16851.

Aguirre-Ghiso JA. (2007). Models, mechanisms and clinical evidence for cancer dormancy. *Nat Rev Cancer* **7:** 834-846.

Alexander NR, Branch KM, Parekh A, Clark ES, Iwueke IC, Guelcher SA & Weaver AM. (2008). Extracellular matrix rigidity promotes invadopodia activity. *Curr Biol* **18:** 1295-1299.

Artym VV, Matsumoto K, Mueller SC & Yamada KM. (2011). Dynamic membrane remodeling at invadopodia differentiates invadopodia from podosomes. *Eur J Cell Biol* **90:** 172-180.

Artym VV, Yamada KM & Mueller SC. (2009). ECM degradation assays for analyzing local cell invasion. *Methods Mol Biol* **522:** 211-219.

Artym VV, Zhang Y, Seillier-Moiseiwitsch F, Yamada KM & Mueller SC. (2006). Dynamic interactions of cortactin and membrane type 1 matrix metalloproteinase at invadopodia: defining the stages of invadopodia formation and function. *Cancer Res* **66:** 3034-3043.

Azimifar SB, Bottcher RT, Zanivan S, Grashoff C, Kruger M, Legate KR, Mann M & Fassler R. (2012). Induction of membrane circular dorsal ruffles requires co-signalling of integrin-ILK-complex and EGF receptor. *J Cell Sci* **125:** 435-448.

Badowski C, Pawlak G, Grichine A, Chabadel A, Oddou C, Jurdic P, Pfaff M, Albiges-Rizo C & Block MR. (2008). Paxillin phosphorylation controls invadopodia/podosomes spatiotemporal organization. *Mol Biol Cell* **19:** 633-645.

Balasubramanian N, Meier JA, Scott DW, Norambuena A, White MA & Schwartz MA. (2010). RalA-exocyst complex regulates integrin-dependent membrane raft exocytosis and growth signaling. *Curr Biol* **20:** 75-79.

Balasubramanian N, Scott DW, Castle JD, Casanova JE & Schwartz MA. (2007). Arf6 and microtubules in adhesion-dependent trafficking of lipid rafts. *Nat Cell Biol* **9:** 1381-1391.

Baldassarre M, Pompeo A, Beznoussenko G, Castaldi C, Cortellino S, McNiven MA, Luini A & Buccione R. (2003). Dynamin participates in focal extracellular matrix degradation by invasive cells. *Mol Biol Cell* **14:** 1074-1084.

Barsky SH, Siegal GP, Jannotta F & Liotta LA. (1983). Loss of basement membrane components by invasive tumors but not by their benign counterparts. *Lab Invest* **49:** 140-147.

Berdeaux RL, Diaz B, Kim L & Martin GS. (2004). Active Rho is localized to podosomes induced by oncogenic Src and is required for their assembly and function. *J Cell Biol* **166:** 317-323.

Blood CH & Zetter BR. (1990). Tumor interactions with the vasculature: angiogenesis and tumor metastasis. *Biochim Biophys Acta* **1032:** 89-118.

Bowden ET, Barth M, Thomas D, Glazer RI & Mueller SC. (1999). An invasion-related complex of cortactin, paxillin and PKCmu associates with invadopodia at sites of extracellular matrix degradation. *Oncogene* **18:** 4440-4449.

Bowden ET, Onikoyi E, Slack R, Myoui A, Yoneda T, Yamada KM & Mueller SC. (2006). Co-localization of cortactin and phosphotyrosine identifies active invadopodia in human breast cancer cells. *Exp Cell Res* **312:** 1240-1253.

Boyd NF, Rommens JM, Vogt K, Lee V, Hopper JL, Yaffe MJ & Paterson AD. (2005). Mammographic breast density as an intermediate phenotype for breast cancer. *Lancet Oncol* **6:** 798-808.

Brabek J, Constancio SS, Shin NY, Pozzi A, Weaver AM & Hanks SK. (2004). CAS promotes invasiveness of Src-transformed cells. *Oncogene* **23:** 7406-7415.

Brabek J, Constancio SS, Siesser PF, Shin NY, Pozzi A & Hanks SK. (2005). Crk-associated substrate tyrosine phosphorylation sites are critical for invasion and metastasis of SRC-transformed cells. *Mol Cancer Res* **3:** 307-315.

Branch KM, Hoshino D & Weaver AM. (2012). Adhesion rings surround invadopodia and promote maturation. *Biology Open* **000:** 1-12.

Bravo-Cordero JJ, Marrero-Diaz R, Megias D, Genis L, Garcia-Grande A, Garcia MA, Arroyo AG & Montoya MC. (2007). MT1-MMP proinvasive activity is regulated by a novel Rab8-dependent exocytic pathway. *Embo J* **26:** 1499-1510.

Bravo-Cordero JJ, Oser M, Chen X, Eddy R, Hodgson L & Condeelis J. (2011). A novel spatiotemporal RhoC activation pathway locally regulates cofilin activity at invadopodia. *Curr Biol* **21:** 635-644.

Burgstaller G & Gimona M. (2004). Actin cytoskeleton remodelling via local inhibition of contractility at discrete microdomains. *J Cell Sci* **117:** 223-231.

Burns S, Thrasher AJ, Blundell MP, Machesky L & Jones GE. (2001). Configuration of human dendritic cell cytoskeleton by Rho GTPases, the WAS protein, and differentiation. *Blood* **98:** 1142-1149.

Caldieri G, Capestrano M, Bicanova K, Beznoussenko G, Baldassarre M & Buccione R. (2012). Polarised apical-like intracellular sorting and trafficking regulates invadopodia formation and degradation of the extracellular matrix in cancer cells. *Eur J Cell Biol*.

Caldieri G, Giacchetti G, Beznoussenko G, Attanasio F, Ayala I & Buccione R. (2009). Invadopodia biogenesis is regulated by caveolin-mediated modulation of membrane cholesterol levels. *J Cell Mol Med* **13:** 1728-1740.

Calle Y, Carragher NO, Thrasher AJ & Jones GE. (2006). Inhibition of calpain stabilises podosomes and impairs dendritic cell motility. *J Cell Sci* **119:** 2375-2385.

Callister WD. (2000). *Fundamentals of materials science and engineering: An Interactive E-Text*. John Wiley & Sons, Hoboken, NJ.

Cantley LC. (2002). The phosphoinositide 3-kinase pathway. *Science* **296:** 1655-1657.

Chabadel A, Banon-Rodriguez I, Cluet D, Rudkin BB, Wehrle-Haller B, Genot E, Jurdic P, Anton IM & Saltel F. (2007). CD44 and beta3 integrin organize two functionally distinct actin-based domains in osteoclasts. *Mol Biol Cell* **18:** 4899-4910.

Chan KT, Cortesio CL & Huttenlocher A. (2009). FAK alters invadopodia and focal adhesion composition and dynamics to regulate breast cancer invasion. *J Cell Biol* **185:** 357-370.

Chen WT. (1989). Proteolytic activity of specialized surface protrusions formed at rosette contact sites of transformed cells. *J Exp Zool* **251:** 167-185.

Chen WT, Chen JM, Parsons SJ & Parsons JT. (1985). Local degradation of fibronectin at sites of expression of the transforming gene product pp60src. *Nature* **316:** 156-158.

Chen WT, Lee CC, Goldstein L, Bernier S, Liu CH, Lin CY, Yeh Y, Monsky WL, Kelly T, Dai M & et al. (1994). Membrane proteases as potential diagnostic and therapeutic targets for breast malignancy. *Breast Cancer Res Treat* **31:** 217-226.

Chen WT, Olden K, Bernard BA & Chu FF. (1984). Expression of transformation-associated protease(s) that degrade fibronectin at cell contact sites. *J Cell Biol* **98:** 1546-1555.

Cheresh DA. (1987). Human endothelial cells synthesize and express an Arg-Gly-Asp-directed adhesion receptor involved in attachment to fibrinogen and von Willebrand factor. *Proc Natl Acad Sci U S A* **84:** 6471-6475.

Chuang YY, Tran NL, Rusk N, Nakada M, Berens ME & Symons M. (2004). Role of synaptojanin 2 in glioma cell migration and invasion. *Cancer Res* **64:** 8271-8275.

Clark ES, Whigham AS, Yarbrough WG & Weaver AM. (2007a). Cortactin is an essential regulator of matrix metalloproteinase secretion and extracellular matrix degradation in invadopodia. *Cancer Res* **67:** 4227-4235.

Clark K, Langeslag M, Figdor CG & van Leeuwen FN. (2007b). Myosin II and mechanotransduction: a balancing act. *Trends Cell Biol* **17:** 178-186.

Collin O, Na S, Chowdhury F, Hong M, Shin ME, Wang F & Wang N. (2008). Self-organized podosomes are dynamic mechanosensors. *Curr Biol* **18:** 1288-1294.

Collin O, Tracqui P, Stephanou A, Usson Y, Clement-Lacroix J & Planus E. (2006). Spatiotemporal dynamics of actin-rich adhesion microdomains: influence of substrate flexibility. *J Cell Sci* **119:** 1914-1925.

Cooper JA, Gould KL, Cartwright CA & Hunter T. (1986). Tyr527 is phosphorylated in pp60c-src: implications for regulation. *Science* **231:** 1431-1434.

Coopman PJ, Do MT, Thompson EW & Mueller SC. (1998). Phagocytosis of cross-linked gelatin matrix by human breast carcinoma cells correlates with their invasive capacity. *Clin Cancer Res* **4:** 507-515.

Cornfine S, Himmel M, Kopp P, El Azzouzi K, Wiesner C, Kruger M, Rudel T & Linder S. (2011). The kinesin KIF9 and reggie/flotillin proteins regulate matrix degradation by macrophage podosomes. *Mol Biol Cell* **22:** 202-215.

Crimaldi L, Courtneidge SA & Gimona M. (2009). Tks5 recruits AFAP-110, p190RhoGAP, and cortactin for podosome formation. *Exp Cell Res* **315:** 2581-2592.

Cukierman E, Pankov R, Stevens DR & Yamada KM. (2001). Taking cell-matrix adhesions to the third dimension. *Science* **294:** 1708-1712.

Dai DL, Makretsov N, Campos EI, Huang C, Zhou Y, Huntsman D, Martinka M & Li G. (2003). Increased expression of integrin-linked kinase is correlated with melanoma progression and poor patient survival. *Clin Cancer Res* **9:** 4409-4414.

Danen EH, Sonneveld P, Brakebusch C, Fassler R & Sonnenberg A. (2002). The fibronectin-binding integrins alpha5beta1 and alphavbeta3 differentially modulate RhoA-GTP loading, organization of cell matrix adhesions, and fibronectin fibrillogenesis. *J Cell Biol* **159:** 1071-1086.

David-Pfeuty T & Singer SJ. (1980). Altered distributions of the cytoskeletal proteins vinculin and alpha-actinin in cultured fibroblasts transformed by Rous sarcoma virus. *Proc Natl Acad Sci U S A* **77:** 6687-6691.

del Pozo MA, Alderson NB, Kiosses WB, Chiang HH, Anderson RG & Schwartz MA. (2004). Integrins regulate Rac targeting by internalization of membrane domains. *Science* **303:** 839-842.

del Pozo MA, Balasubramanian N, Alderson NB, Kiosses WB, Grande-Garcia A, Anderson RG & Schwartz MA. (2005). Phospho-caveolin-1 mediates integrin-regulated membrane domain internalization. *Nat Cell Biol* **7:** 901-908.

del Rio A, Perez-Jimenez R, Liu R, Roca-Cusachs P, Fernandez JM & Sheetz MP. (2009). Stretching single talin rod molecules activates vinculin binding. *Science* **323:** 638-641.

Deryugina EI, Ratnikov B, Monosov E, Postnova TI, DiScipio R, Smith JW & Strongin AY. (2001). MT1-MMP initiates activation of pro-MMP-2 and integrin alphavbeta3 promotes maturation of MMP-2 in breast carcinoma cells. *Exp Cell Res* **263:** 209-223.

Desai B, Ma T & Chellaiah MA. (2008). Invadopodia and matrix degradation, a new property of prostate cancer cells during migration and invasion. *J Biol Chem* **283:** 13856-13866.

Destaing O, Planus E, Bouvard D, Oddou C, Badowski C, Bossy V, Raducanu A, Fourcade B, Albiges-Rizo C & Block MR. (2010). beta1A integrin is a

master regulator of invadosome organization and function. *Mol Biol Cell* **21:** 4108-4119.

Diaz B, Shani G, Pass I, Anderson D, Quintavalle M & Courtneidge SA. (2009). Tks5-dependent, nox-mediated generation of reactive oxygen species is necessary for invadopodia formation. *Sci Signal* **2:** ra53.

Doyle AD, Wang FW, Matsumoto K & Yamada KM. (2009). One-dimensional topography underlies three-dimensional fibrillar cell migration. *J Cell Biol* **184:** 481-490.

Edwards LA, Woo J, Huxham LA, Verreault M, Dragowska WH, Chiu G, Rajput A, Kyle AH, Kalra J, Yapp D, Yan H, Minchinton AI, Huntsman D, Daynard T, Waterhouse DN, Thiessen B, Dedhar S & Bally MB. (2008). Suppression of VEGF secretion and changes in glioblastoma multiforme microenvironment by inhibition of integrin-linked kinase (ILK). *Mol Cancer Ther* **7:** 59-70.

Ellerbroek SM, Wu YI, Overall CM & Stack MS. (2001). Functional interplay between type I collagen and cell surface matrix metalloproteinase activity. *J Biol Chem* **276:** 24833-24842.

Engler A, Bacakova L, Newman C, Hategan A, Griffin M & Discher D. (2004). Substrate compliance versus ligand density in cell on gel responses. *Biophys J* **86:** 617-628.

Enomoto A, Murakami H, Asai N, Morone N, Watanabe T, Kawai K, Murakumo Y, Usukura J, Kaibuchi K & Takahashi M. (2005). Akt/PKB regulates actin organization and cell motility via Girdin/APE. *Dev Cell* **9:** 389-402.

Esfandiarei M, Yazdi SA, Gray V, Dedhar S & van Breemen C. (2010). Integrin-linked kinase functions as a downstream signal of platelet-derived growth factor to regulate actin polymerization and vascular smooth muscle cell migration. *BMC Cell Biol* **11:** 16.

Ezratty EJ, Partridge MA & Gundersen GG. (2005). Microtubule-induced focal adhesion disassembly is mediated by dynamin and focal adhesion kinase. *Nat Cell Biol* **7:** 581-590.

Fidler IJ. (2003). The pathogenesis of cancer metastasis: the 'seed and soil' hypothesis revisited. *Nat Rev Cancer* **3:** 453-458.

Fincham VJ, Wyke JA & Frame MC. (1995). v-Src-induced degradation of focal adhesion kinase during morphological transformation of chicken embryo fibroblasts. *Oncogene* **10:** 2247-2252.

Folkman J. (1971). Tumor angiogenesis: therapeutic implications. *N Engl J Med* **285:** 1182-1186.

Franco SJ, Rodgers MA, Perrin BJ, Han J, Bennin DA, Critchley DR & Huttenlocher A. (2004). Calpain-mediated proteolysis of talin regulates adhesion dynamics. *Nat Cell Biol* **6:** 977-983.

Friedl P & Alexander S. (2011). Cancer invasion and the microenvironment: plasticity and reciprocity. *Cell* **147:** 992-1009.

Friedl P & Wolf K. (2009). Proteolytic interstitial cell migration: a five-step process. *Cancer Metastasis Rev* **28:** 129-135.

Friedland JC, Lee MH & Boettiger D. (2009). Mechanically activated integrin switch controls alpha5beta1 function. *Science* **323:** 642-644.

Fruman DA, Meyers RE & Cantley LC. (1998). Phosphoinositide kinases. *Annu Rev Biochem* **67:** 481-507.

Gaidano G, Bergui L, Schena M, Gaboli M, Cremona O, Marchisio PC & Caligaris-Cappio F. (1990). Integrin distribution and cytoskeleton organization in normal and malignant monocytes. *Leukemia* **4:** 682-687.

Galvez BG, Matias-Roman S, Yanez-Mo M, Sanchez-Madrid F & Arroyo AG. (2002). ECM regulates MT1-MMP localization with beta1 or alphavbeta3 integrins at distinct cell compartments modulating its internalization and activity on human endothelial cells. *J Cell Biol* **159:** 509-521.

Gawden-Bone C, Zhou Z, King E, Prescott A, Watts C & Lucocq J. (2010). Dendritic cell podosomes are protrusive and invade the extracellular matrix using metalloproteinase MMP-14. *J Cell Sci* **123:** 1427-1437.

Geiger B & Yamada KM. (2011). Molecular architecture and function of matrix adhesions. *Cold Spring Harb Perspect Biol* **3**.

Giampieri S, Manning C, Hooper S, Jones L, Hill CS & Sahai E. (2009). Localized and reversible TGFbeta signalling switches breast cancer cells from cohesive to single cell motility. *Nat Cell Biol* **11:** 1287-1296.

Gianni D, Diaz B, Taulet N, Fowler B, Courtneidge SA & Bokoch GM. (2009). Novel p47(phox)-related organizers regulate localized NADPH oxidase 1 (Nox1) activity. *Sci Signal* **2:** ra54.

Giannone G & Sheetz MP. (2006). Substrate rigidity and force define form through tyrosine phosphatase and kinase pathways. *Trends Cell Biol* **16:** 213-223.

Gill JK, Maskarinec G, Pagano I & Kolonel LN. (2006). The association of mammographic density with ductal carcinoma in situ of the breast: the Multiethnic Cohort. *Breast Cancer Res* **8:** R30.

Gimona M, Buccione R, Courtneidge SA & Linder S. (2008). Assembly and biological role of podosomes and invadopodia. *Curr Opin Cell Biol* **20:** 235-241.

Gligorijevic B, Wyckoff J, Yamaguchi H, Wang Y, Roussos ET & Condeelis J. (2012). N-WASP-mediated invadopodium formation is involved in intravasation and lung metastasis of mammary tumors. *J Cell Sci* **125:** 724-734.

Grass GD, Bratoeva M & Toole BP. (2012). Regulation of invadopodia formation and activity by CD147. *J Cell Sci* **125:** 777-788.

Guo W & Giancotti FG. (2004). Integrin signalling during tumour progression. *Nat Rev Mol Cell Biol* **5:** 816-826.

Guo WH, Frey MT, Burnham NA & Wang YL. (2006). Substrate rigidity regulates the formation and maintenance of tissues. *Biophys J* **90:** 2213-2220.

Gupton SL & Gertler FB. (2010). Integrin signaling switches the cytoskeletal and exocytic machinery that drives neuritogenesis. *Dev Cell* **18:** 725-736.

Hai CM, Hahne P, Harrington EO & Gimona M. (2002). Conventional protein kinase C mediates phorbol-dibutyrate-induced cytoskeletal remodeling in a7r5 smooth muscle cells. *Exp Cell Res* **280:** 64-74.

Hall DE, Reichardt LF, Crowley E, Holley B, Moezzi H, Sonnenberg A & Damsky CH. (1990). The alpha 1/beta 1 and alpha 6/beta 1 integrin heterodimers mediate cell attachment to distinct sites on laminin. *J Cell Biol* **110:** 2175-2184.

Hanahan D & Weinberg RA. (2000). The hallmarks of cancer. *Cell* **100:** 57-70.

Hanahan D & Weinberg RA. (2011). Hallmarks of cancer: the next generation. *Cell* **144:** 646-674.

Hashimoto S, Onodera Y, Hashimoto A, Tanaka M, Hamaguchi M, Yamada A & Sabe H. (2004). Requirement for Arf6 in breast cancer invasive activities. *Proc Natl Acad Sci U S A* **101:** 6647-6652.

Hauck CR, Hsia DA, Ilic D & Schlaepfer DD. (2002). v-Src SH3-enhanced interaction with focal adhesion kinase at beta 1 integrin-containing invadopodia promotes cell invasion. *J Biol Chem* **277:** 12487-12490.

Hayman EG, Pierschbacher MD & Ruoslahti E. (1985). Detachment of cells from culture substrate by soluble fibronectin peptides. *J Cell Biol* **100:** 1948-1954.

Ho E & Dagnino L. (2012). Epidermal growth factor induction of front-rear polarity and migration in keratinocytes is mediated by integrin-linked kinase and ELMO2. *Mol Biol Cell* **23:** 492-502.

Honda A, Nogami M, Yokozeki T, Yamazaki M, Nakamura H, Watanabe H, Kawamoto K, Nakayama K, Morris AJ, Frohman MA & Kanaho Y. (1999). Phosphatidylinositol 4-phosphate 5-kinase alpha is a downstream effector of the small G protein ARF6 in membrane ruffle formation. *Cell* **99:** 521-532.

Hoshino D, Jourquin J, Emmons WE, Miller T, Goldgof M, Costello K, Tyson DR, Brown B, Prasad NK, Zhang B, Mills GB, Yarbrough WG, Quaranta V, Seiki M & Weaver AM. (in revision). Network analysis of the focal adhesion-invadopodia transition identifies a PI 3-kinase-PKCalpha invasive signaling axis. *Sci Signal*.

Hoshino D, Koshikawa N, Suzuki T, Quaranta V, Weaver AM, Seiki M & Ichikawa K. (2012). Establishment and validation of computational model for MT1-MMP dependent ECM degradation and intervention strategies. *PLoS Comput Biol* **8:** e1002479.

Hotary K, Li XY, Allen E, Stevens SL & Weiss SJ. (2006). A cancer cell metalloprotease triad regulates the basement membrane transmigration program. *Genes Dev* **20:** 2673-2686.

Hsu SC, TerBush D, Abraham M & Guo W. (2004). The exocyst complex in polarized exocytosis. *Int Rev Cytol* **233:** 243-265.

Hunter T. (1987). A tail of two src's: mutatis mutandis. *Cell* **49:** 1-4.

Isaac BM, Ishihara D, Nusblat LM, Gevrey JC, Dovas A, Condeelis J & Cox D. (2010). N-WASP has the ability to compensate for the loss of WASP in macrophage podosome formation and chemotaxis. *Exp Cell Res* **316:** 3406-3416.

Itoh Y & Seiki M. (2006). MT1-MMP: a potent modifier of pericellular microenvironment. *J Cell Physiol* **206:** 1-8.

Johnson HW & Schell MJ. (2009). Neuronal IP3 3-kinase is an F-actin-bundling protein: role in dendritic targeting and regulation of spine morphology. *Mol Biol Cell* **20:** 5166-5180.

Kanehisa J, Yamanaka T, Doi S, Turksen K, Heersche JN, Aubin JE & Takeuchi H. (1990). A band of F-actin containing podosomes is involved in bone resorption by osteoclasts. *Bone* **11:** 287-293.

Katsumi A, Orr AW, Tzima E & Schwartz MA. (2004). Integrins in mechanotransduction. *J Biol Chem* **279:** 12001-12004.

Kaverina I, Stradal TE & Gimona M. (2003). Podosome formation in cultured A7r5 vascular smooth muscle cells requires Arp2/3-dependent de-novo actin polymerization at discrete microdomains. *J Cell Sci* **116:** 4915-4924.

Kessenbrock K, Plaks V & Werb Z. (2010). Matrix metalloproteinases: regulators of the tumor microenvironment. *Cell* **141:** 52-67.

Kim AS, Kakalis LT, Abdul-Manan N, Liu GA & Rosen MK. (2000). Autoinhibition and activation mechanisms of the Wiskott-Aldrich syndrome protein. *Nature* **404:** 151-158.

Kong F, Garcia AJ, Mould AP, Humphries MJ & Zhu C. (2009). Demonstration of catch bonds between an integrin and its ligand. *J Cell Biol* **185:** 1275-1284.

Koshikawa N, Mizushima H, Minegishi T, Iwamoto R, Mekada E & Seiki M. (2010). Membrane type 1-matrix metalloproteinase cleaves off the NH2-terminal portion of heparin-binding epidermal growth factor and converts it into a heparin-independent growth factor. *Cancer Res* **70:** 6093-6103.

Kubow KE & Horwitz AR. (2011). Reducing background fluorescence reveals adhesions in 3D matrices. *Nat Cell Biol* **13:** 3-5; author reply 5-7.

Kufe DW, Holland JF, Frei E & American Association for Cancer Research. (2006). *Holland Frei cancer medicine 7*. BC Decker, Hamilton, Ont.; Lewiston, NY [distributor].

Labernadie A, Thibault C, Vieu C, Maridonneau-Parini I & Charriere GM. (2010). Dynamics of podosome stiffness revealed by atomic force microscopy. *Proc Natl Acad Sci U S A* **107:** 21016-21021.

Lahlou H & Muller WJ. (2011). beta1-integrins signaling and mammary tumor progression in transgenic mouse models: implications for human breast cancer. *Breast Cancer Res* **13:** 229.

Laug WE, DeClerck YA & Jones PA. (1983). Degradation of the subendothelial matrix by tumor cells. *Cancer Res* **43:** 1827-1834.

Lehti K, Allen E, Birkedal-Hansen H, Holmbeck K, Miyake Y, Chun TH & Weiss SJ. (2005). An MT1-MMP-PDGF receptor-beta axis regulates mural cell investment of the microvasculature. *Genes Dev* **19:** 979-991.

Levental KR, Yu H, Kass L, Lakins JN, Egeblad M, Erler JT, Fong SF, Csiszar K, Giaccia A, Weninger W, Yamauchi M, Gasser DL & Weaver VM. (2009). Matrix crosslinking forces tumor progression by enhancing integrin signaling. *Cell* **139:** 891-906.

Li S, Lao J, Chen BP, Li YS, Zhao Y, Chu J, Chen KD, Tsou TC, Peck K & Chien S. (2003). Genomic analysis of smooth muscle cells in 3-dimensional collagen matrix. *Faseb J* **17:** 97-99.

Li T, Sun L, Miller N, Nicklee T, Woo J, Hulse-Smith L, Tsao MS, Khokha R, Martin L & Boyd N. (2005). The association of measured breast tissue characteristics with mammographic density and other risk factors for breast cancer. *Cancer Epidemiol Biomarkers Prev* **14:** 343-349.

Li XY, Ota I, Yana I, Sabeh F & Weiss SJ. (2008). Molecular dissection of the structural machinery underlying the tissue-invasive activity of membrane type-1 matrix metalloproteinase. *Mol Biol Cell* **19:** 3221-3233.

Linder S & Aepfelbacher M. (2003). Podosomes: adhesion hot-spots of invasive cells. *Trends Cell Biol* **13:** 376-385.

Linder S, Wiesner C & Himmel M. (2011). Degrading devices: invadosomes in proteolytic cell invasion. *Annu Rev Cell Dev Biol* **27:** 185-211.

Liu J, Yue P, Artym VV, Mueller SC & Guo W. (2009a). The role of the exocyst in matrix metalloproteinase secretion and actin dynamics during tumor cell invadopodia formation. *Mol Biol Cell* **20:** 3763-3771.

Liu S, Yamashita H, Weidow B, Weaver AM & Quaranta V. (2009b). Laminin-332-beta1 integrin interactions negatively regulate invadopodia. *J Cell Physiol* **223:** 134-142.

Lizarraga F, Poincloux R, Romao M, Montagnac G, Le Dez G, Bonne I, Rigaill G, Raposo G & Chavrier P. (2009). Diaphanous-related formins are required for invadopodia formation and invasion of breast tumor cells. *Cancer Res* **69:** 2792-2800.

Lock P, Abram CL, Gibson T & Courtneidge SA. (1998). A new method for isolating tyrosine kinase substrates used to identify fish, an SH3 and PX domain-containing protein, and Src substrate. *Embo J* **17:** 4346-4357.

Lorenz M, Yamaguchi H, Wang Y, Singer RH & Condeelis J. (2004). Imaging sites of N-wasp activity in lamellipodia and invadopodia of carcinoma cells. *Curr Biol* **14:** 697-703.

Lu X, Lu D, Scully M & Kakkar V. (2008). The role of integrins in cancer and the development of anti-integrin therapeutic agents for cancer therapy. *Perspect Medicin Chem* **2:** 57-73.

Lucas JT, Jr., Salimath BP, Slomiany MG & Rosenzweig SA. (2010). Regulation of invasive behavior by vascular endothelial growth factor is HEF1-dependent. *Oncogene* **29:** 4449-4459.

Luxenburg C, Geblinger D, Klein E, Anderson K, Hanein D, Geiger B & Addadi L. (2007). The architecture of the adhesive apparatus of cultured osteoclasts: from podosome formation to sealing zone assembly. *PLoS One* **2:** e179.

Machesky LM, Mullins RD, Higgs HN, Kaiser DA, Blanchoin L, May RC, Hall ME & Pollard TD. (1999). Scar, a WASp-related protein, activates nucleation of actin filaments by the Arp2/3 complex. *Proc Natl Acad Sci U S A* **96:** 3739-3744.

Mader CC, Oser M, Magalhaes MA, Bravo-Cordero JJ, Condeelis J, Koleske AJ & Gil-Henn H. (2011). An EGFR-Src-Arg-cortactin pathway mediates functional maturation of invadopodia and breast cancer cell invasion. *Cancer Res* **71:** 1730-1741.

Madsen CD & Sahai E. (2010). Cancer dissemination--lessons from leukocytes. *Dev Cell* **19:** 13-26.

Magalhaes MA, Larson DR, Mader CC, Bravo-Cordero JJ, Gil-Henn H, Oser M, Chen X, Koleske AJ & Condeelis J. (2011). Cortactin phosphorylation regulates cell invasion through a pH-dependent pathway. *J Cell Biol* **195:** 903-920.

Mandal S, Johnson KR & Wheelock MJ. (2008). TGF-beta induces formation of F-actin cores and matrix degradation in human breast cancer cells via distinct signaling pathways. *Exp Cell Res* **314:** 3478-3493.

Marchisio PC, Cirillo D, Naldini L, Primavera MV, Teti A & Zambonin-Zallone A. (1984). Cell-substratum interaction of cultured avian osteoclasts is mediated by specific adhesion structures. *J Cell Biol* **99:** 1696-1705.

Marchisio PC, Cirillo D, Teti A, Zambonin-Zallone A & Tarone G. (1987). Rous sarcoma virus-transformed fibroblasts and cells of monocytic origin display a peculiar dot-like organization of cytoskeletal proteins involved in microfilament-membrane interactions. *Exp Cell Res* **169:** 202-214.

Martin GS. (1970). Rous sarcoma virus: a function required for the maintenance of the transformed state. *Nature* **227:** 1021-1023.

Matias-Roman S, Galvez BG, Genis L, Yanez-Mo M, de la Rosa G, Sanchez-Mateos P, Sanchez-Madrid F & Arroyo AG. (2005). Membrane type 1-matrix metalloproteinase is involved in migration of human monocytes and is regulated through their interaction with fibronectin or endothelium. *Blood* **105:** 3956-3964.

Miesenbock G, De Angelis DA & Rothman JE. (1998). Visualizing secretion and synaptic transmission with pH-sensitive green fluorescent proteins. *Nature* **394:** 192-195.

Miyauchi A, Hruska KA, Greenfield EM, Duncan R, Alvarez J, Barattolo R, Colucci S, Zambonin-Zallone A, Teitelbaum SL & Teti A. (1990). Osteoclast cytosolic calcium, regulated by voltage-gated calcium channels and extracellular calcium, controls podosome assembly and bone resorption. *J Cell Biol* **111:** 2543-2552.

Mizutani K, Miki H, He H, Maruta H & Takenawa T. (2002). Essential role of neural Wiskott-Aldrich syndrome protein in podosome formation and degradation of extracellular matrix in src-transformed fibroblasts. *Cancer Res* **62:** 669-674.

Mofrad MR, Golji J, Abdul Rahim NA & Kamm RD. (2004). Force-induced unfolding of the focal adhesion targeting domain and the influence of paxillin binding. *Mech Chem Biosyst* **1:** 253-265.

Monsky WL, Lin CY, Aoyama A, Kelly T, Akiyama SK, Mueller SC & Chen WT. (1994). A potential marker protease of invasiveness, seprase, is localized on invadopodia of human malignant melanoma cells. *Cancer Res* **54:** 5702-5710.

Moore SW, Roca-Cusachs P & Sheetz MP. (2010). Stretchy proteins on stretchy substrates: the important elements of integrin-mediated rigidity sensing. *Dev Cell* **19:** 194-206.

Moreau V, Tatin F, Varon C & Genot E. (2003). Actin can reorganize into podosomes in aortic endothelial cells, a process controlled by Cdc42 and RhoA. *Mol Cell Biol* **23:** 6809-6822.

Mueller SC & Chen WT. (1991). Cellular invasion into matrix beads: localization of beta 1 integrins and fibronectin to the invadopodia. *J Cell Sci* **99 (Pt 2):** 213-225.

Mueller SC, Ghersi G, Akiyama SK, Sang QX, Howard L, Pineiro-Sanchez M, Nakahara H, Yeh Y & Chen WT. (1999). A novel protease-docking function of integrin at invadopodia. *J Biol Chem* **274:** 24947-24952.

Murphy DA & Courtneidge SA. (2011). The 'ins' and 'outs' of podosomes and invadopodia: characteristics, formation and function. *Nat Rev Mol Cell Biol* **12:** 413-426.

Nakahara H, Howard L, Thompson EW, Sato H, Seiki M, Yeh Y & Chen WT. (1997). Transmembrane/cytoplasmic domain-mediated membrane type 1-matrix metalloprotease docking to invadopodia is required for cell invasion. *Proc Natl Acad Sci U S A* **94:** 7959-7964.

Nakahara H, Mueller SC, Nomizu M, Yamada Y, Yeh Y & Chen WT. (1998). Activation of beta1 integrin signaling stimulates tyrosine phosphorylation of p190RhoGAP and membrane-protrusive activities at invadopodia. *J Biol Chem* **273:** 9-12.

Nakahara H, Nomizu M, Akiyama SK, Yamada Y, Yeh Y & Chen WT. (1996). A mechanism for regulation of melanoma invasion. Ligation of alpha6beta1 integrin by laminin G peptides. *J Biol Chem* **271:** 27221-27224.

Nakamura I, Duong le T, Rodan SB & Rodan GA. (2007). Involvement of alpha(v)beta3 integrins in osteoclast function. *J Bone Miner Metab* **25:** 337-344.

Nemir S & West JL. (2009). Synthetic materials in the study of cell response to substrate rigidity. *Ann Biomed Eng* **38:** 2-20.

Nusblat LM, Dovas A & Cox D. (2011). The non-redundant role of N-WASP in podosome-mediated matrix degradation in macrophages. *Eur J Cell Biol* **90:** 205-212.

Oikawa T, Itoh T & Takenawa T. (2008). Sequential signals toward podosome formation in NIH-src cells. *J Cell Biol* **182:** 157-169.

Ooms LM, Horan KA, Rahman P, Seaton G, Gurung R, Kethesparan DS & Mitchell CA. (2009). The role of the inositol polyphosphate 5-phosphatases in cellular function and human disease. *Biochem J* **419:** 29-49.

Orr AW, Ginsberg MH, Shattil SJ, Deckmyn H & Schwartz MA. (2006). Matrix-specific suppression of integrin activation in shear stress signaling. *Mol Biol Cell* **17:** 4686-4697.

Oser M, Dovas A, Cox D & Condeelis J. (2011). Nck1 and Grb2 localization patterns can distinguish invadopodia from podosomes. *Eur J Cell Biol* **90:** 181-188.

Oser M, Yamaguchi H, Mader CC, Bravo-Cordero JJ, Arias M, Chen X, Desmarais V, van Rheenen J, Koleske AJ & Condeelis J. (2009). Cortactin regulates cofilin and N-WASp activities to control the stages of invadopodium assembly and maturation. *J Cell Biol* **186:** 571-587.

Osiak AE, Zenner G & Linder S. (2005). Subconfluent endothelial cells form podosomes downstream of cytokine and RhoGTPase signaling. *Exp Cell Res* **307:** 342-353.

Owens LV, Xu L, Craven RJ, Dent GA, Weiner TM, Kornberg L, Liu ET & Cance WG. (1995). Overexpression of the focal adhesion kinase (p125FAK) in invasive human tumors. *Cancer Res* **55:** 2752-2755.

Pan YR, Chen CL & Chen HC. (2011). FAK is required for the assembly of podosome rosettes. *J Cell Biol* **195:** 113-129.

Pantel K & Brakenhoff RH. (2004). Dissecting the metastatic cascade. *Nat Rev Cancer* **4:** 448-456.

Parekh A, Ruppender NS, Branch KM, Sewell-Loftin MK, Lin J, Boyer PD, Candiello JE, Merryman WD, Guelcher SA & Weaver AM. (2011). Sensing and modulation of invadopodia across a wide range of rigidities. *Biophys J* **100:** 573-582.

Parekh A & Weaver AM. (2009). Regulation of cancer invasiveness by the physical extracellular matrix environment. *Cell Adh Migr* **3:** 288-292.

Pasapera AM, Schneider IC, Rericha E, Schlaepfer DD & Waterman CM. (2010). Myosin II activity regulates vinculin recruitment to focal adhesions through FAK-mediated paxillin phosphorylation. *J Cell Biol* **188:** 877-890.

Paszek MJ, Zahir N, Johnson KR, Lakins JN, Rozenberg GI, Gefen A, Reinhart-King CA, Margulies SS, Dembo M, Boettiger D, Hammer DA & Weaver VM. (2005). Tensional homeostasis and the malignant phenotype. *Cancer Cell* **8:** 241-254.

Pelham RJ, Jr. & Wang Y. (1997). Cell locomotion and focal adhesions are regulated by substrate flexibility. *Proc Natl Acad Sci U S A* **94:** 13661-13665.

Pignatelli J, Tumbarello DA, Schmidt RP & Turner CE. (2012). Hic-5 promotes invadopodia formation and invasion during TGF-beta-induced epithelial-mesenchymal transition. *J Cell Biol* **197:** 421-437.

Poincloux R, Lizarraga F & Chavrier P. (2009). Matrix invasion by tumour cells: a focus on MT1-MMP trafficking to invadopodia. *J Cell Sci* **122:** 3015-3024.

Poste G & Fidler IJ. (1980). The pathogenesis of cancer metastasis. *Nature* **283:** 139-146.

Prigent M, Dubois T, Raposo G, Derrien V, Tenza D, Rosse C, Camonis J & Chavrier P. (2003). ARF6 controls post-endocytic recycling through its downstream exocyst complex effector. *J Cell Biol* **163:** 1111-1121.

Provenzano PP, Inman DR, Eliceiri KW, Knittel JG, Yan L, Rueden CT, White JG & Keely PJ. (2008a). Collagen density promotes mammary tumor initiation and progression. *BMC Med* **6:** 11.

Provenzano PP, Inman DR, Eliceiri KW, Trier SM & Keely PJ. (2008b). Contact guidance mediated three-dimensional cell migration is regulated by Rho/ROCK-dependent matrix reorganization. *Biophys J* **95:** 5374-5384.

Quintavalle M, Elia L, Condorelli G & Courtneidge SA. (2011). MicroRNA control of podosome formation in vascular smooth muscle cells in vivo and in vitro. *J Cell Biol* **189:** 13-22.

Rajadurai CV, Havrylov S, Zaoui K, Vaillancourt R, Stuible M, Naujokas M, Zuo D, Tremblay ML & Park M. (2012). Met receptor tyrosine kinase signals through a cortactin-Gab1 scaffold complex, to mediate invadopodia. *J Cell Sci*.

Remacle A, Murphy G & Roghi C. (2003). Membrane type I-matrix metalloproteinase (MT1-MMP) is internalised by two different pathways and is recycled to the cell surface. *J Cell Sci* **116:** 3905-3916.

Ren J & Guo W. (2012). ERK1/2 regulate exocytosis through direct phosphorylation of the exocyst component Exo70. *Dev Cell* **22:** 967-978.

Roca-Cusachs P, Gauthier NC, Del Rio A & Sheetz MP. (2009). Clustering of alpha(5)beta(1) integrins determines adhesion strength whereas alpha(v)beta(3) and talin enable mechanotransduction. *Proc Natl Acad Sci U S A* **106:** 16245-16250.

Rohatgi R, Ho HY & Kirschner MW. (2000). Mechanism of N-WASP activation by CDC42 and phosphatidylinositol 4, 5-bisphosphate. *J Cell Biol* **150:** 1299-1310.

Rohatgi R, Ma L, Miki H, Lopez M, Kirchhausen T, Takenawa T & Kirschner MW. (1999). The interaction between N-WASP and the Arp2/3 complex links Cdc42-dependent signals to actin assembly. *Cell* **97:** 221-231.

Rohatgi R, Nollau P, Ho HY, Kirschner MW & Mayer BJ. (2001). Nck and phosphatidylinositol 4,5-bisphosphate synergistically activate actin polymerization through the N-WASP-Arp2/3 pathway. *J Biol Chem* **276:** 26448-26452.

Rottiers P, Saltel F, Daubon T, Chaigne-Delalande B, Tridon V, Billottet C, Reuzeau E & Genot E. (2009). TGFbeta-induced endothelial podosomes mediate basement membrane collagen degradation in arterial vessels. *J Cell Sci* **122:** 4311-4318.

Rowe RG & Weiss SJ. (2008). Breaching the basement membrane: who, when and how? *Trends Cell Biol* **18:** 560-574.

Saarikangas J, Zhao H & Lappalainen P. (2010). Regulation of the actin cytoskeleton-plasma membrane interplay by phosphoinositides. *Physiol Rev* **90:** 259-289.

Sabeh F, Ota I, Holmbeck K, Birkedal-Hansen H, Soloway P, Balbin M, Lopez-Otin C, Shapiro S, Inada M, Krane S, Allen E, Chung D & Weiss SJ. (2004). Tumor cell traffic through the extracellular matrix is controlled by the membrane-anchored collagenase MT1-MMP. *J Cell Biol* **167:** 769-781.

Sabeh F, Shimizu-Hirota R & Weiss SJ. (2009). Protease-dependent versus -independent cancer cell invasion programs: three-dimensional amoeboid movement revisited. *J Cell Biol* **185:** 11-19.

Saitoh M, Ishikawa T, Matsushima S, Naka M & Hidaka H. (1987). Selective inhibition of catalytic activity of smooth muscle myosin light chain kinase. *J Biol Chem* **262:** 7796-7801.

Sakai T, Li S, Docheva D, Grashoff C, Sakai K, Kostka G, Braun A, Pfeifer A, Yurchenco PD & Fassler R. (2003). Integrin-linked kinase (ILK) is required for polarizing the epiblast, cell adhesion, and controlling actin accumulation. *Genes Dev* **17:** 926-940.

Sakurai-Yageta M, Recchi C, Le Dez G, Sibarita JB, Daviet L, Camonis J, D'Souza-Schorey C & Chavrier P. (2008). The interaction of IQGAP1 with the exocyst complex is required for tumor cell invasion downstream of Cdc42 and RhoA. *J Cell Biol* **181:** 985-998.

Santner SJ, Dawson PJ, Tait L, Soule HD, Eliason J, Mohamed AN, Wolman SR, Heppner GH & Miller FR. (2001). Malignant MCF10CA1 cell lines derived from premalignant human breast epithelial MCF10AT cells. *Breast Cancer Res Treat* **65:** 101-110.

Sawada Y, Tamada M, Dubin-Thaler BJ, Cherniavskaya O, Sakai R, Tanaka S & Sheetz MP. (2006). Force sensing by mechanical extension of the Src family kinase substrate p130Cas. *Cell* **127:** 1015-1026.

Sawai H, Okada Y, Funahashi H, Matsuo Y, Takahashi H, Takeyama H & Manabe T. (2006). Integrin-linked kinase activity is associated with interleukin-1 alpha-induced progressive behavior of pancreatic cancer and poor patient survival. *Oncogene* **25:** 3237-3246.

Schmidt S, Nakchbandi I, Ruppert R, Kawelke N, Hess MW, Pfaller K, Jurdic P, Fassler R & Moser M. (2011). Kindlin-3-mediated signaling from multiple integrin classes is required for osteoclast-mediated bone resorption. *J Cell Biol* **192:** 883-897.

Schober M, Raghavan S, Nikolova M, Polak L, Pasolli HA, Beggs HE, Reichardt LF & Fuchs E. (2007). Focal adhesion kinase modulates tension signaling to control actin and focal adhesion dynamics. *J Cell Biol* **176:** 667-680.

Schoumacher M, Goldman RD, Louvard D & Vignjevic DM. (2010). Actin, microtubules, and vimentin intermediate filaments cooperate for elongation of invadopodia. *J Cell Biol* **189:** 541-556.

Scott RW, Hooper S, Crighton D, Li A, Konig I, Munro J, Trivier E, Wickman G, Morin P, Croft DR, Dawson J, Machesky L, Anderson KI, Sahai EA & Olson MF. (2010). LIM kinases are required for invasive path generation by tumor and tumor-associated stromal cells. *J Cell Biol* **191:** 169-185.

Seals DF, Azucena EF, Jr., Pass I, Tesfay L, Gordon R, Woodrow M, Resau JH & Courtneidge SA. (2005). The adaptor protein Tks5/Fish is required for podosome formation and function, and for the protease-driven invasion of cancer cells. *Cancer Cell* **7:** 155-165.

Serrano I, McDonald PC, Lock FE & Dedhar S. (2012). Role of the integrin-linked kinase (ILK)/Rictor complex in TGFbeta-1-induced epithelial-mesenchymal transition (EMT). *Oncogene*.

Siegel R, Naishadham D & Jemal A. (2012). Cancer statistics, 2012. *CA Cancer J Clin* **62:** 10-29.

Smith-Pearson PS, Greuber EK, Yogalingam G & Pendergast AM. (2010). Abl kinases are required for invadopodia formation and chemokine-induced invasion. *J Biol Chem* **285:** 40201-40211.

Spaderna S, Schmalhofer O, Hlubek F, Berx G, Eger A, Merkel S, Jung A, Kirchner T & Brabletz T. (2006). A transient, EMT-linked loss of basement membranes indicates metastasis and poor survival in colorectal cancer. *Gastroenterology* **131:** 830-840.

Spiczka KS & Yeaman C. (2008). Ral-regulated interaction between Sec5 and paxillin targets Exocyst to focal complexes during cell migration. *J Cell Sci* **121:** 2880-2891.

Sporn MB. (1996). The war on cancer. *Lancet* **347:** 1377-1381.

Stanchi F, Grashoff C, Nguemeni Yonga CF, Grall D, Fassler R & Van Obberghen-Schilling E. (2009). Molecular dissection of the ILK-PINCH-parvin triad reveals a fundamental role for the ILK kinase domain in the late stages of focal-adhesion maturation. *J Cell Sci* **122:** 1800-1811.

Steffen A, Le Dez G, Poincloux R, Recchi C, Nassoy P, Rottner K, Galli T & Chavrier P. (2008). MT1-MMP-dependent invasion is regulated by TI-VAMP/VAMP7. *Curr Biol* **18:** 926-931.

Stewart DA, Cooper CR & Sikes RA. (2004). Changes in extracellular matrix (ECM) and ECM-associated proteins in the metastatic progression of prostate cancer. *Reprod Biol Endocrinol* **2:** 2.

Straight AF, Cheung A, Limouze J, Chen I, Westwood NJ, Sellers JR & Mitchison TJ. (2003). Dissecting temporal and spatial control of cytokinesis with a myosin II Inhibitor. *Science* **299:** 1743-1747.

Stylli SS, Stacey TT, Verhagen AM, Xu SS, Pass I, Courtneidge SA & Lock P. (2009). Nck adaptor proteins link Tks5 to invadopodia actin regulation and ECM degradation. *J Cell Sci* **122:** 2727-2740.

Tague SE, Muralidharan V & D'Souza-Schorey C. (2004). ADP-ribosylation factor 6 regulates tumor cell invasion through the activation of the MEK/ERK signaling pathway. *Proc Natl Acad Sci U S A* **101:** 9671-9676.

Tarone G, Cirillo D, Giancotti FG, Comoglio PM & Marchisio PC. (1985). Rous sarcoma virus-transformed fibroblasts adhere primarily at discrete

protrusions of the ventral membrane called podosomes. *Exp Cell Res* **159:** 141-157.

Tatin F, Varon C, Genot E & Moreau V. (2006). A signalling cascade involving PKC, Src and Cdc42 regulates podosome assembly in cultured endothelial cells in response to phorbol ester. *J Cell Sci* **119:** 769-781.

Tomari T, Koshikawa N, Uematsu T, Shinkawa T, Hoshino D, Egawa N, Isobe T & Seiki M. (2009). High throughput analysis of proteins associating with a proinvasive MT1-MMP in human malignant melanoma A375 cells. *Cancer Sci* **100:** 1284-1290.

Uehata M, Ishizaki T, Satoh H, Ono T, Kawahara T, Morishita T, Tamakawa H, Yamagami K, Inui J, Maekawa M & Narumiya S. (1997). Calcium sensitization of smooth muscle mediated by a Rho-associated protein kinase in hypertension. *Nature* **389:** 990-994.

Ueno T, Falkenburger BH, Pohlmeyer C & Inoue T. (2011). Triggering actin comets versus membrane ruffles: distinctive effects of phosphoinositides on actin reorganization. *Sci Signal* **4:** ra87.

Van Goethem E, Guiet R, Balor S, Charriere GM, Poincloux R, Labrousse A, Maridonneau-Parini I & Le Cabec V. (2011). Macrophage podosomes go 3D. *Eur J Cell Biol* **90:** 224-236.

Varon C, Tatin F, Moreau V, Van Obberghen-Schilling E, Fernandez-Sauze S, Reuzeau E, Kramer I & Genot E. (2006). Transforming growth factor beta induces rosettes of podosomes in primary aortic endothelial cells. *Mol Cell Biol* **26:** 3582-3594.

Vicente-Manzanares M, Ma X, Adelstein RS & Horwitz AR. (2009). Non-muscle myosin II takes centre stage in cell adhesion and migration. *Nat Rev Mol Cell Biol* **10:** 778-790.

Wang HB, Dembo M, Hanks SK & Wang Y. (2001). Focal adhesion kinase is involved in mechanosensing during fibroblast migration. *Proc Natl Acad Sci U S A* **98:** 11295-11300.

Wang J, Taba Y, Pang J, Yin G, Yan C & Berk BC. (2009). GIT1 mediates VEGF-induced podosome formation in endothelial cells: critical role for PLCgamma. *Arterioscler Thromb Vasc Biol* **29:** 202-208.

Wang Y, Botvinick EL, Zhao Y, Berns MW, Usami S, Tsien RY & Chien S. (2005). Visualizing the mechanical activation of Src. *Nature* **434:** 1040-1045.

Wang Y & McNiven MA. (2012). Invasive matrix degradation at focal adhesions occurs via protease recruitment by a FAK-p130Cas complex. *J Cell Biol* **196:** 375-385.

Weaver AM. (2006). Invadopodia: specialized cell structures for cancer invasion. *Clin Exp Metastasis* **23:** 97-105.

Weaver AM. (2009). Regulation of cancer invasion by reactive oxygen species and Tks family scaffold proteins. *Sci Signal* **2:** pe56.

Webb BA, Jia L, Eves R & Mak AS. (2007). Dissecting the functional domain requirements of cortactin in invadopodia formation. *Eur J Cell Biol* **86:** 189-206.

Webb DJ, Donais K, Whitmore LA, Thomas SM, Turner CE, Parsons JT & Horwitz AF. (2004). FAK-Src signalling through paxillin, ERK and MLCK regulates adhesion disassembly. *Nat Cell Biol* **6:** 154-161.

Weichselbaum RR, Dahlberg W, Beckett M, Karrison T, Miller D, Clark J & Ervin TJ. (1986). Radiation-resistant and repair-proficient human tumor cells may be associated with radiotherapy failure in head- and neck-cancer patients. *Proc Natl Acad Sci U S A* **83:** 2684-2688.

Weiner TM, Liu ET, Craven RJ & Cance WG. (1993). Expression of focal adhesion kinase gene and invasive cancer. *Lancet* **342:** 1024-1025.

Wennstrom S, Hawkins P, Cooke F, Hara K, Yonezawa K, Kasuga M, Jackson T, Claesson-Welsh L & Stephens L. (1994). Activation of phosphoinositide 3-kinase is required for PDGF-stimulated membrane ruffling. *Curr Biol* **4:** 385-393.

Wheeler AP, Smith SD & Ridley AJ. (2006). CSF-1 and PI 3-kinase regulate podosome distribution and assembly in macrophages. *Cell Motil Cytoskeleton* **63:** 132-140.

Wickstrom SA & Fassler R. (2011). Regulation of membrane traffic by integrin signaling. *Trends Cell Biol* **21:** 266-273.

Wickstrom SA, Lange A, Hess MW, Polleux J, Spatz JP, Kruger M, Pfaller K, Lambacher A, Bloch W, Mann M, Huber LA & Fassler R. (2010). Integrin-linked kinase controls microtubule dynamics required for plasma membrane targeting of caveolae. *Dev Cell* **19:** 574-588.

Wiesner C, Faix J, Himmel M, Bentzien F & Linder S. (2010). KIF5B and KIF3A/KIF3B kinesins drive MT1-MMP surface exposure, CD44 shedding,

and extracellular matrix degradation in primary macrophages. *Blood* **116:** 1559-1569.

Winograd-Katz SE, Brunner MC, Mirlas N & Geiger B. (2011). Analysis of the signaling pathways regulating Src-dependent remodeling of the actin cytoskeleton. *Eur J Cell Biol* **90:** 143-156.

Wolf K, Mazo I, Leung H, Engelke K, von Andrian UH, Deryugina EI, Strongin AY, Brocker EB & Friedl P. (2003). Compensation mechanism in tumor cell migration: mesenchymal-amoeboid transition after blocking of pericellular proteolysis. *J Cell Biol* **160:** 267-277.

Wolf K, Wu YI, Liu Y, Geiger J, Tam E, Overall C, Stack MS & Friedl P. (2007). Multi-step pericellular proteolysis controls the transition from individual to collective cancer cell invasion. *Nat Cell Biol* **9:** 893-904.

Wu C & Dedhar S. (2001). Integrin-linked kinase (ILK) and its interactors: a new paradigm for the coupling of extracellular matrix to actin cytoskeleton and signaling complexes. *J Cell Biol* **155:** 505-510.

Wyckoff JB, Pinner SE, Gschmeissner S, Condeelis JS & Sahai E. (2006). ROCK- and myosin-dependent matrix deformation enables protease-independent tumor-cell invasion in vivo. *Curr Biol* **16:** 1515-1523.

Xiao H, Bai XH, Wang Y, Kim H, Mak AS & Liu M. (2012). MEK/ERK pathway mediates PKC activation-induced recruitment of PKCzeta and MMP-9 to podosomes. *J Cell Physiol*.

Yamaguchi H, Lorenz M, Kempiak S, Sarmiento C, Coniglio S, Symons M, Segall J, Eddy R, Miki H, Takenawa T & Condeelis J. (2005). Molecular mechanisms of invadopodium formation: the role of the N-WASP-Arp2/3 complex pathway and cofilin. *J Cell Biol* **168:** 441-452.

Yamaguchi H, Pixley F & Condeelis J. (2006). Invadopodia and podosomes in tumor invasion. *Eur J Cell Biol* **85:** 213-218.

Yamaguchi H, Takeo Y, Yoshida S, Kouchi Z, Nakamura Y & Fukami K. (2009). Lipid rafts and caveolin-1 are required for invadopodia formation and extracellular matrix degradation by human breast cancer cells. *Cancer Res* **69:** 8594-8602.

Yamaguchi H, Yoshida S, Muroi E, Kawamura M, Kouchi Z, Nakamura Y, Sakai R & Fukami K. (2010). Phosphatidylinositol 4,5-bisphosphate and PIP5-kinase Ialpha are required for invadopodia formation in human breast cancer cells. *Cancer Sci* **101:** 1632-1638.

Yamaguchi H, Yoshida S, Muroi E, Yoshida N, Kawamura M, Kouchi Z, Nakamura Y, Sakai R & Fukami K. (2011). Phosphoinositide 3-kinase signaling pathway mediated by p110alpha regulates invadopodia formation. *J Cell Biol* **193:** 1275-1288.

Yeatman TJ. (2004). A renaissance for SRC. *Nat Rev Cancer* **4:** 470-480.

Yu HG, Nam JO, Miller NL, Tanjoni I, Walsh C, Shi L, Kim L, Chen XL, Tomar A, Lim ST & Schlaepfer DD. (2011). p190RhoGEF (Rgnef) promotes colon carcinoma tumor progression via interaction with focal adhesion kinase. *Cancer Res* **71:** 360-370.